STUDIA UNIVERSITATIS
BABEŞ-BOLYAI

BIOLOGIA

1/2010

ANUL LV **2010**

S T U D I A

UNIVERSITATIS BABEŞ-BOLYAI

BIOLOGIA

1

Desktop Editing Office: 51ST B.P. Hasdeu, Cluj-Napoca, Romania, Phone + 40 264-40.53.52

CUPRINS – CONTENT – SOMMAIRE – INHALT

All authors are responsible for submitting manuscripts in comprehensible US or UK English and ensuring scientific accuracy.

STUDIA UNIVERSITATIS BABEŞ – BOLYAI, BIOLOGIA, LV, 1, 2010, p. 3-15

COMPARATIVE BIOMETRIC STUDY OF CRAYFISH POPULATIONS IN THE ANINA MOUNTAINS (SW ROMANIA) HYDROGRAPHIC BASINS

LUCIAN PÂRVULESCU[1]

SUMMARY. The paper presents data concerning the biometric aspects of two crayfish species from the rivers of the Anina Mts: the stone crayfish (*Austropotamobius torrentium*) and the noble crayfish (*Astacus astacus*). The populations of the two species are not evenly distributed within the three hydrographic basins of the investigated area: Bârzava, Caraş, and Nera. Thus, through the discriminant analysis of the measured parameters we were able to identify several parameters that proved to be highly related to the differentiation of the studied specimens into hydrographic basins; these specimens have been afterwards the subject of the ANOVA type analysis. The study revealed that, whereas the *A. torrentium* populations from the Caraş basin present high significantly differences in comparison to the populations analysed in the Nera basin, the *A. astacus* populations from the Caraş basin differ significantly from those of the Bârzava basin. As far as the morphometric differences between the two sexes are concerned, the most powerful and visible distinctions that have been registered for both species can be found at the level of chela, propodus length, dactylus length and width of chela. The maximum dimension of the *A. torrentium* males, as well as the average of these values, is very close to the female one, while for the *A. astacus* the differences between the sexes are much more significant.

Keywords: Anina Mountains, *Astacus astacus*, *Austropotamobius torrentium*, biometry, populations

Introduction

Freshwater crayfish residing in the Romanian aquatic ecosystems belong to the Decapoda orders; they are represented by three indigenous species and an invasive one (Pârvulescu, 2009c). Among these, two indigenous species are present in the Anina Mountains: *Austropotamobius torrentium* (Schrank 1803) and *Astacus astacus* (Linnaeus 1758) (Pârvulescu 2009a). The main purpose of the comparative study regarding the biometry of different populations is to point out the morphological

[1] *West University of Timisoara, Faculty of Chemistry, Biology, Geography, Dept. of Biology, 16A Pestalozzi St., 300115, Timisoara; e-mail: parvulescubio@cbg.uvt.ro*

similarities and dissimilarities between populations that are geographically separated into different hydrographic basins, as a result of diverse environmental influences (Ďuriš *et al.*, 2006; Burba *et al.*, 1999; Papadopol and Diaconu, 1987; Gutiérrez-Yurrita *et al.*, 1996; Streissl and Hödl, 2002). Studies regarding the three indigenous species of crayfish in Romania have also been published by Papadopol and Diaconu, in 1987.

The investigated area, i.e. the Anina Mountains, is located in southwestern Romania; it has a surface of 770 km^2 (Sencu, 1978) most of which is included in two National Parks: Semenic-Cheile Caraşului (Semenic – Caras Gorges) National Park and Cheile Nerei-Beuşniţa (Nera Gorges - Beusnita) National Park. The area of these mountains gathers three hydrographic basins: Bârzava, Caraş and Nera, basins that collect both surface water and ground water. The Caraş and the Nera rivers are the direct tributaries of the Danube River, and the Bârzava River flows into the Danube River, after the confluence with the Timiş River (Ujvari, 1972). The *A. astacus* species lives almost exclusively in the Caraş basin, with the exception of the Buhui stream and the Cândeni River. The Nera basin shows exclusively the presence of the species *A. torrentium*, while the Bârzava basin displays a mixture of populations from both species that can be found in different streams. (Pârvulescu, 2009a).

Taking into consideration the quality of the aquatic habitats, the Bârzava basin is affected by a powerful anthropic impact; on its upper stream there are three artificial dams and various villages which clearly affect the water quality and, implicitly, the quality of the aquatic fauna. The upper stream of the Caraş River presents a very low anthropic impact and registers a very high water quality, with few punctiform exceptions. In the Nera Basin the anthropic impact is scattered along the small villages situated on the stream of the rank 1 tributaries and that alter the water quality, like in the case of the Cândeni creek, where almost an entire popuation was destroyed as a result of the usage of modern detergents within a traditional wash house. (Pârvulescu, 2009b).

Materials and Methods

The biologic samples were collected in August 2008 and June - July 2009, in a total of 52 sampling stations, on all the permanent waters in the upper sector of the Bârzava, Caraş and Nera rivers. Each sampling station comprised at least 200 m of the river under investigation, with similar catching effort. The crayfish were collected using active methods, i.e. direct hand sampling from the waterbed, by checking the galleries within banks and the spaces between roots or rocks.

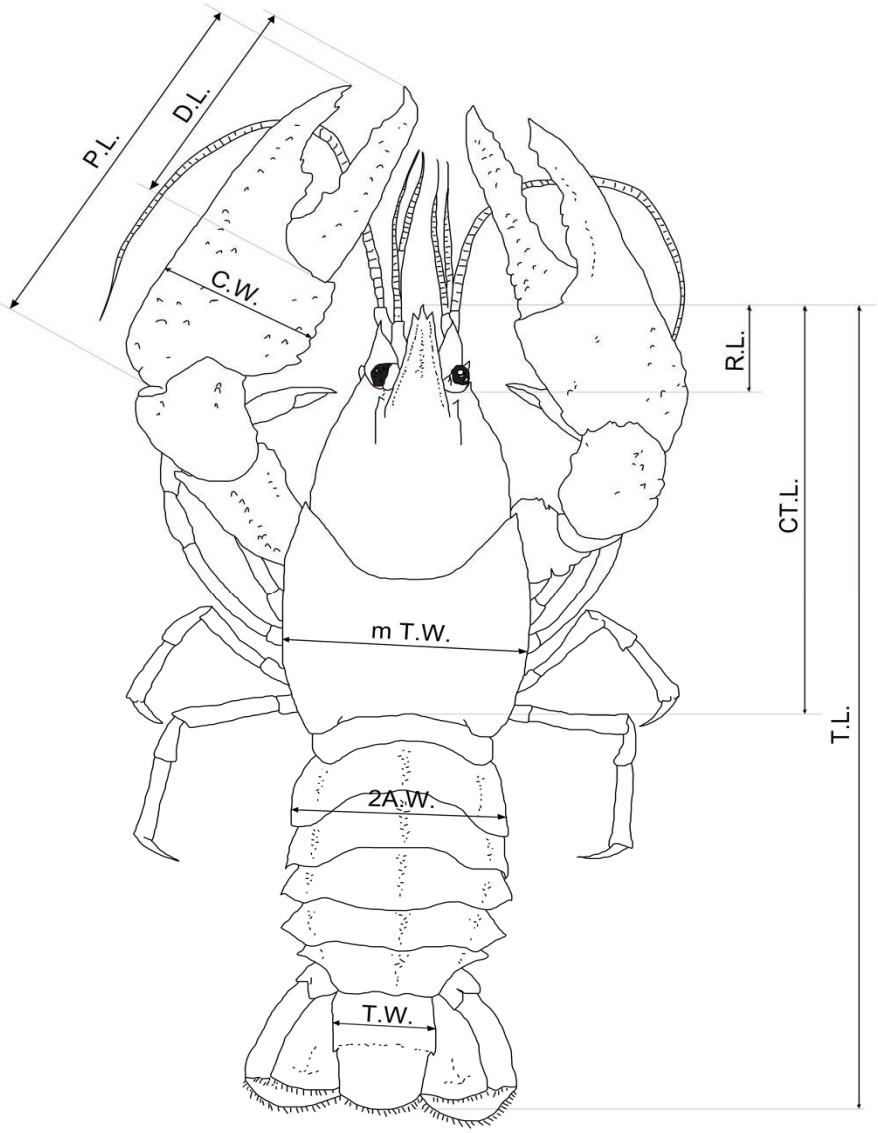

Fig. 1. The biometric parameters measured during the biometric studies for the crayfish from the Anina Mountains

The crayfish were identified *in situ* according to their morphological features, sexed and measured. Subsequently, the specimens were set free exactly in the same location where they had been captured. We have labeled as population all the specimens belonging to one species within each of the three hydrographic basins. For the biometric measurements we have used an electronic Black and Decker caliper with the maximum width of 150 mm and an accuracy of 0.01 mm. The measured parameters (see figure 1) are only those distances which allow the firm grip of the measuring tool. The morphological characteristics measured were: TL – total body length, CTL - cephalothorax (shell) length, mTW - maximum thoracic (shell) width, RL - rostrum length (for the value that indicates the length of the rostrum we subtracted from the value of the cephalothorax length (CTL) the value of the post-orbital cephalothorax length), 2AW – second abdominal segment width, TW – width of telson, PL – propodus length, DL – dactylus length and CW – width of chela. We have measured only the specimens that did not present any sign that both chelae have been regenerated. All specimens have been measured by the same person. The specimens that were smaller than 50 mm total body length have not been measured.

In order to show which of the measured parameters are relevant for the morphological differences, we have processed the data with the help of the discriminant analysis, a technique used to classify cases into categorical-dependent values that helps us obtain pairs of parameters that are significantly different within the lot of the measured data. The means, the standard deviations, the minimum and the maximum as well as the ANOVA tests have also been measured. In order to do this statistical analysis and to create the diagrams, we used the Statistica StatSoft Inc. software (version 7.00 for Windows).

Results

During the investigations performed in the summers of 2008 and 2009 in the rivers of the Anina Mountains, 115 specimens from the *A. torrentium* species and 73 specimens from the *A. astacus* species have been measured. The species are not evenly distributed in all the three hydrographic basins, according to the already published data (Pârvulescu, 2009a). Thus, for the *A. torrentium* species the most representative streams have been the streams of the Nera basin. The species was also found in the Caraş and Bârzava basins. As far as the *A. astacus* species is concerned, the most representative have been the streams from the Caraş basin. The species was also found in the Bârzava basin, especially in the reservoirs. The biometric data have been summarized in Tables 1 and 2.

According to the data from Tables 1 and 2, we can notice that the clearest differences between the sexes are represented by the dimensions of the chelae. However, we cannot use this difference alone if we are to correctly make a distinction between the sexes. Many and diverse situations may appear in nature when the chela may be abnormally well-developed: regeneration after breakage, malformations etc (Pârvulescu *et al.*, 2009).

Table 1.

Biometric data (mm) for the *A. torrentium* species, measured during the summer campaign of 2008-2009, in the Anina Mts. (N = number of specimens).

	Austropotamobius torrentium			
	Male (N=57)		Female (N=58)	
Parameter	Min*-Max	Mean ± SD	Min*-Max	Mean ± SD
TL	50.0-94.0	**69.07** ± 10.862	50.53-93.34	**67.16** ± 10.403
CTL	23.7-48.9	**34.5** ± 6.01	24.6-44.37	**31.46** ± 5.512
RL	4.8-9.1	**6.78** ± 1.072	4.78-9.6	**6.66** ± 1.057
mTW	11.78-27.9	**18.72** ± 3.76	12.3-24.02	**17.04** ± 2.907
2AW	6.17-20.9	**15.33** ± 2.737	11.5-25.43	**16.97** ± 3.486
TW	5.9-13.7	**9.42** ± 1.789	5.93-14.1	**9.37** ± 1.884
PL	16.6-49.9	**29.95** ± 8.021	15.79-33.56	**22.59** ± 4.578
DL	10.08-28.5	**17.23** ± 4.75	8.91-20.45	**13.21** ± 2.757
CW	7.8-19.6	**13.05** ± 3.235	6.75-13.2	**10.05** ± 2.036
Sex ratio	**1:1.017**			

* *Specimens smaller than 50 mm in total length have not been measured*

Table 2.

Biometric data for the (mm) *A. astacus* species, measured during the summer campaign 2008-2009, in the Anina Mts. (N = number of specimens).

	Astacus astacus			
	Male (N=39)		Female (N=34)	
Parameter	Min*-Max	Mean ± SD	Min*-Max	Mean ± SD
TL	61.34-127.34	**99.73** ± 17.978	55.85-108.8	**86.8** ± 14.543
CTL	27.06-68.46	**51.46** ± 10.878	27.82-54.07	**42.98** ± 8.022
RL	5.21-18.8	**12.1** ± 2.671	6.45-12.6	**10.49** ± 1.779
mTW	15.45-49.97	**28.82** ± 7.621	14.42-29.31	**23.24** ± 4.63
2AW	13.17-31.09	**22.93** ± 4.31	12.34-28.26	**21.97** ± 4.655
TW	7.34-18.14	**13.23** ± 2.414	6.83-14.7	**11.38** ± 2.278
PL	20.65-85.5	**47.79** ± 16.925	18.92-42.7	**32.22** ± 8.13
DL	11.69-48.36	**28.08** ± 10.181	10.99-25.6	**19.2** ± 4.778
CW	9.13-32.67	**20.53** ± 6.555	8.19-20.5	**14.43** ± 3.708
Sex ratio	**1:0.871**			

* *Specimens smaller than 50 mm in total length have not been measured*

In order to compare the populations we have resorted to the discriminant analysis that allows to find the most powerful correlated sets of values that could differentiate the specimens from different hydrographic basins. Thus, the correlation

matrix for the *A. torrentium* (Table 3) shows that the most powerful discriminative character is represented by the groups of values propodus length – dactylus length (PL-DL), propodus length – width of chela (PL-CW) and dactylus length – width of chela (DL-CW).

Table 3.

Correlation matrix between the measured parameters for the *A. torrentium* specimens in the Anina Mts. in 2008-2009.

correl.	TL	CTL	RL	mTW	2AW	TW	PL	DL	CW
TL	1.00								
CTL	0.91	1.00							
RL	0.82	0.81	1.00						
mTW	0.95	0.94	0.81	1.00					
2AW	0.84	0.73	0.71	0.76	1.00				
TW	0.75	0.70	0.82	0.73	0.68	1.00			
PL	0.83	0.89	0.73	0.92	0.55	0.62	1.00		
DL	0.82	0.88	0.76	0.90	0.56	0.65	**0.98**	1.00	
CW	0.82	0.87	0.72	0.90	0.56	0.62	**0.97**	**0.95**	1.00

The correlation matrix for the *A. astacus* (Table 4) shows that the most powerful discriminative character is represented by the same groups of values that are relevant for the previous species and by the total length – cephalothorax length (TL-CTL).

Table 4.

Correlation matrix between the parameters measured for the *A. astacus* specimens in the Anina Mts. in 2008-2009.

correl.	TL	CTL	RL	mTW	2AW	TW	PL	DL	CW
TL	1.00								
CTL	**0.97**	1.00							
RL	0.89	0.89	1.00						
mTW	0.92	0.93	0.84	1.00					
2AW	0.92	0.86	0.78	0.82	1.00				
TW	0.80	0.76	0.76	0.72	0.73	1.00			
PL	0.92	0.92	0.83	0.88	0.77	0.72	1.00		
DL	0.91	0.92	0.83	0.86	0.76	0.73	**0.98**	1.00	
CW	0.90	0.90	0.80	0.85	0.77	0.69	**0.97**	**0.96**	1.00

In our studies, for the comparison of these populations, we have used ratio among these parameters. Therefore, for both species we have measured the proportion between propodus and dactylus length, propodus length and chela width, dactylus length and chela width and also total length and cephalothorax length (table 5).

Table 5.

Rapports that show a discriminative character for the crayfish specimens measured in the Anina Mts.

Austropotamobius torrentium		*Astacus astacus*	
Ratio between parameters:	Abbreviation	Ratio between parameters:	Abbreviation
-	**-**	TL and CTL	**TL/CTL**
PL and DL	**PL/DL**	PL and DL	**PL/DL**
PL and CW	**PL/CW**	PL and CW	**PL/CW**
DL and CW	**DL/CW**	DL and CW	**DL/CW**

For our comparison between different populations we have used the ANOVA test, in order to underline the differences between specimens of the same sex, from different hydrographic basins. The individuals of *A. torrentium* species, that inhabit mainly the Nera basin, have also been found well represented in high number of individuals in two streams of the Caraş basin and in five streams of the Bârzava basin. According to the analysis of the diagrams from Figures 2 A, B and C the female populations of crayfish within the three investigated basins are not significantly different. However, we may notice a greater resemblance between the populations of the Nera and of the Bârzava basins.

For *A. torrentium* species the males have been captured in a rather small number of specimens in the Bârzava basin; that is why, for the data analysis only the specimens captured in the Nera and Caraş basins have been taken into account. They display statistically significant differences in the case of the ratio PL/CW ($p=0.01971$) (Fig. 3).

The *A. astacus* species was found in the Anina Mountains only in the Caras and Bârzava basins; in the upper part of the Bârzava River the species was discovered especially in reservoirs. After analyzing the distinct diagrams for the two sexes, we can state that the female populations from the two investigated basins are significantly different concerning the ratio between propodus length and chela width, as well as between dactylus length and chela width (Figs 4 A and B).

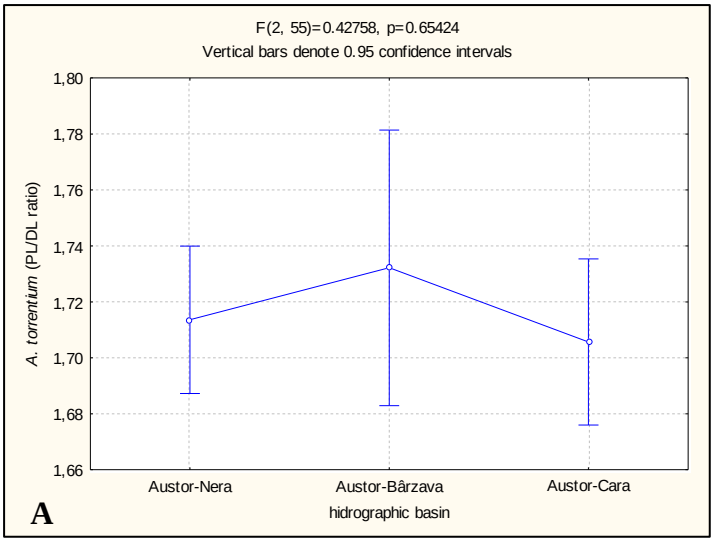

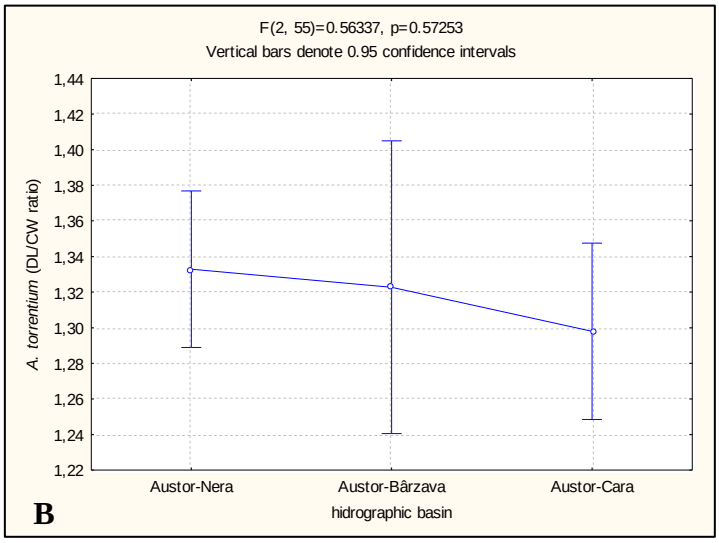

Fig. 2. ANOVA tests for the female specimens of *A. torrentium* from Nera, Bârzava and Caraş hydrographic basins: **A –**for the ratio PL/DL; **B** –for the ratio DL/CW;

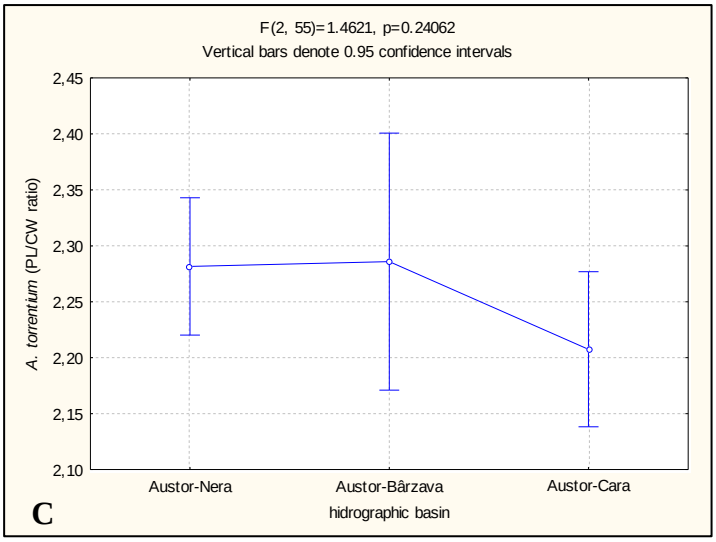

Fig. 3 (continued). ANOVA tests for the female specimens of *A. torrentium* from Nera, Bârzava and Caraş hydrographic basins: **C**- for the ratio PL/CW

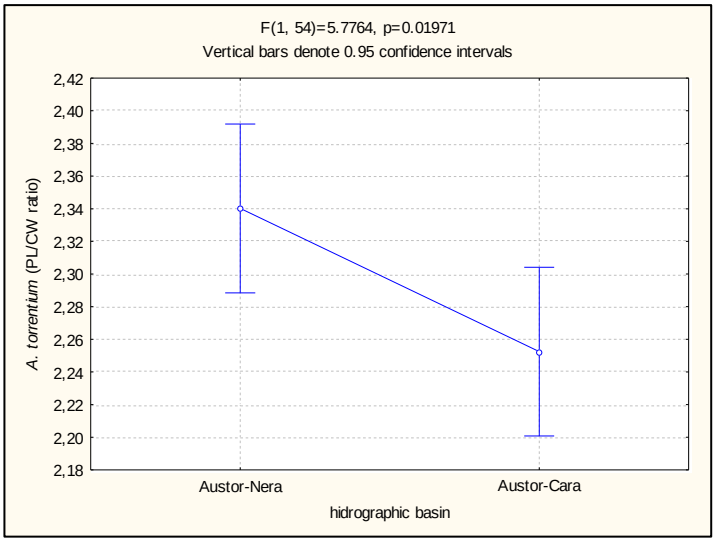

Fig. 4. ANOVA tests for the male specimens of de *A. torrentium* from Nera and Caraş hydrographic, for the ratio PL/CW

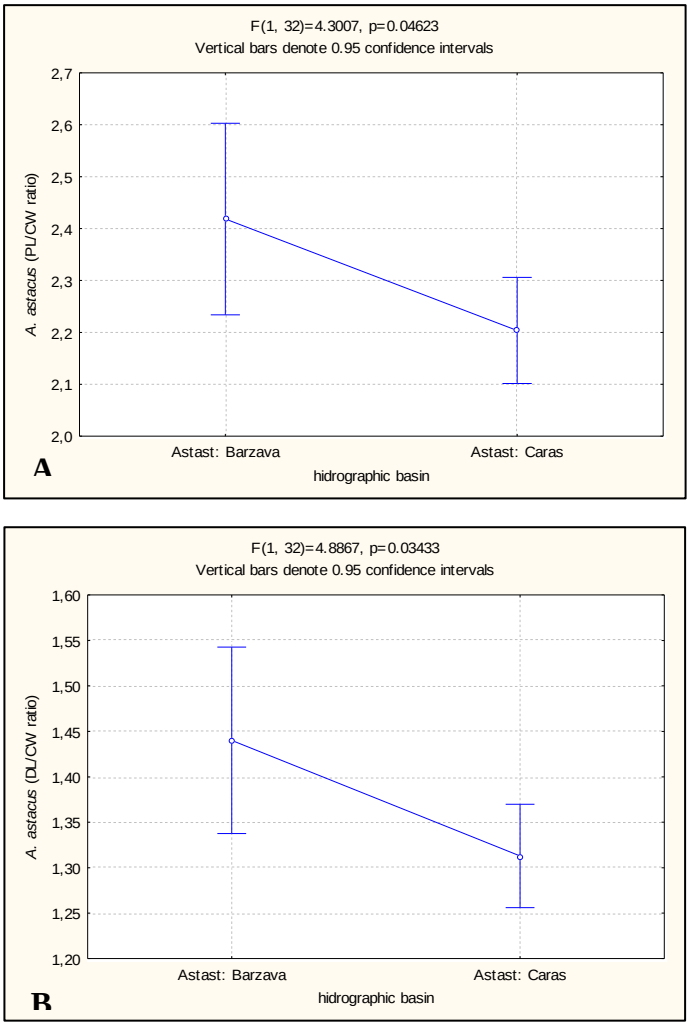

Fig. 5. ANOVA tests for the female specimens of *A. astacus* from the Bârzava and Caraş hydrographic basins: **A** –for the ratio PL/CW; **B** –for the ratio DL/CW

The *A. astacus* males analyzed in the Bârzava basin have been captured in a much smaller number, impossible to analyze statistically.

Discussions

Taking into account the obtained results, we can formulate several sentences regarding the biometric aspects observed in the measured specimens during the summer campaigns of 2008 and 2009 in the Anina Mts.

>For *Austropotamobius torrentium*

1. The maximum dimension of the specimens regarding total length (TL) varies between similar limits for males and females: the largest male specimen has a total body length of 94.00 mm, while the largest female has a total length of 93.34 mm. In comparison with the results existing in the literature the size of the biggest male is with 11.9% larger, while the size of the female is with 16.75% larger the than those measured by Papadopol and Diaconu (1987), on a population from the Nera hydrographic basin (on the Şuşara river).

2. The body characteristics that have registered the greatest differences between the sexes proved to be the parameters of the chelas: the propodus length (PL) being 24.57% smaller for the females than for the males, the dactylus length (DL) being 23.33% smaller for females than for males and the chela width (CW) being 22.98% smaller for the female population than for the male population

3. The average values that have turned out to be higher for the male population are the total length (TL), the cephalothorax length (CTL), the rostrum length (RL), the maximum thoracic width (mTW) and the telson width (TW). For the second abdominal segment width (2AW), the average value of the measured results favors the female population.

>For *Astacus astacus*

1. The maximum dimension of the total length (TL) favors the male population, the largest specimen measuring 127.34 mm, whereas the largest female measured 108.80 mm. In comparison with the results existing in the literature, the size of the larger male is with 2.79%, more reduced, while the size of the female is with 2.85% more reduced than those measured by Papadopol and Diaconu (1987) on a population from the north-eastern part of Romania (from the Bicazu Lake).

2. The body characteristics that have registered the greatest differences between sexes turned out to be the cephalothorax length (CTL) which was 16.47% smaller for the females than for the males, the maximum thoracic width (mTW) being 19.36% smaller for the females than for the males, as well as the parameters of the chelas, namely the propodus length (PL) which is 35.58% smaller for the females than for the males, the dactylus length (DL) which is 31.62% smaller for the female population than for the male population and the chela width (CW) which proved to be 29.71% smaller for females than for males.

3. All the average values measured are larger for the male population in comparison to the female population even for the second abdominal segment width where, due to the eggs, the females should be larger.

Conclusions

Concerning the difference between the populations studied in the Anina Mountains, the *A. torrentium* populations present high significantly biometric differences

between Caraş and Nera hydrographic basins. A possible explanation for the current situation can be represented by the geographical separation. Is known that *A. torrentium* occupies entirely the Nera hydrographic basin and populates only two creeks of Caraş basin.

The difference between the *A. astacus* populations, we can ascertain that the populations are significantly different in the Caraş basin as opposed to the ones measured in the Bârzava basin. In the case of the Bârzava hydrographic basin, and due to the heterogeneity of the populations, we can assume that a restocking in the area of the barrier lakes can be accomplished, probatory documents still have not yet been found.

ACKNOWLEDGMENTS

This study was funded by CNCSIS - Exploratory research projects PCE-4 grant no 1019/2008 „The stone crayfish (*Austropotamobius torrentium*), distribution in Romanian habitats, ecology and genetics of populations". I would like to take this opportunity to give my regards to the Administrators of the Cheile Nerei-Beuşniţa and of the Semenic-Cheile Caraşului National Parks for having facilitated my access to the region; to The Department of The Chemistry, Biology and Geography Faculty within the West University Timişoara for providing me with the topographical maps.

REFERENCES

Burba, A., Vaitkute, N., Kaminskienè, B. (1999): Morphometrics of crayfish species and relationship to the trophic level of waterbodies. *Freshwater Crayfish* **12**: 98-106.

Ďuriš, Z., Drozd, P., Horká, I., Kozák, P., Policar, T. (2006): Biometry and demography of the invasive crayfish *Orconectes limosus* in the Czech Republic. *Bulletin Français de la Pêche et de la Pisciculture* **380-381**: 1215-1228.

Gutiérrez-Yurrita, P.J., Ilhéu, M., Montes, C., Bernardo, J. (1996): Morphometrics of red swamp crayfish from a temporary Marsh (Doñana National Park, Sw. Spain) and temporary stream (Pardiela Stream, S. Portugal). *Freshwater Crayfish* **11**: 384-393.

Papadopol, M., Diaconu, G. (1987): Contributions to the knowledge of the morphology of the Astacid Crayfishes from Romania. *Travaux du Muséum d'Histoire naturelle "Grigore Antipa"* **29**: 55-62

Pârvulescu, L. (2009a) The epigean freshwater malacostracans (Crustacea: Malacostraca) of the rivers in the Anina Mountains (SW Romania). *Studia Universitatis Babeş – Bolyai, seria Biologia* **54** (1): 3-17

Pârvulescu, L. (2009b): Traditional laundry becomes crayfish killer (Cândeni case study). *Crayfish news* **31** (1): 5-6

Pârvulescu, L. (2009c) *Ghid ilustrat pentru identificarea speciilor de raci din România*. Editura Universității din Oradea, Oradea, 28 pp.

Pârvulescu, L., Petrescu, A., Petrescu, I. (2009): Abnormal colors and shapes of the body and the appendages of *Austropotamobius torrentium* (Schrank, 1803) in Romania. *Crayfish News* **31** (3): 6-8

Sencu, V. (1978) *Munții Aninei*, Editura Sport-Turism, București

Streissl, F., Hödl, W. (2002) Growth, morphometrics, size at maturity, sexual dimorphism and condition index of *Austropotamobius torrentium* Schrank. *Hydrobiologia* **477**: 201-208

Ujvari, I. (1972) *Geografia apelor României*, Editura Ştiințifică, Bucureşti

STUDIA UNIVERSITATIS BABEŞ – BOLYAI, BIOLOGIA, LV, 1, 2010, p. 17-30

STRUCTURE AND DYNAMICS OF PREDATOR MITE POPULATIONS (ACARI-MESOSTIGMATA) IN SHRUB ECOSYSTEMS IN PRAHOVA AND DOFTANA VALLEYS.

MINODORA MANU[1]

SUMMARY. The researches of the edaphic predator mite's fauna (Acari-Mesostigmata), were made in three shrubs ecosystems: Nistoreşti and Cornu in Prahova Valley and Lunca Mare in Doftana Valley. 29 species were identified. Each studied area was characterized by a different number of species and numerical density. The relative soil humidity and the type of vegetation, specifically for each shrub ecosystems, influenced the monthly dynamics of the mite populations and their distribution on the soil layers.

Keywords: Acari, mite, populations, shrub ecosystem

Introduction

Similar to other soil mesofauna, population development of Mesostigmata is very much influenced by microclimate, which depends on the structure of the herbaceouas plants, shrubs or trees and on the litter layer (Koehler, 2000; Sadaka and Ponge, 2003; Minor and Norton, 2004; Ruf and Beck, 2005; Ilieva-Makulec *et al*., 2006; Lindberg and Bengtsson, 2006; Bradforda *et al.*, 2007; Salmane and Brumelis, 2008). The soil is their preffered habitat and the dynamics is influenced by different abiotical factors (temperature, pH, humidity, altitude) and by the abundance and quality of the food source (Bowman, 1987; Nielsen, 1999; Halaja *et al*., 2005; Berg and Bengtsson, 2007; Bullinger-Weber *et al*., 2007; Heckmann *et al*., 2007; Lenoir *et al*., 2007). Mesostigmata mites do not change soil structure or plant productivity directly. However, as predators, they influence population dynamics of the other organisms and thereby have an indirect effect on overall ecosystem performance (Koehler, 1999; Ruf and Beck, 2005; Salamona *et al*. 2006).

Studies on the dynamics of the predator mite populations are made especially in forests. Species number varies from 15 in undisturbed open grasslands or shrubs to 25 in ruderal sites and 30-40 in forests (Skorupski, 1997, 2001; Ruf,

[1] *Romanian Academy, Institute of Biology, Department of Ecology, Taxonomy and Nature Conservation, street Splaiul Independenţei, no. 296, code 0603100, PO-BOX 56-53, fax 040212219071, tel. 040212219202, Bucharest, Romania, E-mail address: minodora_stanescu@yahoo.com*

1998; Cortet, 2002; Ruf *et al*., 2003; Hemerik and Brussaard, 2002; Gwiazdowicz and Klemt, 2004; Gwiazdowicz and Kmita, 2004 ; Stănescu and Gwiazdowicz, 2004; Colemana and Whitman, 2005; Seebera *et al*., 2005; Stănescu and Juvara-Balş, 2005; Moraza, 2006, 2007). There are also differences in the abundance of mites among different habitats: their density can be as high as 2000 ind./sq.m. in shrubs, 10000 ind./sq.m. in undisturbed meadows, and even 50000 ind./sq.m. in forests. Studies concerning the structure and dynamics of the soil mite populations (Mesostigmata) are many, in our country as well as in Europe, and were made in different types of habitats (Georgescu, 1981; Solomon, 1985; Skorupski, 1997, 2001; Ruf, 1998; Koehler, 1999, 2000; Salmane, 1999, 2000, 2001; Gwiazdowicz and Szadkowski, 2000; Madej, 2000; Honciuc and Stănescu, 2003; Masan, 2003; Ruf *et al*., 2003; Stănescu and Gwiazdowicz, 2004; Masan and Fenda, 2004; Falcă *et al.*, 2005; Moraza, 2006, 2007; Stănescu and Honciuc, 2006; Gwiazdowicz, 2007; Manu, 2009; Skorupski *et al*., 2009). In Romania, there are few studies on the spatial and temporal dynamics of the mite populations in shrub ecosystems in hilly areas (Paucă Comănescu *et al*. 2000, 2004, 2005, 2008; Honciuc and Manu, 2008; Manu, 2008). Therefore any research regarding this specific habitat could offer important scientific information .

Material and Methods

The study was conducted in 2006, in three different shrub habitats in three localities in Doftana Valley (Lunca Mare village) and Prahova Valley (Cornu and Nistoreşti villages).

The ecosystem from Lunca Mare is an alluvial shrub, characteristic for a hilly-montain area, with *Salix purpurea* (R 4418) (Doniță *et al*., 2005). It is situated at N 45º 20’ 40,1” and E 025º 74’ 51,3”, at 485 m a.s.l., on a flat surface. The soil is sandy-clay, with an increased humidy. The plant association is *Saponario – Salicetum purpurea* (Br.-Bl. 1930). The dominant species of arbustive plants are: *Salix purpurea, Cornus sanguinea, Ligustrum vulgare, Rubus caesius.*

The ecosystem from Cornu is an alluvial shrub, characteristic for a hilly-montain area, with *Salix pupurea* (R 4418) (Doniță *et al*., 2005). It is situated at N 45º 10’ 24,6” and E 025º 42’ 37,6”, at 440 m a.s.l., in a flat surface. The alluvial sandy – clay soil has an incresead humidity. The plant association is *Saliceto (eleagni) – Hippophaëtum* Br.-Bl.et Volk 1940. The dominant plants are: *Salix purpurea, Frangula alnus, Cornus sanguinea, Ligustrum vulgare, Viburnum opulos* and *Viburnum lantana.*

The ecosystem from Nistoreşti is alluvial shrub with *Hippophaë rhamnoides, Salix eleagnos* (R 4417) (Doniță *et al*., 2005). It is situated at N 45º 10’ 03,8” and E 025º 41’ 23,6”, on 510 m altitute, in a plane surface. The alluvial soil has an incresead humidity. The vegetal association is *Saliceto (eleagni) – Hippophaëtum* Br.-Bl.et Volk 1940. The dominant plants are: *Hippophaë rhamnoides, Salix purpurea, Cytisus nigricans, Ligustrum vulgare*.

Soil samples were collected randomly. Ten samples from these areas were collected with MacFadyen soil core (5 cm diameter), up to 10 cm deep, on three layers: litter and fermentation (L),humus (S_1), soil (S_2). The extraction was performed with a modified Berlese-Tullgren extractor, in ethylic alcohol and the mite samples were clarified in lactic acid. The identification of the mites from the Mesostigmata order was carried out to the species level (Gilarov and Bregetova, 1977; Hyatt, 1980; Karg, 1993; Masan and Fenda, 2004).

The statistical analysis was performed with MS Office Excel 2007. The parameters studied were numerical density (no.indiviuals/sq.m.), relative abundance (A%) and Shannon- Wiener diversity index (HS).

The humidity of soil was measured (Table 1).

Table 1.

Average of relative humidity of soil (%) recorded in 2006.

Soil level (cm)	Cornu	Nistoreşti	Lunca Mare
0-10	27.38 ± 1.42	22.56 ± 5.94	34.44 ± 1.32
10-20	19.13 ± 7.61	22.39 ± 5.72	19.05 ± 1.11
20-30	20.21 ± 2.15	18.13 ± 6.18	12.61 ± 2.36
30-40	22.28 ± 0.28	20.52 ± 8.12	18.44 ± 0.89
Average	**22.25** ± 0.94	**20.98** ± 6.49	**21.14** ± 0.21

Results and Discussions

The identification of collected material revealed the presence of 29 species of predatory mites (Acari: Mesostigmata) belonging to the following families: Parasitidae, Veigaidae, Rhodacaridae, Macrochelidae, Pachylaelaptidae, Laelaptidae, Eviphididae, Zerconidae, Trachytidae, Uropodidae. The highest species number was recorded at Nistoreşti (17 species), while the other sites had lower species numbers (Cornu -15 species, Lunca Mare -13 species). The common species identified for the three ecosystems were: *Lysigamasus lapponicus, Veigaia nemorensis, Zercon triangularis, Trachytes aegrota* and Uropoda sp. (Table 2).

Making a comparative analysis of the annual numerical densities from the studied ecosystem, we can remark that the most increased values were recorded at Cornu and Nistoreşti (7900 ind./sq.m. and 7800 ind./sq.m.) and at Lunca Mare the most decreased value (6400 ind./sq.m.). In temporal dynamics, a comparison of this parameter showed that at Lunca Mare, the lowest values were obtained in May and the highest in August.

Table 2.

Mite species identified in studied ecosystems

Species	Lunca Mare	Cornu	Nistoreşti
Lysigamasus sp.	+		
Lysigamasus lapponicus Tragardh, 1910	+	+	+
Lysigamasus neoruncatellus Schweizer, 1961	+		
Leptogamasus tectegynellus Athias-Henriot, 1967		+	
Leptogamasus parvulus Berlese, 1903			+
Eugamasus magnus Kramer, 1876		+	
Veigaia nemorensis C.L.Koch, 1839	+	+	+
Veigaia exigua Berlese, 1917	+		+
Veigaia transisalae Oudemans, 1902			+
Rhodacarellus silesiacus Willmann, 1936		+	
Asca aphidoides Linne, 1758		+	
Asca bicornis Caneastrini and Fanzago, 1887			+
Hypoaspis miles Berlese, 1892	+		+
Hypoaspis aculeifer Caneastrini, 1883	+	+	
Geholaspis mandibularis Berlese, 1904	+		+
Macrocheles carinatus C.L.Koch, 1839	+		
Macrocheles decoloratus C.L.Koch, 1839		+	+
Macrocheles montanus Willmann, 1951		+	+
Pachylaelaps furcifer Oudemans, 1903			+
Olopachys suecicus Sellnick, 1950			+
Eviphis ostrinus C.L. Koch, 1836			+
Zercon triangularis C.L.Koch, 1836	+	+	+
Zercon peltatus C.L.Koch, 1836	+		+
Prozercon sellnicki Schweizer, 1948			+
Prozercon traegardhi Halbert, 1923		+	
Trachytes aegrota C.L.Koch, 1841	+	+	+
Uropoda sp.	+	+	+
Dynichus sp.		+	

The decreased numerical structure in Lunca Mare (especially in May, after the snow was melted) is due to the flood period, which affected the habitat of these predator mites (the organic matter, where they find the food). The temporal evolution

of the numerical densities was different in the other ecosystems. At Cornu, in autumn, the predator mites had a favourable evolution, in comparison with spring, when was recorded a decreasing of the population. In ecosystems from Nistoreşti, in spring and autumn months, due to the favourable bioedaphical conditions (more increased humidity), the gamasid populations increased their number of individuals. In august they decreased considerable (Fig. 1.).

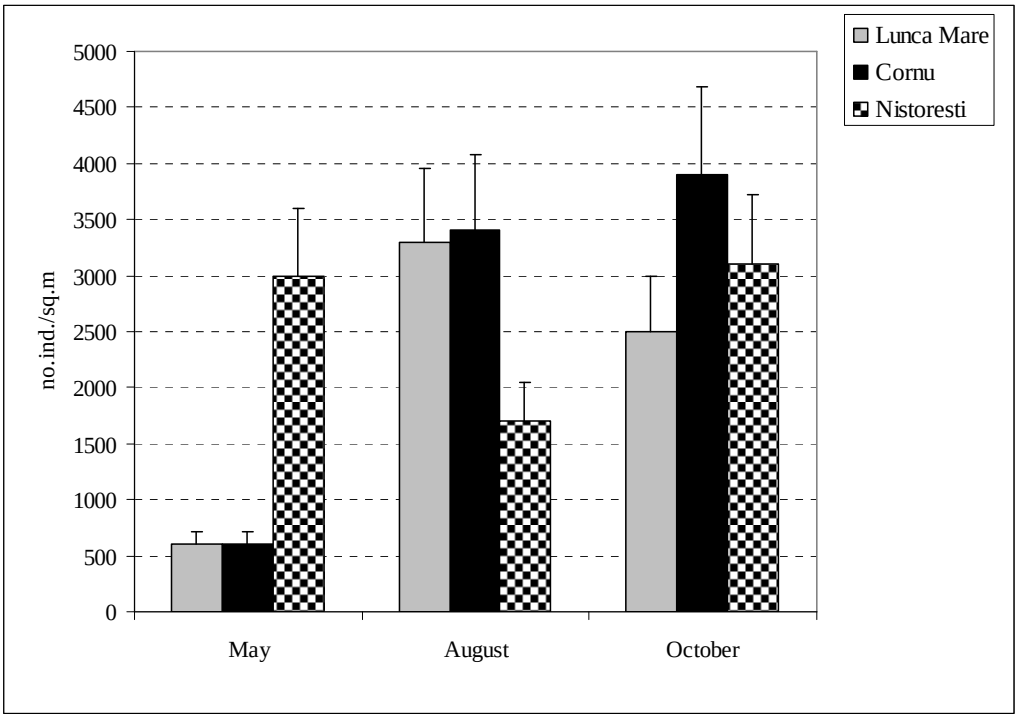

Fig. 1. Numerical densities of the mite's populations from the studied ecosystems.

Taking account of the soil levels, on the litter and fermentation layer, where were recorded the highest values of the humidity (between 27,38%-35,95%), the predator mite's populations had the most increased numerical densities, in all studied areas. The litter and fermentation layer through broken up structure, provided development of the gamasids in better conditions, in comparison with humus and soil layer. In the soil level (S_2) were identified the most decreased number of individuals, with exception of the ecosystem from Lunca Mare. (Fig. 2.).

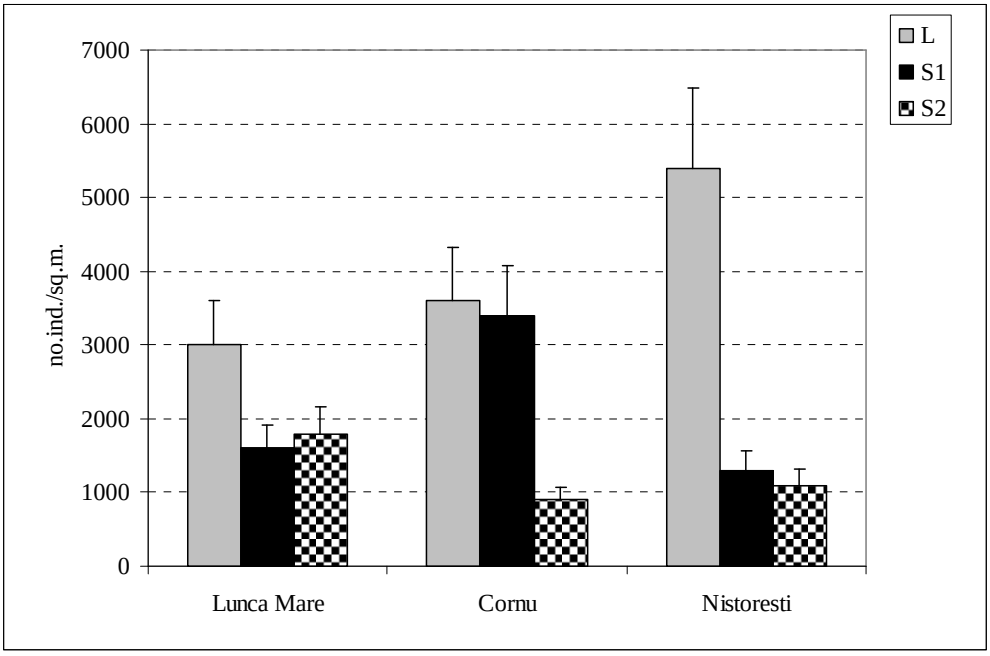

Fig. 2. The numerical densities of the mite's populations from the soil layers of the studied ecosystems.

In this area, the 13 identified species had a total numerical density by 6400 ind./sq.m. To this value a great contribution was brought by the following species: *Veigaia nemorensis*, *Geholaspis mandibularis*, *Hypoaspis aculeifer* and *Trachytes aegrota* (Fig. 3.).

Geholaspis mandibularis is a higrophilous species, which had a wide ecological tolerance, ocurring varied habitats (as litter, humus, detritus, moss, lichens, ant-hills). *Macrocheles carinatus* is a euritopic species, although apparently hygrophilous, it also survive in substrates soaked with water (as inundation zones of flows) (Masan, 2003; Schmolzer, 1995).

In spatial dynamics, at Lunca Mare, in the litter and fermentation layer were recorded the highest values of the numerical densities, in comparison with humus and soil, where these values were more decreased, although the number of identified species doesn't vary too much. The first layer of the soil is a proper habitat for development of other invertebrates (springtails, nematods, enchytreids, etc), which are the food source for the gamasids (Walter and Proctor, 1999). Analysing the temporal dynamics of the species diversity and numerical structure, was showed that in august were recorded the highest values and in may, the smaller ones (Fig. 4) (Table 3).

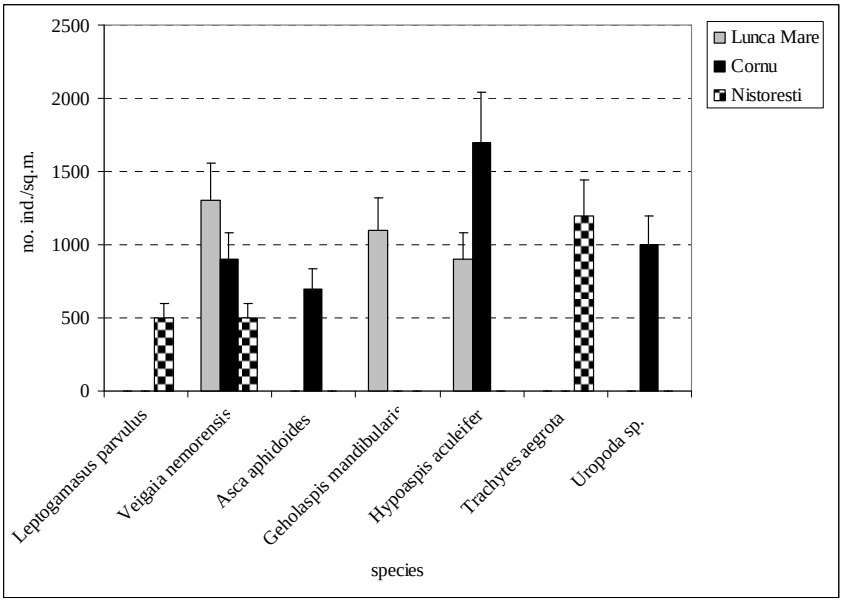

Fig. 3. The numerical densities of the dominant mites in studied ecosystems.

Table 3.

Species diversity (Shannon - Wiener index) of the identified mites species in studied ecosystems

Ecosystem	May	August	October	Annual
Lunca Mare	2.25	2.82	2.61	3.23
Cornu	1.37	3.47	2.85	3.29
Nistoreşti	2.73	3.2	2.78	3.75

In ecosystem from Cornu were identified 15 species, with 7900 ind./sq.m. In humus layer was recorded the most increased number of species, than in litter and fermentation layer and in the last was the soil layer. The humus, which had a reach content of organic matter, action as a trophical additional substratum, determining by its structure an increasing of the species number, providing to the mites optimal environmental conditions.

In temporal dynamics was obtained a high specific diversity in august and a small one in may. From the numerical density point of view, the most favourable evolution of the mite populations was in october and the less propitious in may. In autumn, developing of the litter and fermentation layer is faster, this habitat being prefered by the majority of descomposer invertebrates from soil-trophic source for gamasids (Fig. 5.) (Table 3).

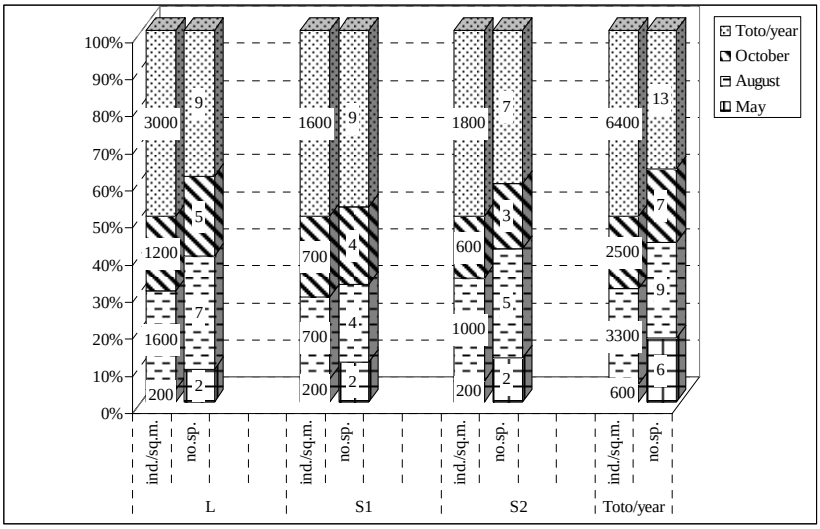

Fig. 4. The numerical densities and the number of species of the mite's, in soil layers in ecosystem from Lunca Mare.

The dominant species were: *Veigaia nemorensis*, *Asca aphidoides*, *Hypoaspis aculeifer* and Uropoda sp. (Fig.3).

These are in majority predator species (as *Veigaia nemorensis, Asca aphidoides*) and poliphagous (as *Hypoaspis aculeifer),* (Buryn and Brandl, 1992; Karg, 1993; Walter and Proctor, 1999). *Veigaia nemorensis* and *Hypoaspis aculeifer* are very spread species, occuring various habitats and their populations are characterised by a high number of individuals (Salmane, 1999, 2001). The small dimension of the species *Asca aphidoides* (310 µm) allows its to migrate in soil till 20 cm depth, being able to survive in unfavourable environmental conditions (soil without organic matter, very decreased humidity – till 16%, high temperature) (Koehler, 1999; Gwiazdowicz,2007).

In ecosystem from Nistoreşti, the mesostigmatid species (17) recorded a total numerical density of 7.800 ind./sq.m. The most increased values of this parameter were obtained by the following predator species: *Leptogamasus parvulus*, *Veigaia nemorensis*, *Trachytes aegrota*, with exception of the last one, which is fungivorous. Their dynamics depends directly of the food availability and indirectly of the environmental factors (Koehler, 1999) (Fig. 3.). On the edaphon level, in the first layer was identified most increased number of species and individuals, in comparison with humus and soil layers, where the values of these parameters were more decreased.

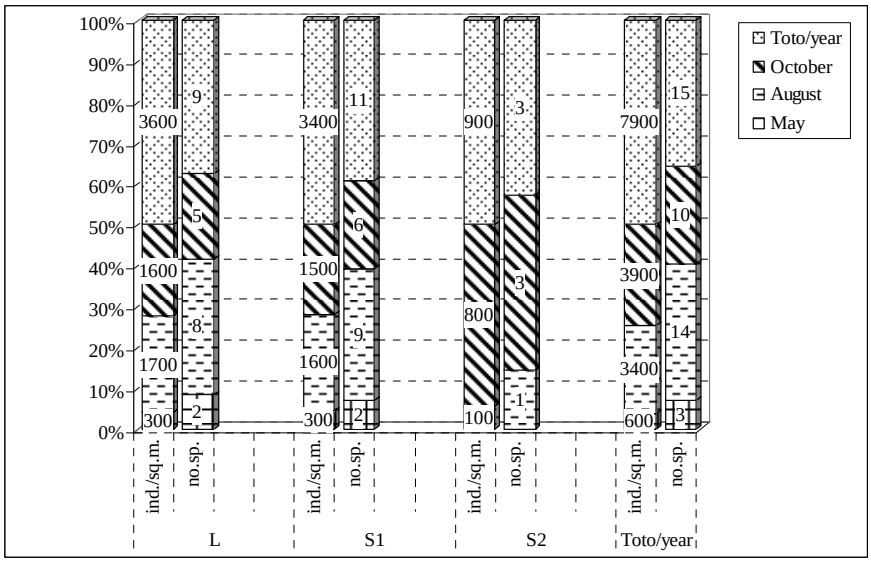

Fig. 5. The numerical densities and the number of species of the mites, in soil layers in ecosystem from Cornu.

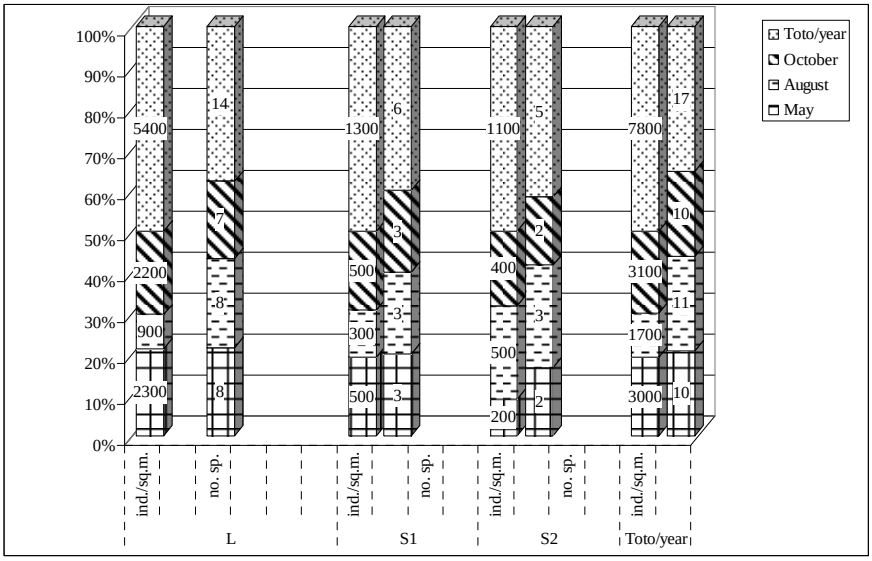

Fig. 6. The numerical densities and the number of species of mites, in soil layers in ecosystem from Nistoreşti.

The monthy analysis of the total numerical density showed that in october was recorded the highest value, very closed to that from may, when due to the development of the litter-fermentation layer and to a more increased soil humidity, the mite's populations had a favourable evolution. The bioedaphical condition from august determined the increase of the species diversity and a decrease of the numerical density, in the same time (Fig. 6.) (Table 3.).

All these structural and dynamical differences of the predator mite populations were due to the specific vegetation and to soil humidity, characteristic for each studied area.

REFERENCES

Bradforda, A.M., Eggersb, T., Newingtonc, J.E., Tordoff, G. (2007) Soil faunal assemblage composition modifies root in-growth to plant litter patches, *Pedobiologia*, **50,** 505—513.

Berg, M.P., Bengtsson, J. (2007) Temporal and spatial variability in soil food web structure, *Oikos*, **116** (11), 1-16.

Bowman, C.E. (1987) Studies on Feeding in the Soil Predatory Mite *Pergamasus longicornis (Berlese)* (Mesostigmata:Parasitidae) Using Dipteran and Microarthropod Prey, *Experimental & Applied A carology*, **3**, 201-206.

Bullinger-Weber, G., Le Bayon, R.C., Guenat, C., Gobat, J.M. (2007) Influence of some physicochemical and biological parameters on soil structure formation in alluvial soils, *European Journal of Soil Biology*, **43**, 57-70.

Buryn, R., Brandl, R. (1992) Are the morphometrics of chelicerae correlated with diet in mesostigmatid mite's (Acari)?, *Exp.Appl.Acarol*. **14** (1),67-82.

Colemana, D.C., Whitman, W.B. (2005) Linking species richness, biodiversity and ecosystem function in soil systems, *Pedobiologia*, **49,** 479—497.

Cortet, J., Ronce, D., Poinsot-Balaguer, N., Beaufreton, C., Chabert, A., Viaux, P., Cancela de Fonseca, J.P. (2002) Impacts of different agricultural practices on the biodiversity of microarthropod communities in arable crop systems, *European Journal of Soil Biology*, **38,** 239−244.

Doniță, C., A. Popescu, M. Paucă Comănescu, S. Mihăilescu, I. Biriş (2005) *Habitatele din România*, editura Tehnică Silvică, Bucureşti, pp. 271.

Falcă, M., Vasiliu, Oromulu, L., Sanda, V., Paucă, Comănescu, M., Honciuc, V., Sanda, M., Purice, D., Dobre, A., Stănescu, M., Onete, M., Biță, Nicolae, C., Ivanescu, C., Șincu, E. D. (2005) The Study of Preliminary and Secondary Producers from Some Alder Depression Forests of the Plain Zone, *Proceedings of the Institute of Biology*, 7, 33-49.

Georgescu, A. (1981) Fauna de Gamasidae (Acarieni) din unele soluri din Munții Bihor, *Crisia*, **25**, 503-513.

Gilarov, M.S., N.G. Bregetova (1977) *Opredeliteli Obitaiuscih v Pocive Clescei, Mesostigmata*, isdatelistvo "Nauka", Leningratkoe, Otdelenie, Leningrad, pp 717.

Gwiazdowicz, D.J., Szadkowski, R. (2000) Mites (Acari, Gamasina) of the Narew National Park, *Fragmenta Faunistica*, 43 (1-8), 91-95.

Gwiazdowicz, D.J., Klemt, J. (2004) Mesostigmatic mites (Acari, Gamasida) in selected microhabitats of the Biebrza National Park (NE Poland), *Biol. lett*., **41(1),** 11-19.

Gwiazdowicz, D., Kmita, M. (2004) Mites (Acari, Mesostigmata) from selected microhabitats of the Ujscie Warty National Park, *Acta Scientiarum Polonorum, Silv. Calendar.Rat. Ind. Lignar.*, **3**(2), 49-55.

Gwiazdowicz, D.J. (2007) *Ascid mite's (Acari, Mesostigmata) from selected forest ecosystems and microhabitats in Poland*, Wydawnictwo Akademii Rolniczej Im. Augusta Cieszkowskiego w Poznan, pp. 247.

Halaja, J., Peckb, R.W., Niwa, C.G. (2005) Trophic structure of a macroarthropod litter food web in managed coniferous forest stands: a stable isotope analysis with d15N and d13C, *Pedobiologia*, **49,** 109—118.

Heckmann, L.H., Ruf, A., Nienstedt, K.M., Krogh, P.H. (2007) Reproductive performance of the generalist predator *Hypoaspis aculeifer* (Acari: Gamasida) when foraging on different invertebrate prey, *Applied soil ecology,* **36,** 130 – 135.

Hemerik, L., Brussaard, L. (2002) Diversity of soil macro-invertebrates in grasslands under restoration succession, *European Journal of Soil Biology,* **38,** 145−150.

Honciuc, V., Stănescu, M. (2003) *Acari Fauna (Mesostigmata; Prostigmata; Oribatida) from Piatra Craiului National Park,* In Researches in Piatra Craiului National Park I, pp. 159-170.

Honciuc, V., M. Manu, (2008) Taxonomia şi ecologia populaţiilor de acarieni edafici (Arachnida, Acari) din tufărişurile de pe Valea Prahovei şi Valea Doftanei. In*: Volumul Lucrărilor Conferinţei Naţionale de Ecologie: ˝Protecţia şi Restaurarea Bio şi Ecodiversităţii",* Editura Ars Doncenti, pp.19-23**.**

Ilieva-Makulec, K., Olejniczak, I., Szanser M. (2006) Response of soil micro- and mesofauna to diversity and quality of plant litter, *European Journal of Soil Biology,* **42,** S244–S249.

Hyatt, K.H. (1980) Mite's of the subfamily Parasitinae (Mesostigmata: Parasitidae) in the British Isles, *Bulletin of the British Museum, Zoology series,* **38** (5), 237-378.

Karg, W. (1993) *Acari (Acarina), Milben Parasitiformes (Anactinochaeta) Cohors Gamasina Leach*, **59,** 1-513.

Koehler, H.H. (1999) Predatory mite's (Gamasina, Mesostigmata), *Agriculture, Ecosystems and Environment* **74**, 395-410.

Koehler, H.H. (2000) Natural regeneration and succession. Results from a 13 years study with reference to mesofauna and vegetation, and implications for management, *Landscape and Urban Planning,* **51,** 123-130.

Lenoir, L., Persson, T., Bengtsson, J., Wallander, H., Wirén, A. (2007) Bottom–up or top–down control in forest soil microcosms? Effects of soil fauna on fungal biomass and C/N mineralization, *Biol Fertil Soils,* **43,** 281–294.

Lindberg, N., Bengtsson, J. (2006) Recovery of forest soil fauna diversity and composition after repeated summer droughts, *Oikos*, **114**, 494-506.

Madej, G. (2000) Gamasina (Arachnida, Acari) of the Sonsk Nature Reserve, *Biological Bulletin of Poznan*, **37**(2), 287-298.

Manu, M. (2008) The influence of some abiotical factors on the structural dynamics of the predatory mite populations (Acari: Mesostigmata) from an ecosystem with *Myricaria germanica* from Doftana Valley (Romania), *Trav. Mus.Nat. D'Hist. Nat."Grigore Antipa"*, **51,** 463-471.

Manu, M. (2009) Ecological research on predatory mite populations (Acari: Mesostigmata) in some Romanian forests, *Biharean Biologist*, **3** (2), 110-116.

Masan, P. (2003) *Macrochelid mite's of Slovakia (Acari, Mesostigmata, Macrochelidae)*, Institute of Zoology, Bratislava, Slovak Academy of Science, pp.149.

Masan, P., Fenda, P. (2004) *Zerconid mite's of Slovakia (Acari, Mesostigmata, Zerconidae),* Institute of Zoology, Bratislava, Slovak Academy of Science, pp.238.

Minor, A.M., Norton, R. (2004) Effects of soil amendments on assemblages of soil mites (Acari: Oribatida, Mesostigmata) in short-rotation willow plantings in central New York, *Can. J. For. Res*., **34,** 1417–1425.

Moraza, M. L. (2006) Efecto de la degradación de un encinar de *Quercus rotundifolia* en la comunidad de ácaros cryptostigmados y mesostigmados (Acari: Cryptostigmata, Mesostigamata), *Revista Ibérica de Aracnología*, **13**, 171-182.

Moraza, M. L. (2007) Composicion, estructura y diversidad de la comunidad de acaros Mesostigmata de un hayedo natural (Fagus sylvatica) del sur de Europa, *Graellsia*, **63(1)**, 35-42.

Nielsen, P.S. (1999). The impact of temperature on activity andconsumption rate of moth eggs by *Blattisocius tarsalis* (Acari: Ascidae), *Experimental & Applied Acarology*, **23**, 149–157.

Paucă, Comănescu, M., Tăcină, A., Vasiliu, Oromulu, L., Honciuc, V., Falcă, M., Onete, M., Purice, D., Stănescu, M., Bujdea, V., Ionescu, M. (2000) Structure of the main biocenotic components in Tamarix shrublands of Prahova and Teleajen floodplain, *Rév. Roum. Biol.- Biol. Végét*., Bucharest, **45**(*2*):155-179.

Paucă, Comănescu, M., Dihoru, G., Onete, M., Vasiliu, Oromulu, L. Falcă, M. Honciuc, V., Stănescu, M., Purice, D., Matei, B. (2004) The diversity of some alluvial shrubland flora and fauna in the Neajlov Floodplain, *Proceedings of the Institute of Biology*, Bucureşti, Romanian Academy, **6**, 105-118.

Paucă, Comănescu, M., Stefănuț, S., Șincu, D., Vasiliu, Oromulu, L., Falcă, M. Honciuc, V., Stănescu, M., Purice, D., Fiera, C. (2005) Biodiversity of alluvial shrubs characteristic to the Câlnişţea River, *Proceedings of the Institute of Biology*, Bucureşti, Romanian Academy, **7,** 87-111.

Paucă, Comănescu, M., Onete, M., Honciuc, V., Vasiliu, Oromulu, L., Manu, M., Fiera, C., Purice, D., Falcă, M., Șincu, D., Ion, M. (2008) Structura unor componente biotice din tufărișurile aluviale colinare, In: *Volumul Lucrărilor Conferinței Naționale de Ecologie: ˝Protecția şi Restaurarea Bio şi Ecodiversității*", Editura Ars Doncenti, pp.165-170.

Ruf, A. (1998) A maturity index for predatory soil mites (Mesostigmata:Gamasina) as an indicator of environmental impacts of pollution on forest soils, *Applied Soil Ecology*, **9**, 447-452.

Ruf, A., Beck, L., Dreher, P., Hund-Rinke, K., Rombke, J., Spelda, J. (2003) A biological classification concept for the assessment of soil quality: "biological soil classification scheme", *Agriculture, Ecosystems and Environment*, **98,** 263-271.

Ruf, A., Beck, L. (2005) The use of predatory soil mite's in ecological soil classification and assessment concepts, with perspectives for oribatid mite's, *Ecotoxicology and Environment Safety*, **62** (2), 290-299.

Sadaka, N., Ponge, J.P. (2003) Soil animal communities in holm oak forests: influence of horizon, altitude and year, *European Journal of Soil Biology*, **39**, 197–207.

Salamona, J., Alpheib, J., Ruf, A., Schaeferb, M., Scheud, S., Schneiderd, K., Su¨hrigb, M., Maraund, M. (2006) Transitory dynamic effects in the soil invertebrate community in a temperate deciduous forest: Effects of resource quality, *Soil Biology and Biochemistry*, **38,** 209–221.

Salamane, I. (1999) Soil free living predatory Gamasina mite's (Acari, Mesostigmata) from the coastal meadows of Riga Gulf, Latvia, *Latvijas Entomologs*, **37,** 104-114.

Salmane, I. (2000) Investigation of the seasonal dynamics of soil Gamasina mite's (Acari: Mesostigmata) in *Pinaceum myrtilosum*, *Latvia Ekologia*, **19** (3), 245-252.

Salmane, I. (2001) A check list of Latvian Gamasina mite's (Acari, Mesostigmata) with short notes to their ecology, *Latvijas Entomologs*, **38,** 21-26.

Salmane, I., Brumelis, G. (2008) The importance of the moss layer in sustaining biological diversity of Gamasina mites in coniferous forest soil, *Pedobiologia*, **52,** 69-76.

Schmolzer, K., Neudorf, W. (1995*) Catalogus Faunae Austriae, teil IX, F. – U.- Ordn: Anactinochaetaa (Parasitiformes),* Verlag der Osterreichischen Akademie der Wissenschaften, pp.179.

Seebera, J., Seeberb, G.U.H., Ko¨sslera, W., Langeld, R., Scheu S., Meyer, E. (2005) Abundance and trophic structure of macrodecomposers on alpine pastureland (Central Alps, Tyrol): effects of abandonment of pasturing, *Pedobiologia*, **49,** 221—228.

Skorupski, M., (1997) Mesostigmata mites from soil habitats of the Pieninz National Park. *Abh. Ber. Naturkundemus., Gorliz*, **69**(2), 201-208.

Skorupski, M. (2001) Mite's (Acari) from the order gamasida in the Wielkopolski National Park, *Fragmenta Faunistica*, **44**, pp.129-167.

Skorupski, M., Butkiewicz, G., Wierzbicka A. (2009) The first reaction of soil mite fauna (Acari, Mesostigmata) caused by conversion of Norway spruce stand in the Szklarska Poręba Forest District, Journal of Forest Science, **55** (5), 234–243.

Solomon, L. (1985) The structure and biomass of the gamasidocenosis from a mountain forest ecosystem, *Analele Stiințifice ale Universității "Al. I. Cuza", Iași*, **31**,21-28.

Stănescu, M., Gwiazdowicz, D., J. (2004) Structure and dynamics of the Gamasina mite's (Acari-Mesostigmata) from a forest with *Picea abies* from Bucegi Massif, *Revue Roum. Biol*., **48** (1-2), 79-88.

Stănescu, M., Gwiazdowicz, D. (2004) Preliminary research on Mesostigmata mites (Acari) from a spruce forest in the Bucegi massif in Romania, *Acta Scientiarum Polonorum, Silv. Calendar.Rat. Ind. Lignar.,* **3**(2), 79-84.

Stănescu, M., Juvara- Balş, I. (2005) Biogeographical distribution of Gamasina mites from Romania (Acari-Mesostigmata), *Revue Roum Biol*., **50** (*1-2*): 57-74.

Stănescu, M., Honciuc, V. (2006) The taxonomical structure of the Epicriina and Gamasina mite's (Mesostigmata: Epicriina, Gamasina) from forestry ecosystems from Bucegi Massif, *Roumanian Journal of Zoology*, **52**, 33-41.

Walter, D.E., Proctor, H., C.(1999) *Mite's – Ecology, Evolution and Behavior. Unsw Press*, printed by Everbest Printing Hong-Kong, pp. 131.

STUDIA UNIVERSITATIS BABEŞ – BOLYAI, BIOLOGIA, LV, 1, 2010, p. 31-44

LEAF-BEETLES (COLEOPTERA, CHRYSOMELIDAE) FROM THE AREA BISTRIȚA BÂRGĂULUI- COLIBIȚA- PIATRA FÂNTÂNELE, A PART OF "NATURE 2000" CUŞMA SITE (NE ROMANIA)

ALEXANDRU CRIŞAN[1]

SUMMARY. A number of 68 leaf beetle species from 9 subfamilies and 32 genera were found in a research made in the North and North-Eastern parts of Cusma Nature 2000 Site, district of Bistrita-Nasaud (Romania). Two endemic species and other 24 rare ones were revealed. Chrysomelinae subfamily and the genera *Chrysolina, Longitarsus* and *Cassida* were the best represented ones. The hygrophilous herbs from Soimului de Sus valley was the habitat with the largest number of species, so as a mezzo-hygrophilous lawn in Piatra Fantanele. Some other habitats are important by their rare or endemic leaf beetle species.

Keywords: leaf-beetles, Cusma "Nature 2000" Site, species list, distribution in habitats

Introduction

Researches made in this area on leaf-beetles constitute a part of the works started by a research group, in order to substantiate the inclusion of the "Cuşma" site (Bistrița-Năsăud district, Romania) in the "Nature 2000" European Ecological Network. It represents the Northern and North-Eastern parts of the proposed site. At first, it were established the most representative habitats of the area, in some representative points: Bistrița Bârgăului river meadow, Popasul Șoimului (the falcon halt); Șoimului de Sus valley (all situated dawn stream of the Colibița barrage), than: Colibița-Mița zones, around the Colibița lake; the Toader's valley; the Dălbidan valley; the area Tăul Zânelor to Strănior glade; the area Piatra Fântânele to Vinului glade (the all situated upstream of the Colibița barrage). In these areas we checked forest habitats (beech forests, mixed forests with broad-leaved species, mixed forests with *Picea* and *Fagus*, pure spruce forests); river meadow habitats (alluvial forests with *Alnus* and *Salix* species, alluvial bushes and clearings); lawn habitats (river meadow lawns, sub-mountain and mountain lawns and hay-lands). No investigations

[1] *Faculty of Biology and Geology, Babes-Bolyai University of Cluj-Napoca, E-mail: acrisan@hasdeu.ubbcluj.ro*

on leaf-beetles group in the area are known in the specific Romanian literature (Bobârnac, 1974; Balog *et al*., 1997; Crişan,1993 a,b, 1994, 1995, 2004, 2006 a,b; Crişan and Teodor, 1994, 2003, 2005: Crişan and Bonea, 1995; Crişan and Druguş, 2001; Crişan *et al*., 1998, 1999, 2000, 2003; Fleck, 1905; Gruev *et al*., 1993; Ieniştea, 1968, 1974; Ieniştea and Negru, 1975; Ilie, 2001; Ilie and Chimisliu, 2000; Konnert-Ionescu, 1963, Maican and Serafim, 2001; Marcu, 1927, 1928, 1936, 1957; Negru, 1968, Negru and roşca, 1967; Roşca, 1973, 1974, 1976; Seidlitz, 1891; Szel *et al*., 1995).

Material and mMethods

The above-mentioned habitats were investigated during the summer 2008 and leaf-beetles adults were collected using an insect net. Barber traps were also positioned and monthly checked, in each type of habitat. Collected insects were put on 80% alcohol and kept dry till the identification made in the laboratory, using an appropriate literature (Kaszab, 1962-1971; Kippenberg and Doberl, 1994; Mohr, 1966; Panin, 1951; Petri, 1912; Rozner, 1996; Warkalowsky, 1993, 2003.)

Results and Discussion

In the table below we present, in taxonomical order, the leaf beetle species identified in the area Bistrița Bârgăului – Colibița – Piatra Fântânele, indicating also the date of collection, the number of caught individuals, the relative abundance, the place and the habitat in which the species were collected. We identified a number of 68 species of leaf beetles, from 9 subfamilies and 32 genera. It represents a great biodiversity of the group in the investigated area. More significantly, most of some common leaf beetle species, an important number of rare and endangered species were identified in the area, in almost each of the leaf beetle subfamilies. For these, the investigated area may constitute a good ecological refuge. From the species considered rare and endangered, comparing with the citations for other parts of the country (see the references!) we emphasize: *Donacia aquatica* şi *Plateumaris affinis* (Donaciinae), *Oulema erichsoni* (Criocerinae), *Cryptocephalus quinquepunctatus* and *Cryptocephalus biguttatus* (Cryptocephalinae), *Chrysolina rufa ssp.squalida, Chrysolina marcasitica, Chrysolina cuprina, Chrysolina lichenis, Oreina virgulata, Oreina bidentata, Hydrotassa marginella, Chrysomela collaris, Gonioctena quinquepunctata, Gonioctena interposita, Gonioctena intermedia* (Chrysomelinae), *Galerucella tenella* (Galerucinae), *Longitarsus rubellus, Longitarsus languidus, Asiorestia femorata, Sphaeroderma rubidum, Dibolia criptocephala, Dibolia chrysocephala, Psylliodes subaenea* (Halticinae), *Cassida stigmatica* (Cassidinae), so that as endemical ones: *Sclerophaedon carpathicus* and *Sclerophaedon carniolicus* (sin *Phaedon transsylvanicus*). The presence of these species arises the value of the zone as a protective and conservative area .

Table 1.

List of the leaf beetle species from the area Bistrița Bârgăului-Colibița- Piatra Fântânele a part of the Nature 2000, "Cusma" Site

Nr. Crt.	Subfamily/ species	Date	Nr. Ind.	Rel. ab. %	Place of capture/ habitat
	I. Donaciinae Kirby, 1837				
1	*Donacia (Donacia) aquatica* (Linnaeis, 1758)	30.07	1	0,19	-Tăul Zânelor, hyg. herbs
2	*Plateumaris (Juliusiana) affinis* (Kunze, 1818)	26.06	18	3,49	-Piatra Fântânele, hyg. herbs
3	*Plateumaris (Juliusiana) consimilis* (Schrank, 1781)	26.06 31.07	8 1	1,55 0,19	-Piatra Fântânele, mezo-hyg. veg. -Mița, Toader's valley, hyg. veg.
	II. Orsodacninae Thomson, 1859				
4	*Orsodacne cerasi* (Linnaeus, 1758)	26.06	1	0,19	-Piatra Fântânele, mezo-hyg. veg.
	III. Criocrinae Latreille, 1807				
5	*Oulema (Haspidolema) erichsoni* (Suffrian, 1841)	24.05	1	0,19	- Șoimului de sus, valley, association with *Coryllus*
6	*Oulema (Oulema) melanopus* (Linnaeus, 1758)	30.04	1	0,19	-Colibita, mez. lawn
	IV. Clytrinae Kirby, 1837				
7	*Labidostomis longimana* (Linnaeus, 1761)	26.06 30.07	1 1	0,19 0,19	-Piatra Fântânele, mez. mountain lawn -Colibița, S. of lake mez. lawn
8	*Smaragdina aurita* (Linnaeus, 1761)	22.05	1	0,19	-Colibița, river meadow on *Salix* sp.
	V. Cryptocephalinae Gyllenhal, 1813				
9	*Cryptocephalus (Cryptocephalus) quinquepunctatus* (Scopoli, 1763)	04.05	1	0,19	-Bistrița Bârgăului, river meadow herbs
10	*Cryptocephalus (Cryptocephalus) hypochoeridis* (Linnaeus, 1758)	26.06 29.07 30.07 30.07	50 7 2 12	9,69 1,35 0,38 2,32	-Piatra Fântânele, mez. lawn -Piatra Fântânele, mez. lawn -Tăul Zânelor, hyg. herbs -Colibița, S of lake, mez. lawn

Table 1. (continued)

Nr. Crt.	Subfamily/ species	Date	Nr. Ind.	Rel. ab. %	Place of capture/ habitat
11	*Cryptocephalus (Cryptocephalus) sericeus* (Linnaeus, 1758)	26.06	8	1,55	-Piatra Fântânele, mez. lawn
		29.07	2	0,38	- Piatra Fântânele, mez. lawn
		30.07	3	0,58	- Colibița, S of lake, mez. lawn
		30.07	3	0,58	-Popasul Șoimului, mez. lawn
		30.07	1	0,19	-Colibița, mez. lawn
12	*Cryptocephalus (Cryptocephalus) bipunctatus* (Linnaeus, 1758)	26.06	5	0,96	-Piatra Fântânele, mez. lawn
		29.07	1	0,19	-Piatra Fântânele, mez. lawn
		30.07	1	0,19	- Colibița, S of lake, mez. lawn
13	*Cryptocephalus (Cryptocephalus) moraei* (Linnaeus, 1758)	26.06	1	0,19	-Piatra Fântânele, mez. lawn
		30.07	5	0,96	- Colibița, S of lake, mez. lawn
14	*Cryptocephalus (Cryptocephalus) biguttatus* (Scopoli, 1763)	26.06	1	0,19	-Piatra Fântânele, mez. lawn
15	Cryptocphalus (Burlinius) bilineatus (Linnaeus, 1767)	22.05	1	0,19	- Șoimului de sus valley hyg. veg.
		30.07	2	0,38	- Colibița, S of lake, mez. lawn
	VI. Chrysomelinae Latreille, 1802				
16	*Leptinotarsa decemlineata*(Say, 1824)	24.06	1	0,19	- Șoimului de sus valley hyg. veg.
		26.06	1	0,19	-Piatra Fântânele, mez. lawn
17	*Chrysolina (Sphaerochrysolina) rufa* (Duftschmid, 1825*) squalida* (Suffrian, 1851)	01.05	6	1,16	- Șoimului de sus valley hyg. veg.
		24.05	19	3,68	- Șoimului de sus valley hyg. veg.
		22.05	2	0,38	- Șoimului de sus, valley, Barber trap
		22.05	3	0,58	-Popasul Șoimului, river meadow herbs
		22.05	1	0,19	-Popasul Șoimului, beech forest, Barber trap

Table 1. (continued)

Nr. Crt.	Subfamily/ species	Date	Nr. Ind.	Rel. ab. %	Place of capture/ habitat
18	*Chrysolina (Sphaeromela) varians* (Schaller, 1783)	01.05	1	0,19	- Șoimului de sus valley hyg. veg.
		24.05	2	0,38	- Șoimului de sus valley hyg. veg.
		25.06	1	0,19	-Colibița, mez. lawn Barber trap
		24.06	2	0,38	-Tăul Zânelor, hyg. veg.
		26.06	1	0,19	-Piatra Fântânele, mezo-hyg. veg.
		30.07	1	0,19	-Tăul Zânelor, hyg. veg.
		31.07	1	0,19	-Mița, Toader's, valley, hyg. veg.
		30.07	2	0,38	-Colibița, mez. lawn
19	*Chrysolina (Ovostoma) olivieri* (Bedel, 1892)	04.05	1	0,19	-Bistrița Bârgăului, river meadow herbs
		24.05	1	0,19	- Șoimului de sus valley hyg. veg.
		24.06	1	0,19	-Colibița, mez. lawn
20	*Chrysolina (Menthastriella) herbacea* (Duftschmid, 1825)	24.05	1	0.19	- Șoimului de sus valley, association with *Coryllus*
		24.06	10	1,93	- Șoimului de sus valley, hyg. veg.
21	*Chrysolina (Cyrtochrysolina) marcasitica* (Germar,1824)	28.05	2	0.38	- Șoimului de sus valley, Barber trap
22	*Chrysolina (Hypericia) cuprina* (Duftschmid 1825)	30.07	1	0,19	- Stegea valley, broad-leaved trees and bushes
23	*Chrysolina (Chrysolina) staphylea* (Linnaeus, 1758)	22.05	2	0.38	-Popasul Șoimului, river meadow herbs
24	*Chrysolina (Heliostola) lichenis* (Richter, 1820)	22.05	1	0,19	- Șoimului de sus valley, Barber trap
25	*Oreina (Allorina) caerulea* (Olivier, 1790)	01.05	1	0,19	-Șoimului de sus valley hyg. veg.
		24.05	12	2,32	-Șoimului de sus valley hyg. veg.
		25.06	3	0,58	-Colibița, mez. hay-land
		26.06	26	5,03	- Piatra Fântânele, mez. clearing
		29.07	1	0,19	- Piatra Fântânele, mez. clearing
26	*Oreina (Virgulatorina) virgulata* (Germar, 1824)	24.05	2	0.38	-Șoimului de sus valley, hyg. veg.

Table 1. (continued)

Nr. Crt.	Subfamily/ species	Date	Nr. Ind.	Rel. ab. %	Place of capture/ habitat
27	*Oreina (Intricatorina) intricata* (Germar, 1824)	04.05	1	0,19	-Bistrița Bârgăului, river meadow herbs
		23.05	1	0,19	-Bistrița Bârgăului, herbs, *Salix* sp.
		24.05	3	0,58	- Șoimului de sus valley, hyg. veg.
		25.06	3	0,58	-Colibița, mez. hay-land
		29.07	6	1,16	- Piatra Fântânele, mez. lawn
		30.07	7	1,35	- Colibița, S de lac, mez. hay-land
28	*Oreina (Allorina) bidentata* Bontems, 1981	24.06	6	1,16	- Șoimului de sus valley, hyg. veg.
29	*Gastrophysa viridula* (De Geer, 1775)	24.06	12	2,32	-Tăul Zânelor, herbs with *Rumex crispus*
		26.06	1	0,19	- Piatra Fântânele, mez. lawn
		30.07	12	2,32	-Tăul Zânelor, herbs with *Rumex crispus*
30	*Sclerophaedon carpathicus* Weise, 1875	26.06	64	12,4	- Piatra Fântânele, on *Caltha* sp., in pure spruce forest
		31.07	4	0,77	-Mița, Toader's valley, hyg. veg.
31	*Sclerophaedon carniolicus* (Germar 1824)	30.07	1	0,19	-Stegea valley, on *Caltha* sp. in broad-leaved trees and bushes
32	*Hydrotassa marginella* (Linnaeus, 1758)	24.06	1	0,19	-Tăul Zânelor, on submersible veg.
		31.07	2	0,38	-Mița, Toader's valley, submersible veg.
33	Plagiodera versicolora (Laicharting, 1781)	24.05	35	6,78	-Colibița, on *Salix* sp.
34	*Linaeidea (Linaeidea) aenea* (Linnaeus, 1758)	23.05	4	0,77	-Colibița, on *Salix*
		24.05	11	2,13	- Șoimului de sus valley, hyg. veg.
		22.06	3	0,58	- Șoimului de sus valley, hyg. veg.
		28.07	2	0,38	-Mița, alluvial forst with *Salix* and *Alnus* on Dălbidan valley
35	*Chrysomela (Pachylina) col*laris (Linnaeus, 1758)	23.05	1	0,19	-Colibița, on *Salix capraea*
36	*Chrysomela (Chrysomela) populi* Linnaeus, 1758	29.07	1	0,19	-Piatra Fântânele, on *Populus tremula*

Table 1. (continued)

Nr. Crt.	Subfamily/ species	Date	Nr. Ind.	Rel. ab. %	Place of capture/ habitat
37	*Gonioctena (Goniomena) quinquepunctata* (Fabricius, 1787)	24.05	1	0,19	- Şoimului de sus, valley, hyg. herbs and bushes
38	*Gonioctena(Goniomena)interposita* (Franz et Palmen 1950)	30.07	1	0,19	-Popasul Soimului, beech forest
39	*Gonioctena (Goniomena) intermedia* (Helliesen, 1913)	30.07	1	0,19	Popasul Soimului beech forest
40	*Phratora (Phratora) tibialis* (Suffrian, 1851)	24.05	1	0,19	- Şoimului de sus, valley on *Salix sp.*
41	*Phratora (Phratora) vitellinae* (Linnaeus, 1758)	24.06	1	0,19	- Şoimului de sus, valley on *Salix sp.*
42	*Phratora (Chaeroceta) vulgatissima* (Linnaeus, 1758)	23.05	4	0,77	-Colibița, on *Salix sp.*
43	*Timarcha (Metallotimarcha) metallica* (Laicharting, 1781)	22.05	2	0,38	- Şoimului de sus, valley, Barber traps
44	*Timarcha (Timarchostoma) goettingensis* (Linnaeus, 1758)	25.06	1	0,19	-Bistrița Bârgăului, alluvial forest with *Salix* and *Alnus*
	VII. Galerucinae Latreille, 1802				
45	*Galerucella (Neogalerucella) tenella* (Linnaeus, 1761)	26.06	1	0,19	- Piatra Fântânele, mez. lawn
46	*Lochmaea capreae* (Linnaeus, 1758)	04.05 23.05 24.05	5 1 14	0,96 0,19 2,71	-Bistrița Bârgăului, on *Salix sp.* -Bistrița Bârgăului, on *Salix sp.* -Valea Şoimului de sus, on *Salix sp.*
47	*Galeruca (Galeruca) tanaceti* (Linnaeus, 1758)	24.06 28.07	2 2	0,38 0,38	- Şoimului de sus, valley, hyg. veg. -Mița, hyg. veg. on Dălbidan valley
48	*Luperus flavipes* (Linnaeus, 1767)	30.07	1	0,19	- Piatra Fântânele, mez. lawn

Table 1. (continued)

Nr. Crt.	Subfamily/ species	Date	Nr. Ind.	Rel. ab. %	Place of capture/ habitat
	VIII. Halticinae Newman 1834				
49	*Longitarsus (Longitarsus) rubellus* (Foudras, 1860)	30.07	1	0,19	- Colibița, S. of the lake, mez. lawn
50	*Longitarsus (Longitarsus) brunnaeus* (Duftschmid, 1825)	25.06	1	0,19	-Popasul Șoimului, river meadow
51	*Longitarsus (Longitarsus) tabidus* (Foudras, 1860)	30.04	1	0,19	-Colibița, mezo-hyg.lawn
52	*Longitarsus (Longitarsus) languidus* (Kutschera, 1863)	30.07	1	0,19	-Popasul Șoimului, river meadow
53	*Longitarsus (Longitarsus) nugrofasciatus* (Goeze, 1777)	22.05	1	0,19	- Șoimului de sus, valley, Barber traps
54	Altica oleracea (Linnaeus, 1758)	24.05 24.06 26.06	1 1 1	0,19 0,19 0,19	- Șoimului de sus, valley, mez. veg. -Tăul Zânelor, on herbs - Piatra Fântânele, mez. lawn
55	*Batophila fallax* Weise, 1888	22.05	2	0,38	- Șoimului de sus, valley, Barber traps
56	*Asiorestia femorata* (Gyllenhal, 1813)	24.06 31.07	1 1	0,19 0,19	-Tăul Zânelor, hyg. veg. Mița,Toader's,valley hyg. veg.
57	*Crepidodera aurata* (Marsham, 1802)	23.05 24.05 24.06	9 1 2	1,74 0,19 0,38	-Bistrița Bârgăului, on *Salix sp*. - Șoimului de sus, valley on *Salix sp.* -Colibița, on *Salix caprea*
58	*Sphaeroderma rubidum* (Graells, 1858)	30.07	1	0,19	-Colibița, mez. lawn
59	*Dibolia (Dibolia) cryptocephala* (Koch, 1803)	26.06	1	0,19	-Popasul Șoimului, river meadow
60	*Dibolia (Dibolia) crysocephala* (Koch, 1803)	26.06	2	0,38	- Piatra Fântânele, mez. lawn
61	*Psylliodes (Psylliodes) napi* (Fabricius, 1792)	25.06	1	0,19	-Popasul Soimului , beech forest
62	*Psylliodes (Psylliodes) subaenea* Kutschera, 1864	25.06	1	0,19	-Popasul Soimului beech forest

Table 1. (continued)

Nr. Crt.	Subfamily/ species	Date	Nr. Ind.	Rel. ab. %	Place of capture/ habitat
	IX. Cassidinae Gyllenhal, 1813				
63	*Cassida (Odontionycha) viridis* Linnaeus, 1758	04.05	5	0,96	-Bistrița Bârgăului alluvial forest with *Salix* and *Alnus*
		24.05	14	2,71	- Șoimului de sus, valley, hyg. veg.
		24.05	3	0,58	- Șoimului de sus, valley, association with *Coryllus* .
		24.06	4	0,77	- Șoimului de sus, valley, hyg. veg.
		24.06	2	0,38	-Tăul Zânelor, on herbs
		28.07	1	0,19	-Mița, hyg. veg. on Dălbidan valley
64	*Cassida (Cassida) rubiginosa* O.F. Muller, 1776	24.06	1	0,19	-Tăul Zânelor, on herbs
		29.07	1	0,19	-Popasul Șoimului, alluvial forest with *Salix* and *Alnus*, Barber traps
65	*Cassida (Cassida) stigmatica* Suffrian, 1844	26.06	1	0,19	- Piatra Fântânele, mezo-hyg. veg.
66	*Cassida (Cassida) vibex* Linnaeus, 1767	24.05	1	0,19	-Popasul Șoimului, alluvial forest with *Salix* and *Alnus*
67	*Cassida (Cassida) pannonica*, Suffrian, 1849	23.05	1	0,19	-Colibița, grazed lawn
		26.06	1	0,19	-Piatra Fântânele, grazed lawn
68	*Cassida (Cassida) prasina* Illiger, 1789	29.07	1	0,19	-Colibița, mez.lawn, Barber trap

***Abbreviations**: Nr. Crt.= current number; Nr. Ind.= number of individuals; Rel. ab.= relative abundance; hyg.= hygrophilous; mezo-hyg.=mezzo-hygrophilous; veg.= vegetation; mez.= mezophilous; S.= South; sp.= species*

Reffering to the distribution of the registered species on subfamilies (Fig. 1.), the Chrysomelinae subfamily have had the greatest number of species, indicating the mezophilous to mezzo-hygrophilous character of the majority of the habitats existing in the investigated area. Also great number of species was registered in Halticinae and Cryptocephalinae subfamilies, indicating the prsence of some mezophilous or mezzo-xerophilous habitats, areas preffered by the majority of the species of these groups. Concerning the gnera, the best represented was *Chrysolina* genus (Fig. 2.) with a large variety of sub-genera (see also Table 1.), followed by *Cryptocephalus*, *Cassida* and

Longitarsus, showing the presence both of mezzo-hygrophilous and mezzo-xerophilous habitats, as well as typical mezophilous ones. Important is the fact that, over the presence of some common genera, also rare ones for the country's fauna are present, like *Hydrotassa, Sclerophaedon, Sphaeroderma, Dibolia*. This fact accentuate the eco-protective value of the researched zone.

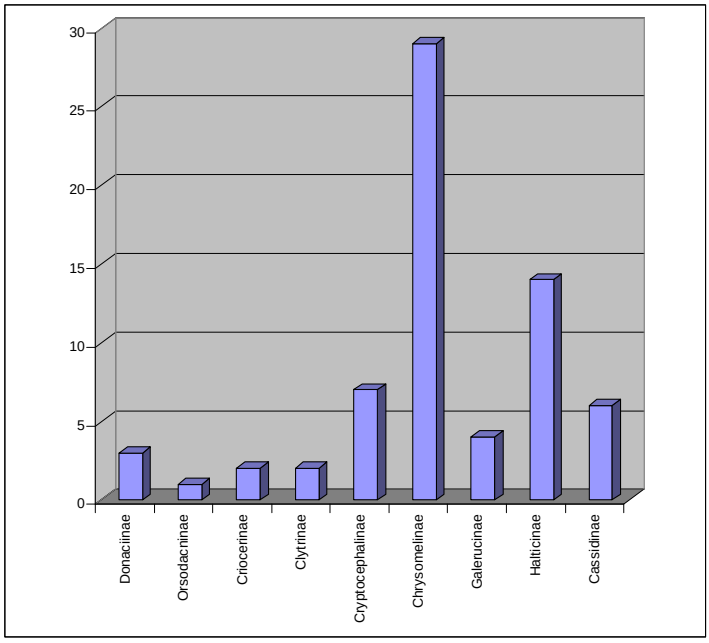

Fig. 1. The distribution on subfamilies and number of species of the leaf-beetles registered in the area Bistrița Bârgăului-Colibița- Piatra Fântânele.

Reffering to the leaf-beetle biodiversity in different habitats of the studied area, (Fig. 3.) we registered a spread of the species on habitats in accord with the different ecological demands of each leaf -betle species or group. Having in mind the ecological characteristics of the habitats existing in the area, as we expected, the greatest number of leaf –beetle species was registered in the herbous vegetation along the Soimului de Sus valley (see column"d" in Fig. 3.), where the plant biodiversity was also great, like in the mezophilous lawn from the Piatra Fântânele zone (column „p", Fig. 3.).Other types of habitats are also important as ecological refuges for different rare or endemic species, even the number of species here registered was not so great. So was for example the case of the hygrophilous vegetation in the spruce forest in Piatra Fântânele area (column "n" Fig. 3.), where the rare endemic species *Sclerophaedon carpathicus* found the best life conditions.

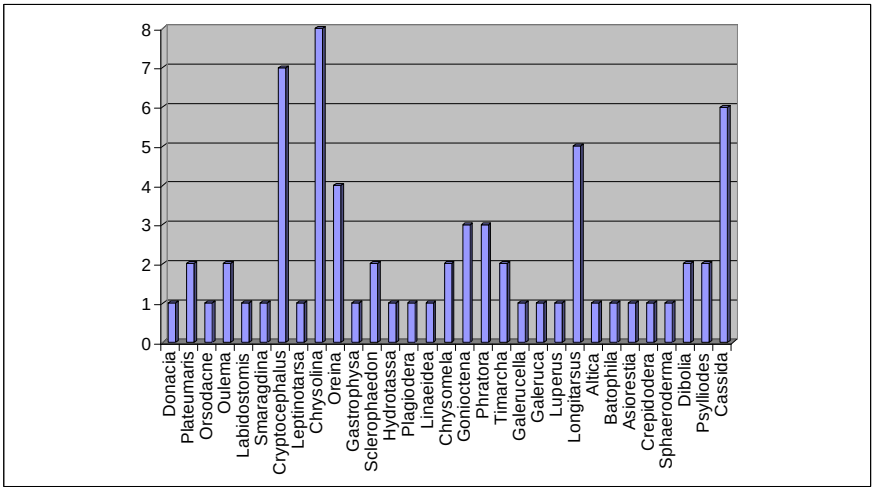

Fig. 2. The distribution on genera and number of species of the leaf-beetles registered in the area Bistrița Bârgăului-Colibița- Piatra Fântânele

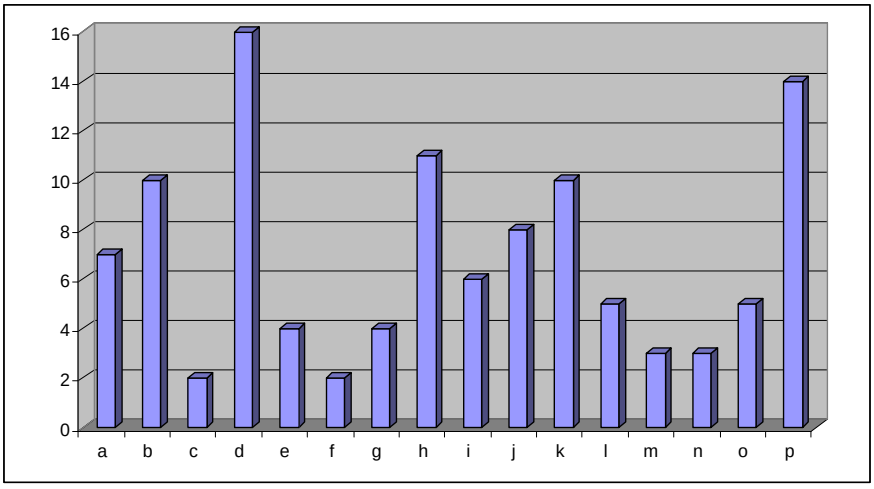

Fig. 3. The distribution of th number of leaf beetle species on habitats in the area Bistrița Bârgăului - Colibița- Piatra Fântânele (**a**- Bistrița Bârgăului, river meadow herbs; **b**- Popasul Șoimului, mezophilous lawn; **c**- Stegea valley, clearing in a mixed forest; **d**- Soimului de Sus valley, hygrophilous herbs; **e** –Șoimului de Sus valley, mezophilous association with *Coryllus*; **f** – Șoimului de Sus valley,mezophilous vegetation; **g** –Șoimului de Sus valley, on *Salix sp.*; **h** – Colibița, mezophilous lawn; **i** – Colibița, on *Salix caprea* ; **j** – Colibița, South of the lake, mezophilous lawn; **k** – Tăul Zânelor, mezo-hygrofilous vegetation; **l** –Toader's valley, hygrophilous vegetation; **m** –Dălbidan valley, mezo-hygrofilous herbs; **n** – Piatra Fântânele, on *Caltha* sp., in pure spruce forest; **o**- Piatra Fântânele, mezo-hygrophilous vegetation; **p**- Piatra Fântânele, mezophilous lawn).

We estimate that the researched area on the whole constitute a good eco-protective zone, fact illustrated also by the presence of a few number of species in only 2-3 types of habitats, following the spread of the plant species, these constituting the single food source for this insect group. Other habitat factors as the altitude, the humidity, the temperature and luminosity mast be taken into consideration in the analyses of leaf-beetle distribution in the habitats.

REFERENCES

Bobarnac B. (1974) Contributii la studiul familiei Chrysomelidae (Ord. Coleoptera) in Oltenia., *Stud. Com. St. Muz. St. Nat. Bacău*, 23-30.

Balog A., Crisan A., Ruicanescu A. (1997) cercetari faunistice asupa unor familii de coleoptere din zona localitatii Hotoan, judetul Satu Mare (Scarabeidae, Cerambicidae, chrysomelidae)., *Bul. Inf. Soc. Lipid. Rom.*, **8** (4), 253-260.

Crişan A. (1993a) Date asupra familiei Chrysomelidae (Coleoptera) în partea sudică a Deltei Dunării., *An. şt. Inst. „Delta Dunării" Tulcea*, 67-74.

Crişan A. (1993b) Cercetări faunistice şi ecologice asupra familiei Chrysomelidae (Coleoptera) în cheile Turzii în 1992., *Studia Univ. "Babeş-Bolyai", Biologia*, **38** (1-2), 59-67.

Crişan A. (1994) Noi date asupra familiei Chrysomelidae (Coleoptera) în Rezervaţia Biodferei „Delta Dunării", *An. şt. Inst. „Delta Dunării" Tulcea*, 159-166.

Crişan A. Teodor L. (1994) Researches on leaf-beetles (Coleoptera, Chrysomelidae) in "Scărița Belioara"Botanical Reservation., *Bul. Inf. Soc. Lipid. Rom.* 7 (3-4): 255-260.

Crişan A. (1995) Cercetări asupra familiei Chrysomelidae (Coleoptera) în Rezervaţia Biosferei "Delta Dunării", cu referire specială la *Stilosomus tamaricis* H-Schaeff. şi *Cryptocephalus gamma* H-Schaeff., *Bul. Inf. Soc. Lipid. Rom.* **6** (1-2), 145-149.

Crişan A., Bonea V. (1995) Studiu faunistic asupra crizomelidelor (Coleoptera, Chrysomelidae) din zona Arcalia, (Jud. Bistriţa-Năsăud)., *Bul. Inf. Soc. Lipid. Rom.* **6** (3-4), 305-317.

Crişan A., Popa V., Teodor L. (1998) Leaf-beetles (Coleoptera: Chrysomelidae) from the area "Cheile Someşului Cald- Ic Ponor", Romania., *Bul. Inf. Soc. Lipid. Rom.* **9** (1-2), 127-132.

Crişan A., Popa V., Teodor L. (1999) Studies on leaf-beetle fauna (Coleoptera: Chrysomelidae) in "Someşului Cald Gorges" area, Romania., *Bul. Inf. Soc. Lipid. Rom.*, **10** (1-4), 131-135.

Crişan A., Teodor L., Nistor L. (2000) Data on leaf-beetle fauna (Coleoptera, Chrysomelidae) in the North-West Transsylvania (Romania)., *Bul. Inf. Soc. Lipid. Rom.* **11,** (1-4), 115-122.

Crişan A., Druguş M. (2001) Studiul faunistic şi ecologic al crizomelidelor (Coleoptera, Chrysomelidae) din zona de confluenţă a Târnavelor., *Bul. Inf. Soc. Lipid. Rom.* **12,** (1-4), 191-200.

Crişan A., Teodor L. (2003) Researches on leaf-beetles (Coleoptera Chrysomelidae) from the upper Arieş River basin., *Bul. Inf. Soc. Lipid. Rom.* **13** (1-4)

Crisan. A. (2004) Studii de biodiversitate in ecosisteme naturale din bazinul Ariesului., Rev. Pol st. Scient., Nr spec. 2005, 1/17-17/17

Crisan A., Teodor L., Crisan M. (2003) Studies on leaf-beetles (Coleoptera, Chrysomelidae) from the middle Aries River basin (Câmpeni-Buru area), *Entomol. Rom.*, **8-9**, 2003/2004, 13-28.

Crisan A., Teodor L. (2005) Leaf beetle biodiversity in the low Aries river basin (Chrysomelidae, Coleoptera, Insecta), *Entomol. Rom.*, **10**, 43-52.

Crisan A. (2006) Comparative analysis of leaf-beetles (Coleoptera, Chrysomellidae) from the scientific researvs Scărița-Belioara, Cheile Turzii and Cheile Turului (Transylvania county, Romania), *Studia Univ. "Babes-Bolyai", Biologia*, **51** (2), 3-13

Crisan A. (2006) Researches on leaf-beetles (Coleoptera, Chrysomelidae) in the black pine of Banat (*Pinus nigra banatica*) habitate and adjacent areas from the "Domogled-Valea Cernei" National Park (Romania), *Entomol. Rom.*, **11**, 13-18.

Fleck E. (1905) Die Coleopteren Rumaniens., *Bul. Soc Şt.*, **14** (1-6), 680-735.

Gruev P., Merkl O., Vig K. (1993) Geographical distribution of Halticinae (Coleoptera, Chrysomelidae) in Romania, *Ann. Hist. Nat. Mus. Hung.*, **85**, 75-132.

Ieniştea M.A. (1968) L'entomofaune de l Île de Letea (Delta du Danube), ord. Coleoptera (pars)., *Trav. Mus. Hist. Nat. "Gr. Antipa"*, **8**, 81-93.

Ieniştea M.A. (1974) Contribution a la connaisance des coleopteres du Delta du Danube (la "grind" Caraorman)., *Trav. Mus. Hist. Nat. "Gr. Antipa"*, **14**, 239-249.

Ieniştea M.A., Negru Ş. (1975) *Seria monografică "Porțile de Fier", Coleoptera*, Ed. Acad. Rom., Bucureşti, 193-214.

Ilie A.L. (2001) Cercetări privind fauna de crizomelide (Coleoptera, Chrysomelidae) din municipiul Craiova şi împrejurimi., *Bul. Inf. Soc. Lipid. Rom.* 1**2,** (1-4), 201-208.

Ilie A.L., Chimisliu C. (2000) Catalogul speciilor de crizomelide din colecția Muzeului Olteniei, Craiova, *Bul. Inf. Soc. Lipid. Rom.*, **10** (1-2), 153-158.

Kaszab Z. (1962-1971) *Magyarorszag allatvilaga, Bogarok IV/B (Fauna Hungariae, Coleoptera IV/B)*, Akad. Kiado, Budapest.

Kippenberg H., Doberl M. (1994) Familie Chrysomelidae, In Lohse & Lucht "*Die Kafer Mitteleuropas*", Supplementband, Krefeld.

Konnert-Ionescu A. (1963) Halticinae recorded from Romania till 1961., *Trav. Mus. Hist. Nat "Gr. Antipa"*, **4**, 251-268.

Maican S., Serafim R. (2001) Chrysomelidae (Coleoptera) from Maramureş (Romania)., *Trav. Muz. Nat. Hist Natur"Grigore Antipa"*, **43**, 199-233.

Marcu O. (1927) Neue Coleopteren aus der Bucovina., *Bul. Fac. Şt. Cernăuți*, **1** (2), 413-423.

Marcu O. (1928) Beitrage zur Coleopterenfauna der Bucovina., *Bull. Sci. Ec. Polytech.*, Timişoara, 4-11.

Marcu O. (1936) Coleopterenfunde aus der Bucovina., *Bull. sect. sci. Acad. Roum.*, **16**,:1-6.

Marcu O. (1957) Contribuții la cunoaşterea faunei coleopterelor Transilvaniei., *Bul. Univ. V. Babeş şi I. Bolyai, ser. Şt. Nat*, **1**. (1-2), 527-544.

Mohr K.H. (1966) Chrysomelidae, In Freude, Harde, Lohse "*Die Kefer Mitteleuropas*", Goekeund Evers-Krefeld, Zurich, 95-299.

Negru Ș. (1968) L entomofaune de l île de Letea (Delta du Danube), ord. Coleoptera (pars)., *Trav. Mus. Hist. Nat. "Gr. Antipa"*, **9**, 81-83.

Negru Ș., Roşca A. (1967) L entomofaune des forets du Sud de la Doubroudja, ord.Coleoptera (pars), *Trav. Mus. Hist. Nat. "Gr. Antipa"*, **7**, 119-145.

Panin S. (1951) *Determinatorul coleopterelor dăunătoare şi folositoare din R.P. Romînă*, Ed. Lit. Șt. Did., Bucureşti, 126-150.

Petri K. (1912) *Siebenburgens Kaferfauna auf Grund ichrer Erforschung bis zum Jahre 1911*, Buchdruckerei Jus. drotleff, Hermannstadt, 253-286.

Roşca A. (1973) Contributions a la connaissance du genre *Cryptocephalus* Foucr. (Coleoptera, Chrysomelidae) en Roumanie., *Trav. Mus. Hist. Nat. "Gr. Antipa"*, **13**, 143-154.

Roşca A. (1974) Contributions a la connaissance du genre *Chrysomela* L. (Coleoptera, Chrysomelidae) en Roumanie., *Trav. Mus. Hist. Nat. "Gr. Antipa"*, **14**, 250-259.

Roşca A. (1976) L entomofaune du Nord de la Dobrogea, la zone Măcin – Tulcea- Niculițel, ord. Coleoptera (pars)., *Trav. Mus. Hist. Nat. "Gr. Antipa"*, **17**, 145-152.

Rozner I. (1996) An update list of the Chrysomelidae of Hungary and the adjoining parts of the Carpathian Basin (Coleoptera), *Folia Entomol. Hung.*, **57**, 234-260.

Seidlitz G. (1891) *Fauna Transsylvanica, die Kafer (Coleoptera) Siebenburgens*, Hartungsche Verlagsdruckerei, Konigsberg, 753-823.

Szel G., Rozner I., Kocs I. (1995) Contribuții la cunoaşterea coleopterelor din Transilvania (România) pe baza colectărilor din ultimii ani., *Acta Muz. Secuiesc al Ciucului*, Muz. Naț. Secuiesc, 73-92.

Warkalowsky A. (1993) *Fauna Polski- Fauna Poloniae- Chrysomelidae (Coleoptera, Insecta), Tom. 15*, Pol. Akad. Nauk., Warszawa.

Warkalowsky A. (2003) *Chrysomelidae, the leaf-beetles of Europe and Mediterranean area*, Natura optima dux, Warszawa, 656 pp.

STUDIA UNIVERSITATIS BABEŞ – BOLYAI, BIOLOGIA, LV, 1, 2010, p. 45-59

PLATFORM INITIATION, CLUTCH INITIATION AND CLUTCH SIZE IN COLONIAL GREAT CRESTED GREBES *PODICEPS CRISTATUS*

ANDRÉ KONTER[1]

SUMMARY. Data of platform initiation, clutch initiation and clutch size of colonial Great Crested Grebes *Podiceps cristatus* were collected over a period of four years and analyzed with respect to seasonal patterns and possible differences between experienced birds and first-time breeders. Extraordinary large (above 5 eggs) and small (below 3 eggs) clutch sizes were analyzed separately and possible cases of conspecific brood parasitism were documented. Average full clutch sizes of Great Crested Grebes were seasonally decreasing and it was concluded that this should be the norm. The seasonal decline in final nest content was triggered by seasonally increasing numbers of small clutches and in parallel decreasing numbers of exceptionally large clutches. Also, parasitic egg reception increased average clutch size more in early than in later clutches. Brood parasitism was a major component in exceptionally large clutches. At least for experienced birds, the not parasitized clutch size should be comprised of 3 to 5 eggs. Differences in nesting density inside the colony could possibly explain part of the parasitic egg laying. Adverse weather conditions leading to the destruction of part of the platforms were found to play an important role, too. The breeding parameters associated with small clutches pointed at a high likelihood that these could have originated from inexperienced females that could have laid later in the season and produced fewer eggs.

Keywords: brood parasitism, clumping of nests, clutch initiation, clutch size, colonial breeding, experience, platform initiation, *Podiceps cristatus*.

Introduction

Clutch size in the Great Crested Grebe (*Podiceps cristatus*) is variable and ranges from 1-2 to 8-9 eggs (Dittberner 1996, Fjeldså 2004, Ilicev and Flint 1985, Vlug 1983), but more commonly is comprised between 3 and 5 (Dittberner 1996, Ilicev and Flint 1985, Konter 2001, Melde 1973, Simmons 1989). Different studies on the subject found seasonally decreasing clutch sizes, independently from whether the grebes nested solitarily or colonially (Blinov *et al*. 1981, Fjeldså 2004, Goc 1986, Henriksen 1992, Ulenaers and Dhondt 1991). The most commonly accepted explanation for this phenomenon is that experienced grebes breed earlier in the

[1] *Collaborator of the Museum of Natural History, L-2345 Luxembourg, E-mail: podiceps@pt.lu*

season and produce on average larger-sized clutches than inexperienced grebes that initiate their egg laying later (Bukacinska *et al.* 1993, Goc 1986, Henriksen 1992, Lammi 1985 *in* Ulenaers and Dhondt 1991).

According to Fjeldså (2004), in grebes eggs can occasionally be laid in foreign nests. While he expects this brood parasitism to be relatively common in the least hostile species, it might be rare in territorial species even if these form colonies. Moskal and Marsalek (1986) and Vlug (1983) however report of conspecific brood parasitism in the Great Crested Grebe and Henriksen (1996) found 8% of the nests in his study to contain parasitic eggs. Grebes seem to be unable to differentiate between their own eggs and those of conspecifics. Even three cases where Red-necked Grebes (*P. grisegena)* raised chicks of Great Crested Grebes are known (Vlug 1998) and underline the difficulties grebes may have with egg recognition.

To test the seasonal evolution in clutch size, different nesting parameters on colonial Great Crested Grebes on the Dutch IJsselmeer were collected over four breeding seasons. The study tried to respond to the following questions: Can the principle of seasonally decreasing clutch sizes be confirmed for the colony investigated? To what extent does parasitic egg laying impact clutch sizes found and to what extent could brood parasitism be related to nesting density? How do exceptionally large (over 5 eggs) or exceptionally small (1-2 eggs) full clutches fit into the picture? What qualities could be attributed to individual grebe pairs that laid full clutches outside the common range (3-5 eggs) of egg numbers for the species?

Study Area and Methods

Recording of nesting data of the Great Crested Grebes took place at the Compagnieshaven of Enkhuizen, a yachting harbour located in the western part of the Dutch Lake IJssel or IJsselmeer in spring from 2003 to 2006. The harbour held three groups of nesting pairs qualified as colonies in the sense of Goc (1986) who arbitrarily retained an average distance criterion of 10 m or less between nest platforms to call a Great Crested Grebe concentration a colony. The colony investigated was the Footbridge colony that was observed without disturbance to the grebes from the elevated footbridge just in front of the nesting area. The colony was subdivided into 3 vegetated zones separated called Reed I, Reed II (2 stretches of Reed *Phragmites australis*) and the Bulrush zone covered with *Typha latifolia*. The three zones were separated by stretches clear of vegetation in between. In addition, Reed II was generally wider and denser than Reed I. In each year and for each observation period consisting generally of 3 days over a weekend, the platforms present were recorded on a 1:100-map of the area. The chronology of each platform and the progress in nesting were noted. Generally, 2-3 observers were present with short interruptions from 14.00 to 19.00 hr on Fridays, 06.30 to 19.00 hr on Saturdays and 06.30 to 12.00 hr on Sundays. The nest contents were recorded each time an incubating grebe stood up. Only first clutches, no replacement or second clutches are included in this study. For a complete description of the area and the methods, see Konter 2005 and 2007.

For all 4 years, seasonal changes in clutch sizes were analyzed with respect to the dates of platform initiation and clutch initiation. Clutch sizes were also grouped with respect to their degree of clumping. Clumping of nests was expressed by the number of neighbouring platforms within 3 m (Konter, 2005). The measure of clumping retained was taken at the moment when the maximum density for the colony was reached, independently from clutch initiation dates of the different nests. It was considered that even if clutch initiation was early when the degree of clumping was less, the pressure from not yet settled grebes was proportional to later degrees of clumping.

Full clutches were classified into 3 categories depending on the date of clutch initiation: first egg laid before 11 April, from 11-20 April and after 20 April. During the night from 8 to 9 April 2005, a storm destroyed most of the existing platforms, whether containing eggs or not. Therefore related data were analyzed separately. Full clutch sizes were also classified into 4 categories depending on the date of platform initiation: start of building in March, 1-10 April, 11-20 April, and after 20 April. Only nests in the Reed zones of the colony were considered as the numbers of nests in the Bulrush zone were too limited in each year (between 17 and 23), and therefore did not warrant analysis if the data were distributed into different time or clumping categories.

Full clutches of below 3 and above 5 eggs were considered to be of abnormal size. They were therefore identified and analyzed separately. The breeding parameters of their owners (settlement date, clutch initiation date, time from settlement to clutch initiation) were compared to the average figures for the colony as a whole.

While in 2003 and 2004, the content of each nest was recorded mostly only once per observation weekend, in 2005 and 2006 nest contents were recorded up to 3 times per observation weekend. In order to detect anomalies in the laying patterns of the grebes pointing to possible brood parasitism, I focused on the 2005 and 2006 data of nest contents. The egg-laying interval in the Great Crested Grebe ranges from 1-2 days, but more often occurs every other day (Fjeldså, 2004; Henriksen, 1995, Onno, 1966; Simmons, 1974). Nests were classified as parasitized if an average laying interval of less than 24 hours was detected in a clutch or if the addition of late eggs occurred more than 48 hours after laying of the previous egg.

Statistical Analyses. I used a one-way ANOVA to test for differences in clutch size among nesting-season periods (platform initiation and clutch initiation) and nest-clumping classes. Significant ANOVA results ($P < 0.05$) were followed by Tukey *post hoc* tests for pair wise comparisons. ANOVA and Tukey tests were performed using the VassarStats web site for statistical computation (http://faculty.vassar.edu/lowry/VassarStats.html). All means are given ± SD.

Results

Seasonal Changes in Clutch Size

Except for Reed I in 2003, the average clutch size of nests inside the Reeds showed a seasonal decrease in relation to the date of clutch initiation. While the decrease was not significant for Reed I in most of the years, it was significant for Reed II in all years. Aggregated figures for all years displayed significant declines for Reed I ($P<0.05$) and even highly significant declines for Reed II ($P<0.0001$) and for both Reed parts combined ($P<0.0001$). For Reed II and for all Reeds, the pair wise comparisons of the values between the periods using the Tukey test proved significant decreases, too (Table 1).

Table 1.

Average full clutch size of grebe nests in the Reeds in relation to the date of clutch initiation (in parentheses number of clutches; for 2005, clutches still incomplete and destroyed by the storm on 8 April were not considered).

Date of first egg		Before 11 April	11-20 April	After 20 April	One-way ANOVA			Tukey test
		Mean ± SD	Mean ± SD	Mean ± SD	*F*-value	df	*P*	Periods that differ (*P*)
2003	Reed I	3.92 ± 0.79 (12)	3.58 ± 1.08 (12)	3.82 ± 0.40(11)	0.5	2, 32	0.60	
	Reed II	4.33 ± 0.50 (9)	3.77 ± 0.95 (22)	3.50 ± 0.62 (18)	3.4	2, 46	0.04	1-3 (<0.05)
	Total	4.10 ± 0.70 (21)	3.71 ± 1.00 (34)	3.62 ± 0.56 (29)	2.4	2, 81	0.10	
2004	Reed I	4.25 ± 0.50 (4)	4.25 ± 0.45 (12)	4.09 ± 0.70 (11)	0.3	2, 24	0.78	
	Reed II	4.33 ± 0.58 (3)	4.14 ± 0.56 (22)	3.50 ± 0.89 (16)	4.3	2, 38	0.02	
	Total	4.29 ± 0.49 (7)	4.18 ± 0.52 (34)	3.74 ± 0.86 (27)	3.8	2, 65	0.03	
2005	Reed I	4.87± 0.83 (8)	3.82 ± 0.40 (11)	3.80 ± 1.13 (10)	4.7	2, 26	0.02	1-2, 1-3 (<0.05)
	Reed II	5.46 ± 1.45 (13)	3.95 ± 0.51 (20)	3.58 ± 0.90 (12)	14.0	2, 42	0.0001	1-2, 1-3 (<0.01)
	Total	5.24 ± 1.26 (21)	3.90 ± 0.47 (31)	3.68 ± 0.99 (22)	18.7	2, 71	0.0001	1-2, 1-3 (<0.01)
2006	Reed I	4.38 ± 0.74 (8)	4.00 ± 0.82 (4)	3.90 ± 0.57 (10)	1.1	2, 19	0.34	
	Reed II	4.69 ± 0.79 (16)	4.44 ± 1.10 (18)	3.67 ± 0.72 (15)	5.4	2, 46	0.008	1-3 (<0.01), 2-3 (<0.05)
	Total	4.58 ± 0.78 (24)	4.36 ± 1.05 (22)	3.76 ± 0.66 (25)	6.4	2, 68	0.003	1-3 (<0.01), 2-3 (<0.05)
All years	**Reed I**	**4.31 ± 0.82 (32)**	**3.90 ± 0.75 (39)**	**3.90 ± 0.73 (42)**	**3.3**	**2, 110**	**0.04**	
	Reed II	**4.83 ± 1.07 (41)**	**4.06 ± 0.84 (82)**	**3.56 ± 0.76 (61)**	**26.1**	**2, 181**	**0.0001**	**1-2, 1-3, 2-3 (<0.01)**
	Total	**4.60 ± 1.00 (73)**	**4.01 ± 0.81 (121)**	**3.70 ± 0.76 (103)**	**24.6**	**2, 294**	**0.0001**	**1-2, 1-3 (<0.01), 2-3 (<0.05)**

Seasonal variation of clutch sizes in relation to the start of platform building exhibited a less clear trend although a general tendency towards smaller clutches for platforms started later appeared. Taking each year separately, the declines were only significant for Reed II ($P<0.05$) and for all Reeds ($P<0.01$) in 2005. For all years combined, early platforms in Reed II and in all Reeds contained significantly bigger clutches than platforms built 11-20 April or after 20 April ($P<0.001$; Table 2).

Table 2.

Average full clutch size of grebe nests in the Reeds in relation to the date of platform initiation (in parentheses number of clutches).

Date of platform start		In March	1-10 April	11-20 April	After 20 April	One-way ANOVA			Tukey test
		Mean ± SD	Mean ± SD	Mean ± SD	Mean ± SD	*F*-value	df	*P*	Periods that differ (*P*)
2003	Reed I	3.72 ± 0.75 (18)	3.88 ± 1.25 (8)	3.75 ± 0.50 (4)	3.60 ± 0.55 (5)	0.1	3,31	0.95	
	Reed II	4.00 ± 0.75 (26)	3.91 ± 0.83 (11)	3.38 ± 1.06 (8)	3.29 ± 0.76 (7)	2.2	3,48	0.10	
	Total	3.89 ± 0.75 (44)	3.89 ± 0.99 (19)	3.50 ± 0.90 (12)	3.42 ± 0.67 (12)	1.6	3,83	0.19	
2004	Reed I	4.38 ± 0.74 (8)	4.20 ± 0.42 (10)	4.00 ± 0 (6)	4.00 ± 0.81 (4)	0.7	3, 24	0.57	
	Reed II	4.17 ± 0.58 (12)	3.86 ± 0.38 (7)	3.70 ± 0.67 (10)	3.75 ± 0.50 (4)	1.4	3, 29	0.26	
	Total	4.25 ± 0.64 (20)	4.06 ± 0.43 (17)	3.81 ± 0.54 (16)	3.88 ± 0.64 (8)	2.0	3, 57	0.12	
2005	Reed I	4.23 ± 1.01 (13)	4.00 ± 0.58 (7)	3.40 ± 1.34 (5)	3.67 ± 0.58 (3)	1.0	3, 24	0.41	
	Reed II	4.90 ± 1.34 (21)	4.33 ± 0.89 (12)	3.67 ± 0.87 (9)	3.75 ± 0.46 (8)	4.0	3, 46	0.013	1-3 (<0.05)
	Total	4.65 ± 1.25 (34)	4.21 ± 0.79 (19)	3.57 ± 1.02 (14)	3.73 ± 0.47 (11)	4.6	3, 74	0.005	1-3 (<0.05)
2006	Reed I	4.11 ± 0.93 (9)	4.20 ± 0.84 (5)	4.29 ± 0.49 (7)	3.00 ± 0 (2)	1.5	3, 19	0.24	
	Reed II	4.59 ± 0.79 (17)	4.22 ± 0.94 (18)	3.91 ± 1.30 (11)	4.00 ± 0 (2)	1.2	3, 44	0.34	
	Total	4.42 ± 0.86 (26)	4.22 ± 0.90 (23)	4.06 ± 1.06 (18)	3.50 ± 0.58 (4)	1.4	3, 67	0.24	
All years	**Reed I**	**4.04 ± 0.87 (48)**	**4.07 ± 0.78 (30)**	**3.91 ± 0.75 (22)**	**3.64 ± 0.63 (14)**	**1.1**	**3, 110**	**0.36**	
	Reed II	**4.41 ± 1.00 (76)**	**4.12 ± 0.84 (48)**	**3.68 ± 0.99 (38)**	**3.62 ± 0.59 (21)**	**7.4**	**3, 179**	**0.0001**	**1-3, 1-4 (<0.01)**
	Total	**4.27 ± 0.96 (124)**	**4.10 ± 0.81 (78)**	**3.77 ± 0.91 (60)**	**3.63 ± 0.60 (35)**	**7.3**	**3, 293**	**0.0001**	**1-3, 2-4 (<0.05), 1-4 (<0.01)**

When combining both criteria to analyze clutch sizes in relation to the dates of platform and clutch initiation (years 2005-2006, Table 3), the results revealed again seasonal declines in each category. However, early settlers in March 2005 that rather quickly laid their first egg contradicted this trend. Due to unfavourable weather conditions, the early settlers in March 2006 all had to wait for an extended period of time before initiating their clutches.

Data in Table 3 suggests that early settlers in March did not necessarily quickly lay their first egg and that even waiting for over 20 days before clutch initiation was not exceptional among first settlers. Data of 2005 were biased by a storm that destroyed nearly all platforms in early April. Thus, March-platforms having received no egg when blown away were not included in the statistics. In all years, some of the March-platforms experienced their clutch initiation over 30 days after platform initiation while at the same time some of the April-settlers laid their first egg within a few days.

Table 3.

Average full clutch size in the Reeds in relation to the date of platform initiation and the time span from platform initiation to clutch initiation in 2005 and 2006 (in parentheses number of clutches).

Date of platform initiation		In March		1-10 April		11-20 April		After 20 April	
		2005	2006	2005	2006	2005	2006	2005	2006
Time span	< 6 days	3.67 (3)	---	4.25 (8)	4.38 (8)	4.00 (12)	4.20 (10)	3.71 (7)	3.50 (2)
	SD	1.15	---	0.89	0.74	0.80	1.32	0.49	0.71
	6-10 days	4.20 (10)	4.83 (6)	3.86 (7)	4.33 (9)	3.67 (3)	4.20 (5)	3.50 (2)	---
	SD	1.03	0.983	0.69	1.22	0.58	0.48	0.71	---
	> 10 days	4.95 (19)	4.30 (20)	4.00 (3)	3.75 (4)	2.67 (3)	3.50 (4)	---	---
	SD	1.47	0.801	0	0.50	1.53	0.58	---	---

Nesting Density and Clutch Size

Nesting density was measured by the degree of clumping (number of neighbouring nests within 3 m) and clutches were grouped accordingly (Table 4). In both Reed zones, nests clumped at degree 0 held on average the largest clutches in 2003, 2004 and 2005, but not in 2006. In 2006, nests most heavily clumped contained the largest clutches and in nests clumped at degrees 0 or 1-2, markedly smaller average clutches are observed (Figure 1).

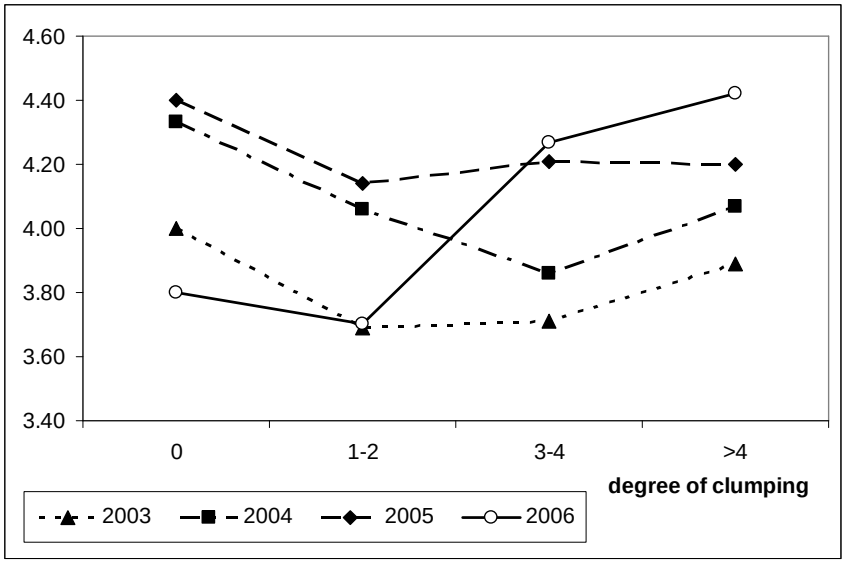

Fig. 1. Average clutch size in relation to degree of nest clumping

Inside the Bulrush zone, comparisons were difficult due to the limited amount of data and the generally lower nesting density, and the results have to be considered with care. In all years, non-clumped nests held more eggs than nests clumped at degrees 1-2. In 2003 and 2005, higher degrees of clumping resulted in increasing average clutch sizes. In 2006, a gradual decline of clutch size with increasing degrees of clumping was noted, and this trend was exactly opposite to the evolution inside the Reeds in the same year.

The pattern of clumping for the colony as a whole was similar to that for the Reeds, with no uniform pattern for the four-year period of this study. One-way ANOVA testing of the evolution of clutch size in relation to the degree of clumping performed for the colony as a whole nevertheless proved significant differences in clutch size for 2006 ($P<0.005$) and for all years combined ($P<0.05$; Table 4).

Table 4.

Average full clutch size in the grebe colony in relation to nest clumping (in parentheses number of clutches).

Section	Number of clumped nests	2003	2004	2005	2006	All years
		Mean ± SD	Mean ± SD	Mean ± SD	Mean ± SD	Mean ± SD
Reed I & II	0	4.00 ± 0 (2)	4.33 ± 0.52 (6)	4.40 ± 0.89 (5)	3.80 ± 0.45 (5)	4.17 ± 0.62 (18)
	1-2	3.69 ± 1.03 (13)	4.06 ± 0.68 (16)	4.14 ± 0.71 (22)	3.70 ± 0.48 (10)	3.95 ± 0.76 (61)
	3-4	3.71 ± 0.92 (34)	3.86 ± 0.85 (21)	4.21 ± 1.17 (28)	4.27 ± 0.88 (22)	3.99 ± 0.99 (105)
	>4	3.89 ± 0.69 (38)	4.07 ± 0.65 (29)	4.20 ± 1.41 (25)	4.42 ± 0.98 (38)	4.15 ± 0.96 (130)
Bulrush	0	4.00 ± 0 (1)	4.33 ± 0.58 (3)	3.60 ± 0.98 (5)	3.67 ± 0.58 (3)	3.83 ± 0.72 (12)
	1-2	3.40 ± 0.84 (10)	3.56 ± 0.53 (9)	3.44 ± 1.01 (9)	3.55 ± 0.69 (11)	3.49 ± 0.76 (39)
	3-4	4.00 ± 0.63 (11)	---	4.00 ± 0 (1)	3.00 ± 0 (1)	3.92 ± 0.67 (13)
	>4	---	---	---	---	---
Colony	0	4.00 ± 0 (3)	4.33 ± 0.50 (9)	4.00 ± 0.94 (10)	3.75 ± 0.46 (8)	4.03 ± 0.67 (30)
	1-2	3.57 ± 0.94 (23)	3.88 ± 0.67 (25)	3.94 ± 0.85 (31)	3.62 ± 0.59 (21)	3.77 ± 0.79 (109)
	3-4	3.78 ± 0.88 (45)	3.86 ± 0.85 (21)	4.21 ± 1.17 (29)	4.22 ± 0.88 (23)	3.98 ± 0.96 (118)
	>4	3.89 ± 0.69 (38)	4.07 ± 0.65 (29)	4.20 ± 1.41 (25)	4.42 ± 0.98 (38)	4.15 ± 0.96 (130)
One-way ANOVA	*F*- value	0.8	1.3	0.4	4.7	3.3
	df	3, 105	3, 80	3, 91	3, 86	3, 374
	P	0.47	0.28	0.75	0.005	0.019
Tukey test	Periods that differ (*P*)				2-4 (<0.05)	

Exceptionally Small Clutches

Inside the Reeds, full clutches with a maximum of 2 eggs summed up to a total of 10 in all 4 years (Table 5). With respect to the average clutch initiation date inside the Reeds for the colony as a whole (that showed little variation over the 4 years and was 16 April ±1day), 6 pairs initiated their clutches later, 1 on the mean date and 3 earlier. The average numbers of waiting days from platform to clutch initiation inside the Reeds for all years combined were 17 days for March platforms, 10 days for first decade of April platforms, 6 days for second decade of April platforms and 5 days for later platforms. From the 6 late small clutches, 2 platforms were

started in March and waited 28-33 days before receiving a first egg. One platform was started in the first decade of April and clutch initiation was 21 days later. Three platforms appeared in the second decade of April and waited 2, 7, and 15 days before egg laying started. The nest with clutch initiation on the average date appeared in early April and held its first egg 13 days later. For the 3 early clutches, the platforms appeared in March, 1st and 2nd decade of April and egg laying started respectively 20 days, 20 days and 5days later.

Nine of the 10 nests with small clutches were clumped with at least 3 other nests (Table 5). The last nest, already built towards mid-March in 2003, held 2 eggs and was not clumped. It was located within rather poor stands of Reed and had the nearest neighbour at 3.65 m. Clutch initiation occurred a bit more than one month after platform initiation.

Table 5.

Total number of full clutches with one or two eggs (small clutches) versus number with more than five eggs (large clutches) in relation to nest clumping 2003-2006.

	Reeds									**Bulrush**			
	Number of clumped nests									**Number of clumped nests**			
	0	0	0	0	0	5	6	7	8	0	1	2	>3
Small-large clutches	1-1	0-0	0-1	6-2	0-2	1-1	0-6	1-2	1-2	1-0	2-0	2-0	0-0
Total clutches	16	16	34	42	35	29	35	19	11	18	22	41	66
% that are small clutches	6.7	0	0	14.3	0	3.4	0	5.3	9.1	5.6	9.1	4.9	0
% that are large clutches	6.7	0	2.9	4.8	5.7	3.4	17.1	10.5	18.2	/	/	/	/

In total 5 small clutches were counted in the Bulrush zone (Table 5). The average clutch initiation dates were quite variable over the 4 years and they were 25 April 2003, 25 April 2004, 16 April 2005 and 19 April 2006. The average numbers of waiting days from platform to clutch initiation inside the Bulrush for all years combined were 21 days for March platforms, 11 days for first decade of April platforms, 5 days for second decade of April platforms and 4 days for later platforms. With respect to these dates, 2 small clutches were initiated later and 3 on the average dates. For the 2 late clutches, the platforms were started in March and in the third decade of April and they waited for 31 and 6 days before holding an egg. For the 3 others, 2 platforms appeared in March and needed 26 and 39 days before egg laying was started, the other was built in the second decade of April and received a first egg within 2 days. The five small clutches were recorded in nests clumped at degrees 0 (n=1), 1 (n=2) or 2 (n=2).

Clutch initiation dates of all small clutches fell twice into the first decade of April, 5 times into the second and 8 times into the third. Thus, the number of small clutches goes seasonally increasing (Table 6).

Table 6.

Summary of characteristics associated with small clutches in the Reeds and in the Bulrush.

Platform Initiation (D=decade)	**Clutch initiation with respect to average date for the colony**					
	Earlier		On the average date		Later	
	3		4		8	
	Waiting time from platform to clutch initiation		**Waiting time from platform to clutch initiation**		**Waiting time from platform to clutch initiation**	
	Below average	Above average	Below average	Above average	Below average	Above average
March		1		2		3
1D April		1		1		1
2D April	1		1		1	2
3D April						1
Total	1	2	1	3	1	7

Exceptionally Large Clutches

All 17 full clutches with more than 5 eggs were laid in the Reed zones and none of them was recorded in 2003 (Table 5). 16 of these clutches were started prior to the average laying date for the Reeds, 13 of them more than 5 days earlier, the other 3 just 1 or 2 days earlier. The 17th clutch was initiated on the average date. 10 of the really early large clutches knew a platform initiation in March and they waited for 4, 6, 11, 12, 12, 17, 18, 20, 20 and 20 days before receiving a first egg. 2 platforms appeared during the first decade of April and waited for 6 days each before initiating a clutch and one platform was started during the second decade of April to hold an egg 3 days later. For the 3 clutches initiated just prior to the average date, one platform appeared in March and received an egg after 26 days, the remaining 2 were initiated in the first decade of April and held an egg 5 and 10 days later. The only clutch started on the average day knew its platform initiation during the second decade of April and a clutch initiation 4 days later.

15 of the 17 clutches (88%) occurred in nests clumped with at least 3 other nests and 10 (59%) in nests clumped with at least 6 additional nests. One nest holding a full clutch of 6 eggs was located in a narrow part of Reed I. It was clumped with 2 other nests and had its nearest neighbour at 2.3 m. The platform started on 25 March 2005 received its first egg on 5 April. The last platform was located at the beginning of Reed II where the stands of vegetation were much spaced and therefore prohibited having very close neighbours. It was started on 20

March 2005 and received its first egg on 15 April, some days after the storm. The next nest was at a distance of 3.9 m. Nesting parameters associated with large clutches are summarized in Table 7.

Table 7.

Summary of characteristics associated with large clutches in the Reeds and in the Bulrush.

Platform Initiation (D=decade)	**Clutch initiation with respect to average date for the colony**					
	Earlier			On the average date		
	13			4*		
	Waiting time from platform to clutch initiation			**Waiting time from platform to clutch initiation**		
	Below average	On average	Above average	Below average	On average	Above average
March	5	1	4			1
1D April		2		1	1	
2D April	1			1		
Total	6	3	4	2	1	1

** including 3 clutches laid 1-2 days prior to the average date*

Nests with Possible Parasitic Eggs

To test the hypothesis that large-sized clutches may have been laid by more than one female, data collected in 2005 and 2006 were analyzed with respect irregular laying patterns (laying interval < 24 h or > 48 h) to detect possible cases of brood parasitism.

In 2005, a Storm Night of 8-9 April reduced most of the platforms, whether containing eggs or not, to floating heaps (Konter, 2007). 7 pairs (6 inside the Reeds and one inside the Bulrush) salvaged at least one egg and thereafter 6 of them exhibited an irregular egg laying pattern receiving in total a minimum of 10 parasitic eggs (9 inside the Reeds, 1 one inside the Bulrush). Two clutches of 3 eggs and one clutch of 4 eggs inside the Reeds were completely destroyed during the storm. The replacement clutches initiated shortly afterwards were parasitized 5 times. One additional clutch started immediately after the storm received 2 eggs not laid by the owners. In summary, 9 Reed and 1 Bulrush nests contained at the end 16 and 1 parasitic eggs.

5 Reed clutches initiated in the second decade of April in 2005 were subject to parasitism and received in total 7 eggs after a laying interruption of 3 days and longer.

In 2006, 7 early clutches in the Reed zone received each one egg after a prolonged laying interruption (3-15 days). In the Bulrush section, 2 early nests also received each one late egg. 3 Reed clutches initiated in the second decade of April were subject to late parasitism and received a total of 7 eggs after laying interruptions of 6-13 days.

Deducting detected egg parasitism from clutch sizes, mean values were reduced by 0.43 to 4.81 eggs in early April 2005 and by 0.45 to 3.45 eggs in mid-April 2005. In 2006 the respective decreases were of 0.29 and 0.39 to 4.29 and 4.05 eggs. It is also noteworthy that in 2005 for 6 large clutches out of 9, parasitic egg reception was proved whereas in 2006 this was the case for 5 out of 7. From the 17 large clutches in total, 11 were initiated in the first decade of April, 6 in the second and none in the third.

Discussion

The asynchronous platform and clutch initiation by Great Crested Grebes revealed in this study appears to be rather common, even in colonial nesting of the species (Berthoud, 1963; Blinov *et al.*, 1981; Henriksen, 1992; Koshelev, 1977; Koshelev and Chernichko, 1985; Leys *et al*., 1969; Van IJzendoorn, 1967). At least for the Netherlands, the asynchronies could be largely triggered by the migratory behaviour of the grebes and their arrival at the breeding grounds in distinct periods whereby late birds are migrants and may be more subject to extended pre-laying periods, depending on their body conditions upon arrival (Ulenaers and Dhondt 1991).

Concerning clutch size evolution, I found only 2 studies that observed seasonal increases of mean clutch sizes. Bukacinska et al. (1993) differentiated between colonial and non-colonial grebes on the same lake. While seasonal clutch size increased by ±0.4 eggs in colonial birds, it declined by ±0.7 eggs in non-colonial birds. Including all nests in a single calculation however resulted in a slight seasonal decline of ±0.15 eggs. Leys et al. (1969) studied the Great Crested Grebes at a site directly adjacent to Lake IJssel and found clutch sizes first to increase and to decrease later. The habitat originated only towards the mid-1960s and therefore could not receive from the start grebes returning to a breeding site known from previous years. It recorded extraordinarily high losses of clutches and platforms (152 nests out of 263 were destroyed in 1967), mostly due to wave action. Direct food availability was poor and the adults were forced to fly to the nearby IJsselmeer to feed. This suggests that the habitat was problematic, especially early in the season, and it should therefore have been avoided to a large extent by experienced grebes or more generally by grebes physically in condition to settle at better sites. We conclude that under normal conditions, average full clutch sizes of Great Crested Grebes should decrease seasonally.

Ulenaers and Dhondt (1991) explained the decreases of nest contents not by age differences of the grebes, but by differences in body conditions of locally wintering and late arriving grebes: females in good condition immediately start laying, otherwise they wait and possibly lay smaller clutches. This study found that the seasonal decline in final nest content was not only triggered by seasonally increasing numbers of small clutches (1 or 2 eggs). In parallel, numbers of exceptionally large clutches (over 5 eggs) decreased seasonally. Also, parasitic egg reception increased

average clutch size more in early than in later clutches and potential parasitism was not detected in any late clutch. It seems also clear that early clutches were more prone to the reception of foreign eggs simply because they existed early when settlement pressure built up. Brood parasitism was proved in 69% of the exceptionally large clutches laid in 2005 and 2006 and it could not be excluded in the remaining 31%. Parasitic egg laying was thus a major component in extraordinary large clutches which in turn contributed to high average clutch sizes. This is in agreement with Vlug (1983) who found the modal clutch of Great Crested Grebes in the Netherlands to hold four eggs and clutches of seven and more eggs are laid most times by two females. Blinov *et al*. (1981) and Goc (1986) support this thesis. Other arguments in favour of the limitation in normal clutch size are the maximum numbers of fledglings of 3 to 4 in the species and the findings of Lyon and Everding (1996) predicting that a non-parasitized full clutch of Eared Grebes *P. nigricollis* holds 3 or 4 eggs and never exceeds 4 eggs while, similarly to Great Crested Grebes, larger clutches occur. We conclude that, at least for experienced Great Crested Grebes, a not parasitized clutch should range between 3 and 5 eggs.

Lyon and Everding (1996) found nest density to influence brood parasitism in the Eared Grebe; high levels of aggression related to dense nesting may provide more opportunities for a parasitic female to sneak onto a momentarily undefended nest. We then could expect more parasitic eggs in denser nesting parts of a colony and therefore generally increasing clutch sizes with increased clumping. This was indeed the case in the colony investigated here in 2006 and for all years combined, but the pattern for the 4 years taken separately was not uniform. Nesting density might therefore only be one out of several factors affecting brood parasitism and may not play a predominant role. Considering only extraordinary large clutches (that had a good chance of having been parasitized), we found no homogenous attributes other than generally early platform and clutch initiation (prior to the mean dates for the colony). It appeared however that adverse weather conditions leading to the destruction of a more or less important part of the platforms might push brood parasitism at least momentarily to higher levels. At Lake Braband, Henriksen (1996) found that 30% of the females lost their clutch before completion through nest destruction and he expected platform loss to be responsible for a more or less important part of parasitic egg laying.

Vlug (1998) argued that fierce nest defence by colonial grebes is possibly an attempt to prevent brood parasitism on their nests. Behavioural tactics so far evolved to avoid parasitism may then still be insufficient and would only limit the degree of conspecific brood parasitism in the species.

Analyzing small clutches more in detail, we observed that their platform initiation dates were mostly late, their waiting times until clutch initiation generally above average (80%) and their start of egg laying occurred either on the average date for the colony as a whole (27%) or later (53%). This pattern could of course be explained by the differences in migratory decisions and in body conditions of the

grebes. Other explanations are however possible. Early reservation of a prime nesting space coupled with delayed clutch initiation means prolonged exposure to aggressiveness of neighbours and new settlers and high energetic costs for platform defence. It is rather unlikely that grebes in poor physical conditions would then invest in early site occupation. They would possibly be better off by first refilling their energetic reserves outside the nesting habitat to move to the colony later. We may also ask to what extent birds in poor physical conditions would be able to defend a platform in a highly competitive context. If we consider in addition that experienced grebes can be expected not to unnecessarily prolong their presence inside a stressful colony and to initiate their clutches with minimal delay, habitat and weather conditions permitting, early settlement coupled with delayed clutch initiation would better fit with birds lacking experience. In line with the preceding, Vlug (2002 for the Red-necked Grebe) speculated that young females lay later in the season, possibly also as a consequence of delayed reproductive development of first-year birds or of their lack of experience for coping appropriately with high levels of intraspecific aggression, and Goc (1986) predicted that clutches of 3 and fewer eggs belong to young females.

In conclusion, Great Crested Grebe colonies are commonly composed of a mix of birds from all age classes and seasonally decreasing average clutch sizes are the norm for the species. This evolution relies on one hand on in time decreasing numbers of extraordinary large clutches and on the other on increasing numbers of small clutches. Not parasitized full clutches are expected not to exceed 5 eggs, otherwise they are laid by more than one female. Conspecific brood parasitism decreases gradually in time. The exceptionally small clutches are initiated later, possibly in their majority by inexperienced females. Under abnormal conditions, deviations from these general patterns are possible. Additional research should analyze to what extent younger birds could settle early in the season and what characteristics are then associated with their nesting.

ACKNOWLEDGEMENTS

Many thanks to Gilbert Laroche, Han Vlug and my wife Maria for their tireless contribution to field work, and to the staff of the Compagnieshaven and the Museum of Natural History in Luxembourg for their support. I am also grateful to Han Vlug for commenting on the first draft of the paper and to Bruce Eichhorst whose most welcome suggestions further improved this publication. Finally I thank the two anonymous reviewers from Studia Biologia whose comments helped in clarifying some issues.

REFERENCES

Adriaensen F., Ulenaers P., Dhondt A.A. 1993. Ringing recoveries and the increase in numbers of European Great Crested Grebes *Podiceps cristatus*. Ardea 81: 59-70.

Berthoud G. 1963. Observations sur une colonie de Grèbes huppés près d'Yverdon. Nos oiseaux 27: 184-186.

Blinov V. N., Koshelev A.I., Yanovskiy A. P. 1981. [Structure of colonies, breeding success and behaviour of the Great Crested Grebe (*Podiceps cristatus*) on Menzelinskoe Lake, West Siberia]. Ekologiya i biotsenoticheskie svyazi pereletnykh ptits Zapadnoi Sibiri, Nauka Publishers, Novosibirsk: 30-48.

Bukacińska M., Bukaciński D., Jabłonski P. 1993. Colonial and Noncolonial Great Crested Grebes (*Podiceps cristatus*) at LakeŁuknajno: Nest Site Characteristics, Clutch Size and Egg Biometry. Colonial Waterbirds 16: 111-119.

Dittberner W. 1996. Die Vogelwelt der Uckermark. Verlag Erich Hoyer, Galenbeck.

Fjeldså J. 2004. The Grebes. Oxford University Press.

Goc M. 1986. Colonial versus territorial breeding of the Great Crested Grebe *Podiceps cristatus* on Lake Druzno. Acta Ornithol. 22: 95-145.

Henriksen K. 1992. Nesting ecology and production of young in the Great Crested Grebe *Podiceps cristatus* in a hypereutrophic Danish lake. Dansk Ornitologisk Forenings Tidsskrift 86:163-168.

Henriksen K. 1995. Intraclutch variation in egg volume of Great Crested Grebes. Condor 97: 826-828.

Henriksen K. 1996. [Intraspecic nest parasitism in the Great Crested Grebe *Podiceps cristatus*]. Dansk Ornitologisk Forenings Tidsskrift 90: 36-37.

Illicev V. D., Flint V. E. 1985. Handbuch der Vögel der Sowjetunion Band 1. Aula Verlag, Wiesbaden.

Konter A. 2001. Grebes of our world. Lynx Edicions, Barcelona.

Konter A. 2005. Annual Building-up of Great Crested Grebe Colonies: An Example from the Dutch IJsselmeer. Waterbirds 28: 351-358.

Konter A. 2007. Response of Great Crested Grebes *Podiceps cristatus* to storm damage of nests. Waterbirds 30: 140-143.

Koshelev A.I. 1977. [Colonial nesting habits of the Great Crested Grebe (*Podiceps cristatus* L.) in the northern part of Lake Menzelinskoe, Western Siberia]. Bulletin of the Moscow Naturalists' Society, Department of Biology: 5-9.

Koshelev A.I., Chernichko I. I. 1985. [Ecological factors determining the nesting type of the Great Crested Grebe]. Theoretical aspects of colonial breeding in birds: 67-72, Nauka Press, Moscow.

Leys H. N., Marbus J., de Wilde J.J.F.E. 1969. [Observations in a colony of Great Crested Grebes (*Podiceps cristatus* L.) in Eastern Flevoland]. De Levende Natuur 72: 97-141.

Lyon B. E., Everding S. 1996. High frequency of conspecific brood parasitism in a colonial waterbird, the Eared Grebe *Podiceps nigricollis*. Journal of Avian Biology 27: 238-244.

Mayr C. 1986. Häufigkeit, Voraussetzungen und Ursachen von Mehrfachbruten des Haubentauchers (Podiceps cristatus). Charadrius 22: 55-68.

Melde M. 1973. Der Haubentaucher - Die Neue Brehm Bücherei, A.Ziemsen Verlag, Wittenberg Lutherstadt.

Moskal J., Marszałek J. 1986. Effect of habitat and nest distribution on the breeding success of the great crested grebe *Podiceps cristatus* on Lake Żarnowieckie. Acta Ornithol. 22: 147-158.

Onno S. 1966. Zur vergleichenden Ökologie der Paläarktischen Taucherarten. Falke 7: 220-226.

Perry K. 2000. The Ecology and Conservation of Great Crested Grebes *Podiceps cristatus* at Lough Neagh, Northern Ireland. Thesis for the degree of Doctor of Philosophy, University of Ulster.

Simmons K.E.L. 1974. Adaptations in the reproductive biology of the Great Crested Grebe. British Birds 67: 413-437.

Simmons K.E.L. 1989. The Great Crested Grebe. Shire Natural History.

Ulenaers P., Dhondt, A. A. 1991. Phenology, habitat choice and reproduction of the Great Crested Grebe *Podiceps cristatus* L., on a fish-farm. Ardea 79: 395-408.

Van IJzendoorn E. J. 1967. [The Great Crested Grebes of the Amstelmeer]. Levende Natuur 70: 284-286.

Vlug J.J. 1983. [The Great Crested Grebe (*Podiceps cristatus*)]. Wetenschappelijke Mededeling van de Koninklijke Nederlandse Natuurhistorische Verenigung 160.

Vlug, J.J. 1998. Brutparsitismus bei Lappentauchern. Corax 17: 169-171.

Vlug J.J. 2002. *Podiceps grisegena* Red-necked Grebe. BWP Update 4: 139-180.

STUDIA UNIVERSITATIS BABEŞ – BOLYAI, BIOLOGIA, LV, 1, 2010, p. 61-65

A MATHEMATICAL MODEL FOR AN EPIDEMIC IN AN OPEN SOCIETY

MOHAMMAD REZA MOLAEI[1]

SUMMARY. In this paper a mathematical model for an infectious disease in an open society is introduced. The parameters of this model are time dependent, and it is an extension of the susceptible, infectious and removed (SIR) models. This model has this ability to determine the speed of recovery rate to protect the society from an epidemic.

Keywords: mortality rate, recovery rate, per capita birth, SIR model

Introduction

Theory of infectious disease epidemics is based on mathematical models for the epidemics. Beside its applications in epidemiology it brings many bright mathematical results in dynamical systems (Bauch and Earn, 2003, Earn, *et al.*, 2000, Korobeinikov and Maini, 2004). In the susceptible, infectious and removed (SIR) model and its extensions, the society is closed and its parameters such as per capita birth and mortality rate are constant numbers. In this paper we consider an open society. It means a society in which individuals enter it and leave it. Moreover its parameters are time dependent. For example the influenza infection in which passengers have essential role in its infection and this model can apply for it. In the next section we introduce this model and then we show that it is an extension of the previous models (Farkas, 2001). Moreover we find a recovery rate as a function of a time as a limitation for the speed of recovery to protect the society from an epidemic of a disease.

The model

We denote the number of individuals at time t by $x(t)$. $S(t)$ is the number of individuals who have no immunity to the infectious agent. We denote the number of individuals who are infected at time t and can transmit the infection to the susceptible individuals by $I(t)$. $R(t)$ is the number of individuals who are immune to

[1] *Department of Mathematics, University of Kerman (Shahid Bahonar), 76169-14111, Kerman, Iran. E-mail: mrmolaei@mail.uk.ac.ir*

the infection and their contacts to the others have no any effect to the transmission. We denote the number of offspring and dead people at time *t* by *B(t)* and *D(t)* respectively. *b(t)* and *d(t)* are the per capita birth and the mortality rate at time *t* respectively. In fact if we choose a discrete small time τ as a unit time, then the per capita birth and the mortality rate at time *t* can be approximated by $\frac{B(t+\tau)-B(t)}{x(t)}$ and $\frac{D(t+\tau)-D(t)}{x(t)}$ respectively.

e(t) is the rate of those who leave the society at time *t*. If *g(t) = 1-d(t)* and if there is no any infection then *x(t)g(t)* is the number of those survive at time *t* and *x(t)g(t)e(t)* is the number of those who leave the society at time *t*. *x(t)g(t)e(t)b(t)* is the number of those who are born at time *t* by the people who leave the society and take their offspring with themselves.

We denote the rate of those who enter the society at time *t* by *c(t)*, and we denote their per capita birth by *f(t)*. If there is no any infection then *x(t)c(t)f(t)* is the number of those who are born by the individuals who enter the society.

An average member of the population at time *t* makes contact to transmit infection is denoted by $\beta(t)x(t)$.

For $t \in R$, and small positive number τ we define *h(t)* and $\alpha(t)$ by $\frac{R(t+\tau)-R(t)}{x(t)}$ and $\frac{I(t+\tau)-I(t)}{x(t)}$ respectively. By choosing a function $u(\tau)$ with $t < u(\tau) < t+\tau$ we can find the following approximations:

$$\frac{S(t+\tau)-S(t)}{\tau} \cong x(t)\frac{b(u)-b(t)}{\tau} - x(t)\frac{g(u)e(u)b(u)-s(t)e(t)b(t)}{\tau} +$$

$$x(t)\frac{c(u)f(u)-c(t)f(t)}{\tau} + \frac{b(t)x(t)u(t)}{\tau} - \frac{\beta(t)S(t)I(t)u(t)}{\tau} - \frac{d(t)S(t)u(\tau)}{\tau}$$

and

$$\frac{I(t+\tau)-I(t)}{\tau} \cong \frac{\beta(t)S(t)I(t)u(\tau)}{\tau} - \frac{d(t)I(t)u(\tau)}{\tau} - \frac{\alpha(t)I(t)u(\tau)}{\tau}.$$

Moreover,

$$\frac{x(t+\tau)-x(t)}{\tau} \cong x(t)\frac{b(u)-b(t)}{\tau} - x(t)\frac{g(u)e(u)b(u)-s(t)e(t)b(t)}{\tau}$$

$$+ x(t)\frac{c(u)f(u)-c(t)f(t)}{\tau} + \frac{b(t)x(t)u(\tau)}{\tau} - \frac{(1-h(t))\alpha(t)I(t)u(\tau)}{\tau} - \frac{d(t)x(t)u(\tau)}{\tau}.$$

So, by tending τ to zero we deduce the following system:

$$\begin{cases} \dot{S}(t) = A[\eta(t)x(t) - \beta(t)S(t)I(t) - d(t)S(t)] \\ \dot{I}(t) = A[\beta(t)S(t)I(t) - d(t)I(t) - \alpha(t)I(t)] \\ \dot{x}(t) = A[\eta(t)x(t) - (1-h(t))\alpha(t)I(t) - d(t)x(t)] \end{cases} \quad (*)$$

where $A = \dot{u}(0)$ is a constant in the interval (0,1].

$\eta(t) = \dot{b}(t) - \dot{g}(t)e(t)b(t) - g(t)e(t)\dot{b}(t) + \dot{c}(t)f(t) + c(t)\dot{f}(t) + b(t)$,
and $S(t) + I(t) + R(t) = x(t)$.

Discussion on the compatibility of the model and its applied results

In the system (*) if we put $e(t) = f(t) = c(t) = \dot{b}(t) = 0, b(t) = d(t)$, and $A = 1$, then we conclude the system:

$$\begin{cases} \dot{S}(t) = -\beta(t)S(t)I(t) \\ \dot{I}(t) = \beta(t)S(t)I(t) - (d(t) + \alpha(t))I(t) \\ \dot{x}(t) = -(1-h(t))\alpha(t)I(t) \end{cases} .$$

When $\beta(t), d(t)$ and $\alpha(t)$ are constant functions and $h(t) = 1$ then the above system reduce to the following SIR model (Farkas, 2001, Kermack and McKendrick, 1927):

$$\begin{cases} \dot{S}(t) = -\beta S(t)I(t) \\ \dot{I}(t) = \beta S(t)I(t) - (d + \alpha)I(t) \\ \dot{x}(t) = 0 \end{cases} .$$

Let $A = 1, e(t) = f(t) = c(t) = 0,$ and let *b(t)* and *d(t)* be two constant functions. Then we conclude the following generalization of the SIR model with the vital dynamics (Brauer, 2008, Hethcote, 1976):

$$\begin{cases} \dot{S}(t) = bx(t) - \beta(t)S(t)I(t) - d(t)S(t) \\ \dot{I}(t) = \beta(t)S(t)I(t) - d(t)I(t) - \alpha(t)I(t) \\ \dot{x}(t) = bx(t) - (1-h(t))\alpha(t)I(t) - d(t)x(t) \end{cases}.$$

In fact when $\alpha(t), \beta(t)$ and *d(t)* are constant functions then we deduce the usual SIR model with the vital dynamics.

In the system (*) if $S(t) = \dfrac{d(t)+\alpha(t)}{\beta(t)}$ then $\dot{I}(t) = 0.$ So $I(t)$ is a constant such as *c*. If we put *S(t)* in the equation

$$\dot{S}(t) = A[\eta(t)x(t) - \beta(t)S(t)I(t) - d(t)S(t)]$$

then we can find the following relation between *x(t)* and *d(t)*:

$$x(t) = \frac{(\dot{d}(t)+\dot{\alpha}(t))\beta(t) - \dot{\beta}(t)(d(t)+\alpha(t))}{A\beta^2(t)}$$

$$+ (d(t)+\alpha(t))c + \frac{d^2(t)}{\beta(t)} + \frac{d(t)\alpha(t)}{\beta(t)}.$$

The equation:

$$\dot{x}(t) = A[\eta(t)x(t) - (1-h(t))\alpha(t)I(t) - d(t)x(t)]$$

determines the recovery rate *h(t)* by:

$$h(t) = 1 + \frac{\dot{x}(t)}{\alpha(t)Ac} + \frac{x(t)(d(t)-\eta(t))}{c\alpha(t)}.$$

So by this recovery rate we can sure that there is no any epidemic of the disease. Moreover if $S(t) < \dfrac{d(t)+\alpha(t)}{\beta(t)}$ then $\dot{I}(t) < 0$ and there is no epidemic, but if $S(t) > \dfrac{d(t)+\alpha(t)}{\beta(t)}$ then there is an epidemic of the disease.

Conclusion

In this paper we try to introduce a new mathematical model which can apply for the diseases which are carried by passengers such as **influenza**. The recovery rate is the main biological result of this model. The consideration of this model from the mathematical viewpoint is also a topic for further research.

Two topics for further research are:

1. What are the limit sets for infectious disease system?

2. Has the system any periodic orbit?

REFERENCES

Bauch, C.T., Earn D.J.D. (2003). Transients and Attractors in Epidemics, *Proc. R. Soc. Lond. B*, **270**, 1573-1578.

Brauer F. (2008). Compartmental Models in Epidemiology, In: *Mathematical Epidemiology (Lecture Notes in Mathematics) 1945*, Brauer F., van der Driessche, P. Wu, J. (Eds.), Springer-Verlag, Heidelberg, pp. 19-79.

Earn, D.J.D., Rohani, P., Bolker, B.M., Grenfell, B.T., (2000). A Simple Model for Complex Dynamical Transitions in Epidemics, *Science*, **287**, 667-670.

Farkas, M. (2001). *Dynamical Models in Biology*, Academic Press, San Diego.

Hethcote, H.W. (1976). Qualitative Analysis for Communicable Disease Models, *Math. Biosci.*, **28**, 335-356.

Kermack, W.O., McKendrick, A.G. (1927). A Contribution to the Mathematical Theory of Epidemics, *Proc. R. Soc. Lond. A*, **115**, 700-721.

Korobeinikov, A. , Maini, P.K. (2004). A Lyapunov Function and Global Properties for SIR and SEIR Epidemiological Models with Nonlinear Incidence, *Math. Biosci. Engin.*, **1**, 57-60.

STUDIA UNIVERSITATIS BABEŞ – BOLYAI, BIOLOGIA, LV, 1, 2010, p. 67-79

ON THE CONDITIONS FOR WHICH THE Atm PROTEIN CAN SWITCH OFF THE DNA DAMAGE SIGNAL IN A p53 MODEL

OMID RABIEIMOTLAGH[1] and ZAHRA AFSHARNEZHAD[2]

SUMMARY. In this paper, we consider a recently developed p53 model which simulates interactions between the proteins p53, Mdm2, Atm and DNA damage signal. We apply analytic methods to answer this question: how can the Atm protein contribute positively in DNA healing process? Indeed, we determine regions of parameters into which the Atm protein can switch off damage signals, or conversely, it can lead DNA to a permanent damage.

Keywords: DNA healing; Mdm2 protein; Atm protein

Introduction

Today, it is probably well known that one of the key players in cancer development is p53, a tumor suppressor. The p53 protein is a transcription factor encoded by a gene whose disruption is associated with approximately 50 to 55 percent of human cancers. The p53 protein acts as a checkpoint in the cell cycle, either preventing or initiating programmed cell death (apoptosis) (Cohen *et al.*, 2008). Regarding to the recent experimental observations, biologists consider three major functions for the p53 protein, as, it arrests the cell cycle, thereby giving the cell time to correct any DNA damage, activates transcription of gene indirectly responsible of DNA repair and can be cause of apoptosis (Chicharmane *et al.*, 2007; Vogelstein *et al.*, 2000). We know that p53 regulates itself through its interaction with an intermediate protein which is called Mdm2 (Harris and Levine, 2005). A recent elementary model which is motivated biologically, formulates this interaction as below

$$\begin{aligned} \dot{x} &= \alpha_0 + \alpha_1 x^n/(k_1 + x^n) - \gamma_1 xy - \gamma_2 x \\ \dot{y} &= \alpha_2 + \alpha_3 x^4/(k_2 + x^4) - \gamma_3 y, \end{aligned} \tag{1}$$

where $x(t)$ and $y(t)$ are dimensionless and stand respectively for $[\mathrm{p35}](t)$ and $[\mathrm{Mdm2}](t)$, [2]. In the first equation above, α_0 shows the production rate of p53, the second therm with coefficient α_1 exists due to positive feedback of p53 on

[1] *Corresponding author, Dept. of Math., University of Birjand, Birjand, Iran, email: omid.rabiei@gmail.com*
[2] *Dept. of Math., Ferdowsi University of Mashhad, Mashhad,Iran, email: afsharnezhad@um.ac.ir*

itself and it is described with a Hill coefficient $n \in N$ which determines the degree of cooperativity of the ligand of p53 binding to the enzyme or receptor (Hill, 1910). The third term represents the active process of ubiquitination of p53 by Mdm2 and the fourth term represents the degradation of p53 independently of Mdm2. Similarly, in the second equation above, α_2 shows the production rate of Mdm2, and second term with coefficient α_3 represents the activation of Mdm2 by p53 with Hill coefficient 4, and the third term represents the degradation of Mdm2 (Chicharmane *et al.*, 2007; Vogelstein *et al.*, 2000; McLure and Lee, 1998).

Another factor in the cell cycle process which acts as a damage sensor, signaling presence of DNA damage, is the Atm protein (Banin *et al.*, 1998: Kurz and Lees-Miller, 2004), The Atm-p protein, a phosphorylated form of Atm, associates in the cell cycle process by controlling production rate of p53. This is the motivation for improving the model (1) by the new model

$$\begin{aligned} \dot{x} &= z + \alpha_1 x^n/(k_1 + x^n) - \gamma_1 xy - \gamma_2 x \\ \dot{y} &= \alpha_2 + \alpha_3 x^4/(k_2 + x^4) - \gamma_3 y, \end{aligned} \tag{2}$$

where $z(t)$ denotes [Atm-p](t). Experimental observations show that amount of Atm and Atm-p holds for the conservative equation [Atm](t) +[Atm-p]$(t) = \mu$, for a positive real constant μ. Also, they are in a reaction for which the phosphorylated form Atm-p promotes further phosphorylation of Atm, hence, once a small amount of Atm-p is produced, it leads to further increase in Atm-p, until all the Atm is converted into its phosphorylated form. This should occur only when a significant DAN damage occurs. So, this process is modelled by the equation

$$\dot{z} = \alpha_{1s} z(\mu - z)/(k_{1s} + \mu - z) - \alpha_{2s} z/((k_{0d} + w)(k_{2s} + z)).$$

Here, $w(t)$ =[Dmg](t) denotes the DNA damage signal, representing amount of DNA damages, and $\mu - z(t) = \mu -$ [Atm-p](t) denotes amount of the Atm protein [2]. The first term of the above equation, with coefficient α_{1s} shows phosphorylation rate of the Atm protein and the second term, with coefficient α_{2s} shows dephosphorylation rate of the Atm protein. The parameter k_{1s} controls dependence of phosphorylation rate of the Atm protein to amount of Atm. Similarly, the parameters k_{2s} and k_{0d} control dependence of dephosphorylation rate of the Atm protein to amount of Atm-p and damage signal.

In order to complete the chain of this interaction, finally, we have to take in account that DNA is repaired by combined actions of Atm-p and p53 which can be modelled as below .

$$\dot{w} = -\alpha_d wzx.$$

Although, all of the equations mentioned above are introduced in [2] separately, but as long as we know, the co-effects of these equations have not considered as a unit system. However, these equations have been studied separately, where the results for bifurcation diagrams and stability of the systems based on numerical solutions show a control system responding to DNA damage signal by inducing p53 oscillations, correct the damage, and finally shut off the oscillations (Tyson, 2006: Benoit *et al.*, 2000). This convinces us to introduce the model below simulating interactions between p53, Atm, Mdm2 and damage signal by the four dimensional ODE .

$$\begin{cases} \dot{x} = z + \alpha_1 x^n/(k_1 + x^n) - \gamma_1 xy - \gamma_2 x \\ \dot{y} = \alpha_2 + \alpha_3 x^4/(k_2 + x^4) - \gamma_3 y \\ \dot{z} = \alpha_{1s} z(\mu - z)/(k_{1s} + \mu - z) - \alpha_{2s} z/((k_{0d} + w)(k_{2s} + z)) \\ \dot{w} = -\alpha_d wzx. \end{cases} \tag{3}$$

We believe that the model (3) has enough motivation because the numerical plots of its equations show a control system responding to DNA damage signal by inducing p53 oscillations, correct the damage, and finally shut off the oscillations [2]. This is in spirit of Ciliberto, Novak and Tyson (2005).

In this paper, for the first time, we consider all the equations of (3) together and apply mathematical methods to indicate behaviors forecasted by the model for the Atm protein and the DNA damage signal. First, we define concept of compatible solution which means that the solution of (3) is biologically motivated. Also, we show that all compatible solutions are entrapped in a region and they are attracted by certain invariant manifolds. Then, we show that the DNA damage signal is affected by dephosphorylation rate of the Atm protein and it is directly in interaction with the p53 protein. This is the key point in DNA healing process, especially where, the DNA damage signal converges to zero. This can be interpreted biologically that DNA will be finally repaired from damages. Therefore, we investigate regions for parameters into which the Atm protein switches off damage signal or conversely leads the DNA to a permanent damage. We also see that the healing process may depend on initial amounts of the proteins. The results and analytic methods of the paper help us to understand the way that parameters control the cell cycle process and let the Atm protein contribute positively in DNA healing process.

Compatible solutions and invariant manifolds

Since variables in equation (3) stand for amount of the proteins or biological components, so, solutions of (3) taking negative values have no biological sense.

Especially they can not have negative initial values. Therefore, for verifying validity of the model, we have to consider solutions beginning from positive initial values and we show that their positive trajectories remain non negative. Furthermore, we assume that amount of the p53 protein and the Mdm2 protein is initially nonzero, however, because of biological facts, amount of the [Atm-p] protein or the DNA damage signal may be initially zero.

Definition 1: *A solution of* (3) *with the initial values* $x(0) = x_0 > 0$, $y(0) = y_0 > 0$, $0 \le z(0) = z_0 \le \mu$, $w(0) = w_0 \ge 0$ *is called a compatible solution.*

It will be shown later that positive trajectories of compatible solutions remain non negative, so they have such adequacy to be called compatible. It is easy to check that the sets (manifolds) $N = R^3 \times \{0\}$ and $N_w = R \times \{0\} \times \{w\}$, $w \in R$, are invariant for (3), that is, any solution of (3) which intersects N (or N_w), is contained in N (in N_w). A solution which is contained in N_w, for some $w \in R$, implies that the Atm-p is constantly zero. Similarly, a solution which is contained in N, implies that amount of damage signal is permanently zero. Although, these invariant sets may be theorically important, but, we are interested to situations which damage signal and the Atm-p protein coexist simultaneously. This is why we do not study these invariant sets here. What makes these sets interesting for us is that each of them can be the ω-limit set for some compatible solutions. Therefore, interaction between the DNA damage signal and other proteins is bifurcated when the ω-limit set of a compatible solution changes from N to N_w or conversely from N_w to N. This change of ω-limit set is biologically important because, as we will see later, it can be interpreted as switching from DNA healing process to DNA permanent damage, or conversely from DNA permanent damage to DNA healing process. This is the reason for introducing bifurcation diagram of the DNA damage signal by change of ω-limit set of compatible solutions. This is summarized in the theorem below

Theorem 2: *Suppose that* $\Lambda = \mu(\mu + k_{1s}) - k_{1s}k_{2s}$, $U = k_{1s}(\mu + k_{1s} + k_{2s})$ *and define*

$$\Delta = (\mu + k_{1s})\alpha_{2s} - \mu k_{0d} k_{2s} \alpha_{1s}, \quad \Omega = \alpha_{2s}\sqrt{U}/\left(\alpha_{1s}(U - \sqrt{U})(\sqrt{U} - k_{1s})\right) - k_{0d}$$

(1) For $\Lambda \le 0$, *change of sign of* Δ *makes a bifurcation for the DNA damage signal. Indeed, for* $\Delta \le 0$, *compatible solutions converge to* N *and for* $\Delta > 0$, *compatible solutions converge to* N_w, *for some* $w \in R$.

(2) For $\Lambda > 0$, *change of sign of* Ω *makes a bifurcation for the DNA damage signal. Indeed, for* $\Omega \le 0$, *some compatible solutions converge to* N *and for* $\Omega > 0$, *all compatible solutions converge to* N_w, *for some* $w \in R$.

The proof of the theorem will be done through a few lemmas. The theorem shows that the bifurcation occurs with respect to the parameters α_{is}, $i = 1,2$ and k_{js}, $j = 0,1,2$;

however, the parameters α_{is}, $i=1,2$, which control phosphorylation and dephosphorylation rate of the Atm protein, are more biologically important. Meanwhile, because the total amount of the Atm protein and its phosphorylated form, Atm-p, is assumed to be constantly μ, so we can consider $\Lambda = \Lambda(k_{1s}, k_{2s})$ and solve the equation $\Lambda = 0$ with respect to k_{2s} and find $k_{2s} = \mu(\mu + k_{1s})/k_{1s}$. This is a curve in plane of k_{is}, $i=1,2$, which acts like a switch between two bifurcation diagrams, that is, down of the curve, the bifurcation diagram is determined by $\Omega = 0$, so we call it Ω region, and in above of it, the bifurcation diagram is determined by $\Delta = 0$, so we call it Δ region. (see figure 1). By putting

$A = \mu + k_{1s}, \quad B = \mu k_{0d} k_{2s}, \quad A^* = \sqrt{U}, \quad B^* = k_{0d}(U - \sqrt{U})(\sqrt{U} - k_{1s}),$

the equations $\Delta = 0$ and $\Omega = 0$ are reformulated respectively by

$A\alpha_{2s} - B\alpha_{1s} = 0, \quad A^*\alpha_{2s} - B^*\alpha_{1s} = 0,$ which are two lines in plane of α_{is}, $i=1,2$. Therefore we can show the bifurcation diagram as figure 2.

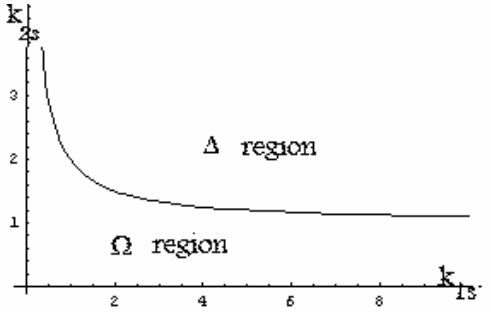

Fig. 1. Typical plot for switch curve, here $\mu = 1$.

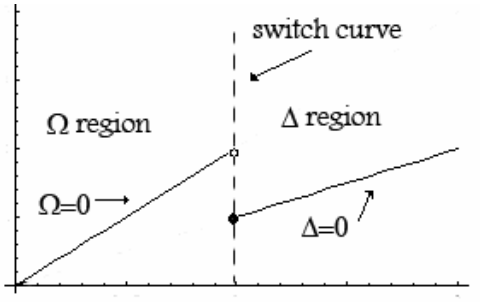

Fig. 2. Typical bifurcation diagram. Since the space of parameters has dimension upper than 3, so we have to simplify it as above. Note that the switch curve is in space of k_{is}, $i=1,2$ and the bifurcation curves are in space of α_{is}, $i=1,2$.

From the bifurcation diagram and theorem 2, we find that if the ratio of phosphorylation and dephosphorylation rate of the Atm protein i.e. α_{1s}/α_{2s} in Δ region is less than or equal to A/B, then DNA is repaired from damages; however, if α_{1s}/α_{2s} is greater than A/B, then DNA contains a permanent damage. Similarly, if the ratio of phosphorylation and dephosphorylation rate of the Atm protein i.e. α_{1s}/α_{2s} in Ω region is less than or equal to A^*/B^*, then DNA may repaired from damages; however, if α_{1s}/α_{2s} is greater than A^*/B^*, then DNA contains a permanent damage. This explains that how parameters of the system can cause the Atm protein to contribute positively in DNA healing process by increasing phosphorylation rate of it, and also, this explains the limitations which exist for this process. This leads us to abbreviate the theorem in a simple but biologically sensible result as below

Summary 3: *In the cell cycle process, if ratio of phosphorylation and dephosphorylation rate of the Atm protein i.e.* α_{1s}/α_{2s} *increases enough (such that* $\alpha_{1s}/\alpha_{2s} \geq \max\{A/B, A^*/B^*\}$*) then the DNA damage signal converges to zero which means biologically promotion in healing process, but if* α_{1s}/α_{2s} *decreases (such that* $\alpha_{1s}/\alpha_{2s} < \min\{A/B, A^*/B^*\}$*) then the DNA damage signal converges to a nonzero constant which biologically means that DNA contains permanent damages.*

Proof of the theorem 2

The proof is done through a few lemmas. First, we can look at phase space vertically such that we see two dimensional plane of z and w. Then, any compatible solution begins from the closure of the region $A = \{(z, w) \mid 0 < z < \mu, w > 0\}$. Also, z axis is N and any point on w axis is N_w, $w \in R$ (see figure 3). Therefore we have the next lemma

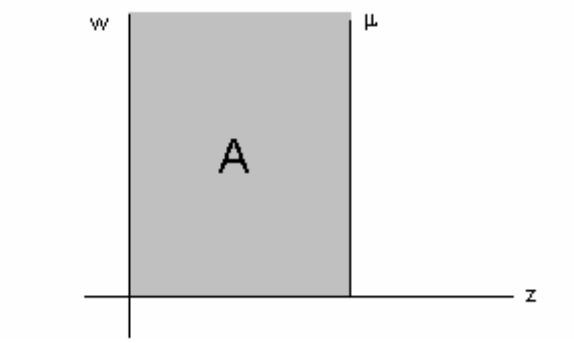

Fig. 3. Appropriate region for compatible solutions. Here, we look at the plane of z and w normally, so any point on the w axis is stands for N_w and the z axis is stands for N.

Lemma 4: *let* $\gamma(t) = (x(t), y(t), z(t), w(t))$ *be a compatible solution and consider the curve* $\tilde{\gamma}(t) = (z(t), w(t))$ *in two dimensional plane of* z *and* w. *The curve* $\tilde{\gamma}(t)$ *dose not intersect* z *-axis or it is contained in it. Similarly,* $\tilde{\gamma}(t)$ *dose not intersect* w *-axis or it is a single point on it.*

In the rest of this section we use notations γ and $\tilde{\gamma}$ as they used in lemma 4. Moreover, we assume that initial amounts of the Atm-p protein and the DNA damage signal are nonzero, that is, the compatible solution $\gamma(t)$ has initial conditions $z(0) = z_0 > 0$ and $w(0) = w_0 > 0$.

Lemma 5: *Let* $T > 0$ *and suppose that* $\{\tilde{\gamma}(t): 0 < t < T\} \subset A$. *Then,* $x(t) > 0$, $y(t) > 0$ *for all* $0 < t < T$.

Proof: Suppose that there exists $t_0 \in (0,T)$ such that for all $t \in (0, t_0)$, $x(t) > 0$ and $x(t_0) = 0$. Then, $x(t)$ must be non increasing function in a left interval of t_0; specially we have $\dot{x}(t_0) \le 0$. But, from the first equation of the model (3), we have $\dot{x}(t_0) = z(t_0) > 0$ which is a contradiction. This means that for all $0 < t < T$ we have $x(t) > 0$. Similarly, if for all $t \in (0, t_0)$, $y(t) > 0$ and $y(t_0) = 0$ then $y(t)$ must be non increasing in a left interval of t_0; specially we have $\dot{y}(t_0) \le 0$. But, from the second equation of the model (3), we have $\dot{y}(t_0) = \alpha_2 + \alpha_3 x^4(t_0)/(k_2 + x^4(t_0)) > 0$ which is a contradiction. This shows that for all $0 < t < T$ we have $y(t) > 0$.

Now we study path of $\tilde{\gamma}$ in A. The forth equation of the model (3) and the lemma 5 imply that $\dot{w} < 0$ in region A; therefore, $w(t)$ is a decreasing map in A. In order to know behavior of $z(t)$, we study the curve $\dot{z}$ =0. From the third equation of the model (3) we have

$$\dot{z} = z\left(\underbrace{\alpha_{1s}(\mu - z)/(k_{1s} + \mu - z) - \alpha_{2s}/((k_{0d} + w)(k_{2s} + z))}_{h(z,w)}\right) = 0.$$

We can solve the equation $h(z,w) = 0$ with respect to w and find $w = g(z)$, where $g(z) = -k_{0d} + \alpha_{2s}(\mu + k_{1s} - z)/(\alpha_{1s}(\mu - z)(k_{2s} + z))$.

It is easy to see that $\lim_{z \to^+ \mu} g(z) = +\infty$. Furthermore, for all $\tilde{\gamma}(t) = (z(t), w(t)) \in A$ with $w(t) < g(z(t))$ we have $\dot{z}(t) < 0$. Similarly, for all $\tilde{\gamma}(t) = (z(t), w(t)) \in A$ with $w(t) > g(z(t))$ we have $\dot{z}(t) > 0$. On the other hand, from lemma 5, if $\tilde{\gamma}(t) \in A$, then $\dot{x} > 0$, hence $\dot{w} < 0$. This shows that if the curve $\tilde{\gamma}(t) \in A$ is close enough to the line $z = \mu$, then $\dot{z} < 0$. Since $\tilde{\gamma}(t)$ dose not

intersects z or w axis, so we conclude that the curve $\tilde{\gamma}(t)$ which starts from a point in A, is contained in A and $w(t)$ is a decreasing map. Therefore next lemma is proven.

Lemma 6: *Suppose that* $\tilde{\gamma}(t)$ *is defined on the interval* $[0,T)$. *Then for all* $t \in [0,T)$, $\tilde{\gamma}(t)$ *is bounded and contained in* A.

Lemma 7: *The compatible solution* $\gamma(t)$ *is defined for all* $t \geq 0$ *and it is positively bounded.*

Proof: Suppose that maximal positive interval of existence for $\gamma(t)$ is $[0,T)$, we makes a contradiction. If $T < +\infty$, then $\lim_{t \to {}^{+}T} \| \gamma(t) \| = +\infty$, (Perko, 1991). From the lemma 6, $\tilde{\gamma}(t)$ is bounded and contained in A, so $\lim_{t \to {}^{+}T} \| (x(t), y(t)) \| = +\infty$. From the lemma 5, for all $t \in [0,T)$ we have $x(t), y(t) > 0$. If $x(t)$ is unbounded then there exits a sequence $0 < t_n \to^{+} T$ such that $x(t_n) \to +\infty$ and $\dot{x}(t_n) \geq 0$. But, from the first equation of the model (3), $\dot{x}(t_n) \to -\infty$ which is a contradiction. Hence $x(t)$ is bounded for $t \in [0,T)$. If $y(t)$ is unbounded then there exits a sequence $0 < t_n \to^{+} T$ such that $y(t_n) \to +\infty$ and $\dot{y}(t_n) \geq 0$. But, from the second equation of the model (3), $\dot{y}(t_n) \to -\infty$ which is a contradiction. Hence for $t \in [0,T)$, $y(t)$ is bounded. This shows that $\gamma(t)$ is bounded and therefore $T = +\infty$. This completes the proof.

Through next lemmas, we will see that graph of $w = g(z)$ which is important for determining behavior of $z(t)$, controls the bifurcation parameters of theorem 2 i.e. Λ, Δ and Ω. It divides A into three distinct region A^{+}, top of the graph, A^{-}, down of the graph and $G(g)$, the graph itself.

$A^{+} = \{(z,w) \in A : w > g(z)\}$, $A^{-} = \{(z,w) \in A : w < g(z)\}$.

Therefore, behavior of $\tilde{\gamma}(t)$ in A is determined by knowing its behavior in A^{+} and A^{-}.

Remark: One more time, we must note that the phase space of (3) is a four dimensional space, but here, we look at this space vertically so that we see two dimensional plane of z and w. Therefore results and theorem for ω-limit sets of flows of two dimensional vector fields are not valid for $\tilde{\gamma}(t)$ in A. Because of this fact, we have to prove following lemmas.

Lemma 8: *The curve* $\tilde{\gamma}(t)$ *which stars in* A^{+} *intersects* $G(g)$ *or converges to a intersection point of* $G(g)$ *and* z *axis.*

Proof: Suppose that $\tilde{\gamma}(0) \in A^+$ and $\tilde{\gamma}(t)$ dose not intersects $G(g)$. From lemma 7, $\tilde{\gamma}(t)$ is bounded and defined for $t \geq 0$. Since $\tilde{\gamma}(t) = (z(t), w(t)) \in A^+$, so $z(t)$ and $w(t)$ are monotone functions, in fact, $z(t)$ is increasing and $w(t)$ is decreasing. Let $\lim_{t\to+\infty}(z(t), w(t)) = (z_1, w_1)$, then from the mean value theorem we have

$$z(t+1) - z(t) = \dot{z}(c_1) = z(c_1)h(z(c_1), w(c_1)),$$
$$w(t+1) - w(t) = \dot{w}(c_2) = -\alpha_d w(c_2)z(c_2)x(c_2),$$

where $|c_i - t| \leq 1$, $i = 1,2$. We can let $t \to +\infty$ and obtain

$$\begin{aligned} 0 &= \lim_{t\to+\infty} z(t+1) - z(t) = z_1 h(z_1, w_1), \\ 0 &= \lim_{t\to+\infty} w(t+1) - w(t) = -\alpha_d w_1 z_1 \lim_{t\to+\infty} x(t). \end{aligned} \tag{4}$$

The first equation shows that $h(z_1, w_1) = 0$ which means that $(z_1, w_1) \in G(g)$. Now, we claim that $\lim_{t\to+\infty} x(t) \neq 0$, if not, one more time applying of the mean value theorem yields

$$x(t+1) - x(t) = \dot{x}(c) = z(c) + \alpha_1 x^n(c)/(k_1 + x^n(c)) - \gamma_1 x(c)y(c) - \gamma_2 x(c),$$

where $|c - t| \leq 1$. Since $y(t)$ is bounded, so if $t \to +\infty$ we obtain $0 = z_1$, which is a contradiction. Therefore, from the second equation of (3) we obtain that $w_1 = 0$, hence $\tilde{\gamma}(t)$ converges to a intersection point of $G(g)$ and z axis. (see figure 4).

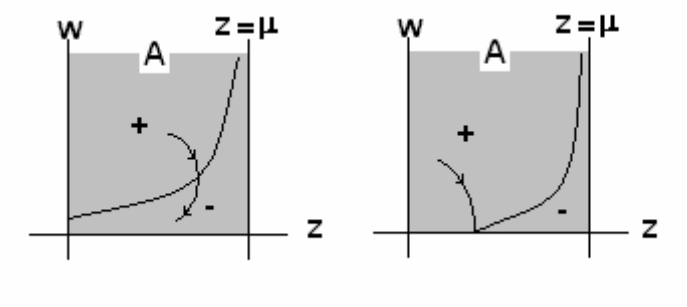

Fig. 4. Typical behavior of $\tilde{\gamma}(t)$.

Lemma 9: *If the curve* $\tilde{\gamma}(t)$ *enters* A^- *then it converges to a intersection point of* $G(g)$ *and* z *axis, or it is converges to a point* $(0, w)$ *on* w *axis with* $w \leq g(0)$.

Proof: Suppose that $t_0 \geq 0$ and $\tilde{\gamma}(t_0) \in A^-$. From lemma 5 and lemma 7, for all $t \geq 0$ we have $\dot{w} < 0$. Therefore, $\tilde{\gamma}(t)$ dose not intersects $G(g)$ for t>0. This means that $\tilde{\gamma}$ is contained in A^- for all $t > t_0$, hence $z(t)$ and $w(t)$ are decreasing for $t > t_0$. Suppose that $\lim_{t\to+\infty}(z(t), w(t)) = (z_1, w_1)$. Same argue as lemma 8 shows that

$$z_1 h(z_1, w_1) = 0, \quad -\alpha_d z_1 w_1 = 0.$$

If $z_1 \neq 0$ then we have $h(z_1, w_1) = 0$ and $w_1 = 0$ which means that (z_1, w_1) is a intersection point of $G(g)$ and z axis. If $z_1 = 0$ then $(0, w_1) \in \overline{A^-}$ is a point on w axis with $w \leq g(0)$. This completes the proof.

Lemma 8 and 9 show that any curve $\tilde{\gamma}(t)$ of a compatible solution $\gamma(t)$ which stars in A, converges to a intersection point of $G(g)$ and z axis or converges to a point on w axis with $w \leq g(0)$. The case of convergence to a intersection point of $G(g)$ and z axis is when the DNA damage signal is damped to zero. Alternatively, If $\tilde{\gamma}(t)$ converges to a point on the w axis then it is the cause that the DNA damage signal contains a permanent damage. Therefore the bifurcation of the DNA damage signal is controlled by $G(g)$ as $\tilde{\gamma}(t)$ is entrapped by $G(g)$ in $A^{\pm}$ and leaded to one of the cases.

The map $w = g(z)$ has two critical point $z_1 = \mu + k_{1s} - \sqrt{k_{1s}(\mu + k_{1s} + k_{2s})}$ and $z_2 = \mu + k_{1s} + \sqrt{k_{1s}(\mu + k_{1s} + k_{2s})}$ which are minimum and maximum point respectively. It is easy to see that $z_1 < \mu < z_2$ and $g(z_1) > g(z_2)$, furthermore, $g(z)$ is increasing for $z_1 \leq z \leq z_2$ and decreasing for $z \notin [z_1, z_2]$. Hence, if $z_1 \leq 0$ then $g(z)$ has no critical point in A and intersection of $G(g)$ and A is a increasing curve, but if $0 < z_1 < \mu$, then z_1 is the only critical point of $g(z)$ in A. In the later case, if $g(0), g(z_1) < 0$ then intersection of $G(g)$ and A is an increasing curves which enters into A from a point on w axis, but if $g(z_1) < 0$ and $g(0) > 0$ then intersection of $G(g)$ and A enters into A from a point on z axis and it contains two curves which are decreasing and increasing respectively. These show that the way which $G(g)$ intersects A is controlled by sing of z_1, $g(z_1)$ and $g(0)$. These make six cases $(a), (b), ..., (f)$ which are listed in table A and showed in figure 5. It is easy to see that $z_1 \leq 0$ if and only if $\Lambda < 0$ and $g(0) \leq 0$ if and only if $\Delta \leq 0$, furthermore $g(z_1) = \Omega$, where Λ, Δ and Ω are bifurcation parameters introduced by the theorem 2. Now, the lemmas 4 to 9 show that behavior of $\tilde{\gamma}$ in each case of table A is as it is shown in figure 6.

If $\Lambda \le 0$ then change of sign of Δ makes a bifurcation which is showed through cases $(a),(b)$ and (c) (see the table A and the figure 6). This proves part (1) of the theorem .

If $\Lambda > 0$ then change of the sign of Ω makes a bifurcation which is showed through cases $(c),(d),(e)$ and (f) (see the table A and the figure 6). This proves part (2) of the theorem.

Table A: here as mentioned before, $g(z_1)$, $0 < z_1 < \mu$, is the only local minimum value for $g(z)$.

$z_1 \le 0,\ g(0) > 0$	(a)
$z_1 \le 0,\ g(0) = 0$	(b)
$g(z_1), g(0) < 0$	(c)
$z_1 > 0,\ g(0) > 0 > g(z_1)$	(d)
$z_1 > 0,\ g(0) > g(z_1) > 0$	(e)
$z_1 > 0,\ g(0) > 0 = g(z_1)$	(f)

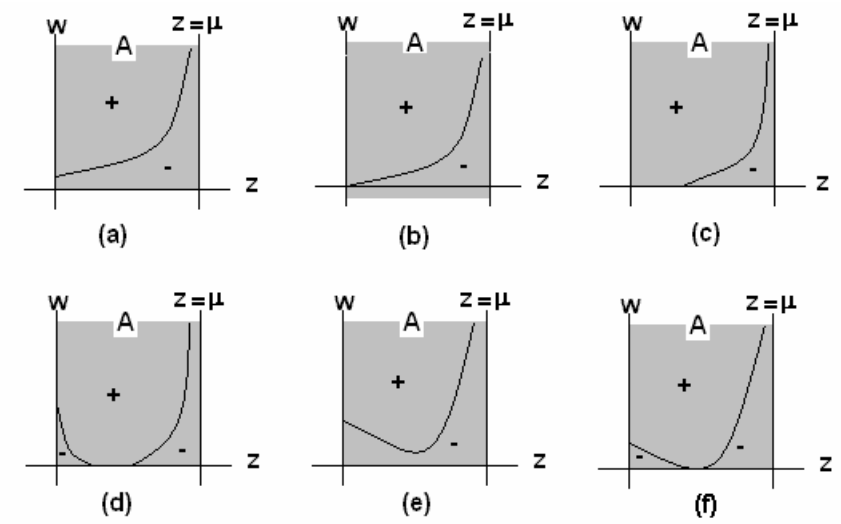

Fig. 5. According to the rows of table A, here we draw all possible plots for $G(g)$.

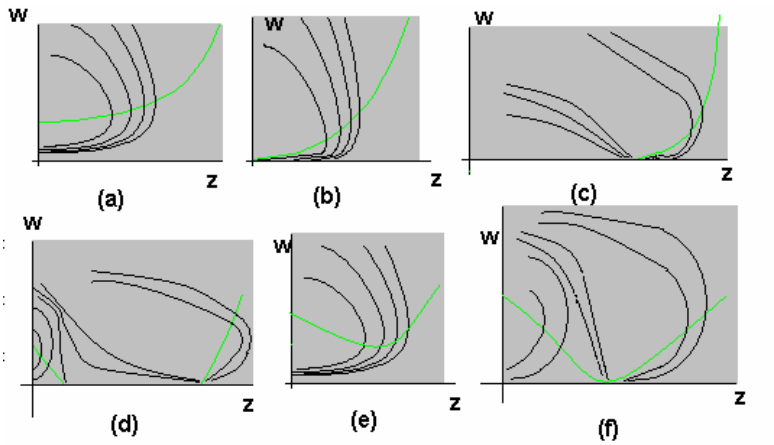

Fig. 6. Certain behavior of $\tilde{\gamma}(t)$ with respect to all possible plots for $G(g)$. Here we can see the effect of $G(g)$ on the convergence of $\tilde{\gamma}$. In fact, according to the what mentioned after theorem 2, $G(g)$ acts like a controller on the DNA healing process .

Dependence on initial values

The part (2) of the theorem 2 states that if $\Lambda > 0$ and $\Omega < 0$ then some compatible solutions converges to N, this means that there may exist compatible solutions converging to N_w, for some $w \in R$. This fact can be seen through the cases (d) and (f) in the table A. This is biologically interesting, because, as it is shown in the figure 6, in these cases, the model forecasts permanent damage for the DNA if the compatible solutions have simultaneously initial low amount of the DNA damage signal and the Atm-p protein. But, the compatible solutions which has initially enough amount of the DNA damage signal, even if they have initially low amount of the Atm-p protein, converge to N. This may occurs because of the fact that, from the second term of the third equation of the model (3), dephosphorylation rate of Atm-p has inverse relation with amount of the DNA damage signal. Therefore, low amount of the DNA damage signal can not force the system to provide enough Atm-p which is necessary for DNA healing process. However, if a compatible solution has enough initial amount of the Atm-p, then it converges to N, hence DNA will be repaired from damages.

ACKNOWLEDGMENT

This research was supported by Ferdowsi University of Mashhad and partly supported by the Center for Research in Modeling and Computation Linear and Nonlinear Systems, Ferdowsi University of Mashhad (Iran).

REFERENCES

Cohen, T., Prus, D., Shia, J., Abu-Wasel, B., Pinto, M. G., Freund, H.R., Stojadinovic, A., Grakov, A., Perets, T., Nissan, A., (2008). Experssion of p53, p27, and KI-67 in corectal cancer patients of various ethnic origins: Clinical and tissue microarray based analysis. *J. Surg. Oncol.*, **97**, 416-422.

Chicharmane, V., Ray, A., Sauro, H. M., Nadim, A., (2007). A model for p53 dynamics triggered by DNA damages. *SIAM J. Appl. Dyn. Syst.*, **6.1**, 61-78.

Vogelstein, V., Lane, D. Levine, A.J. (2000). Surfing the p53 network, *Nature*. **408**, 307-310.

Harris, S.L., Levine, A.J. (2005). The p53 pathway: Positive and negative feedback loops. *Oncogene*, **24**, 2899-2908.

Hill, A.V. (1910). The possible effects of theaggregation of the molecules of hæmoglobin on its dissociation curves *J. Physiol. (London)*, **40,** IV-VII.

McLure, K.G., Lee, P.K.W. (1998). How p53 binds DNA as tetramer. *EMBO J.*, **17**, 3342-3350.

Banin, S., Moyal, L., Shieh, S., Taya, Y., Anderson, C.W., Chessa, L., Smorodinsky, N.I. , Prives, C., Reiss, Y., Shiloh Y., Ziv, Y., (1998). Enhanced phosphorylation of p53 by ATM in response to DNA damage, *Science*, **281**, 1674–1677.

Kurz, E.U., Lees-Miller, S.P. (2004). DNA damage-induced activation of ATM and ATM-dependent signaling pathways, *DNA Repair*, **3**, 889–900.

Tyson, J.J. (2006). Another turn for p53, *Mol. Syst. Biol.*, **2**, doi: 10.1038/msb4100060.\

Benoit, V., Hellin, A.C., Huygen, S., Gielen, J., Bours, V., Merville, M.P. (2000). Additive effect between NF-kappaB subunits and p53 protein for transcriptional activation of human p53 promoter, *Oncogene*, **19,** 4787–4794.

Ciliberto, A., Novak, B., Tyson, J.J. (2005). Steady states and oscillations in the p53-Mdm2 network. *Cell Cycle*, **4**, 107-112.

Perko, L. (1991). *Differential Equations and Dynamical Systems*. 2nd Ed., Springer-Verlag.

STUDIA UNIVERSITATIS BABEŞ – BOLYAI, BIOLOGIA, LV, 1, 2010, p. 81-90

THE INDUCEMENT OF CHLOROPHYLL FLUORESCENCE IN STATE TRANSITIONS UNDER LOW TEMPERATURE IN THE *Mougeotia* ALGA, STRAIN AICB 560

VICTOR BERCEA[1], CRISTIAN COMAN[1] and NICOLAE DRAGOŞ[2]

SUMMARY. The alga was grown using Bold nutritive solution (BBM) with continuous air stirring and illumination with 485 $\mu mol.m^{-2}.s^{-1}$, at 22^0 C, during exponential growth. F_0 has decreased in *state 2* under preillumination and low temperature, and in *state 1*, in the presence of DCMU and methylviologen, F_0 has been the same with the control value. F_m decreased in both *state 1* and *2* which lead to a decrease of the variable fluorescence. The F_v/F_m and the quantum yield decreased significantly in both redox states, highlighting the photoinhibition of the closed reaction centers. The excitation pressure decreased, and in the presence of DBIMB, it increased in *state 1*, which states the growth of the closed Q_A proportion. q_P has increased in *state 1* which emphasizes the growth of the opened Q_A proportion. The increase in the non-photochemical dissipation of the excitation energy is correlated with the excitation pressure. The inducement of chlorophyll fluorescence with quenching analysis on a short period of time in *state 1* and *2* on whole cells marks out the proportionality ratio with the light harvesting antenna size.

Keywords*:* chlorophyll fluorescence; photochemical activity; photosynthetic inhibitors; state 1- state 2 transitions.

Introduction

Organisms with oxygenic photosynthesis have a photoadjustment mechanism for redistribution of the absorbed light energy between the two photosystems PS I and PS II. This mechanism, called *state 1- state 2 transitions*, is thought to be a short term adaptation for eficient usage of light energy in limitation conditions (Bonaventura and Myers, 1969; Vallon *et al.*, 1991; Williams and Allen, 1987). The state transitions involves a reversible redistribution of the light harvesting antenna between PS I and PS II and optimizes the light energy used in photosynthesis through the cyclic electron current (Canaani *et al.*, 1984; Finazzi *et al.*,2002; Weis, 1985).

[1] *Institute of Biological Research, 48 Republicii Street, 400015/Cluj-Napoca, Romania*
[2] *Faculty of Biology and Geology, Babeş-Bolyai University, 5-7 Clinicilor Street, Cluj-Napoca, Romania, E-mail: bercea_victor@yahoo.com.* ***Research supported by CERES Program nr. 54/2006.***

In green plants *state 1* and *state 2* are induced by exposing the leaves at light 1 far-red which exceeds 715 nm and light 2 between 400-600 nm. In *state 2* are generated both the phosphorylation and decoupling of LHC II from the PS II (Canaani *et al.*, 1984). LHC II, dissociated from PS II, migrate towards stromatic lamellas rich in PS I and couple with PS I due to conformational changes which appear in the protein after phosphorylation (Nilsson *et al.*, 1997).

State 1 transition involves dephosphorylation and dissociation of LHC II from PS I and their migration to grana lamellas rich in PS II. The migration of LHC II to PS I by lateral diffusion (*state 1- state 2* transitions) is produced after phosphorylation of LHC II by a protein kinase bound to the thylakoid membrane and activated by the reduction of plastoquinone (PQ) through PS II or other secondary metabolic processes. In oxidative conditions, the kinase is inactivated through oxidation of PQH_2 by PS I and the LHC II are dephosphorylated by a phosphatase (*state 2- state 1* transitions) bound to thylakoids and permanently active (Allen, 1992; Finazzi *et al.*, 2001a; Forti and Caldiroli, 2005). After dephosphorylation, LHC II returns to PS II.

The cytochrome b_6f complexes play a key role in sending the redox signal from plastoquinol to kinase (Wollman, 2001). The first step of signal transmition is the binding of PQH_2 to Q_0 place in the cytochrome b_6f complexes (Vener *et al.*, 1997). Conformational changes are produced in the lumen of the complexe's Rieske subunit after binding of PQH_2 to Q_0, playing an essential role in the LHC II kinase activation (Finazzi *et al.*, 2001 b). The activation signal generated on the lumenal side of the thylakoids where Q_0 is located needs to be transmitted through the bilayer membrane because the active domain of the kinase is located on the stromatic side of the membrane. In this way, the chlorophyll molecules can supply a direct way for transmitting the signal for quinol binding to Q_0 place to a marginal region of the complex, where the kinase is supposed to be located. The region where the chlorophyll ring is exposed towards the lipidic phase is located near the area proposed as kinase- cytochrome b_6f binding site (Zito *et al.*, 1999). In the state transitions LHC II complexes increase the PS I performance and can represent a shifting mechanism between the liniar and cyclic electron current around the PS I (Vallon *et al.*, 1991).

According Finazzi *et al.* (2001a), *state 1* is induced by incubating the cells in dark with continuous agitation, and *state 2* is obtained by dark incubation in anaerobic conditions through argon pumping. Incubating the algae in conditions which promote *state 2* – anaerobic or aerobic conditions and FCCP – generate an electron source passing through the cytochrome b_6f. Reactivation of the liniar electron current between PS II and PS I needs switching from *state 2* to *state 1*, indicated by the concomitent growth of the fluorescence production (F_m).

In this paper we studied the photochemical activity in *Mougeotia* filaments during state transitions under the effect of low temperature in chemically induced anaerobic conditions and in the presence of certain photosynthetic inhibitors.

Materials and methods

The green alga *Mougeotia sp.* (AICB 560) is originated from the Culture Collection of Algae of the Institute of Biological Research, Cluj-Napoca (AICB) (Dragoş *et al.*, 1997). The alga was grown using Bold (BBM) nutritive solution under continuous air stirring and illumination with 485 μmol.m^{-2}.s^{-1}, at 22^0 C, during exponential growth.

Treatment with light, low temperature and inhibitors. The inducement of the chlorophyll fluorescence with quenching analysis on short term was recorded in *state 1* and *2* by using light 1 and 2 after applying this working protocol:

- measurement light – 650 nm
- working manner: saturation pulse

- **V_1**: actinic light excitation at 4112 μmol.m^{-2}.s^{-1} PAR (665 nm) for 10 seconds (for PS II excitation) – *state 2*
- **V_2:** low temperature treatment (0^0 – 2^0C) for 30 minutes followed by actinic light excitation at 4112 μmol.m^{-2}.s^{-1} PAR (665 nm) for 10 seconds - *state 2*
- **V_3:** low temperature treatment (0^0 – 2^0C) for 30 minutes in the presence of FCCP followed by actinic light excitation at 4112 μmol.m^{-2}.s^{-1} PAR (665 nm) for 10 seconds - *state 2*
- **V_4:** low temperature treatment (0^0 – 2^0C) for 30 minutes in the presence of FCCP and iodoacetamide followed by actinic light excitation at 4112 μmol.m^{-2}.s^{-1} PAR (665 nm) for 10 seconds - *state 2*
- **V_5:** low temperature treatment (0^0 – 2^0C) for 30 minutes in the presence of FCCP, DCMU and methylviologen followed by far-red light excitation (730 nm) for 10 seconds - *state 1*
- **V_6:** low temperature treatment (0^0 – 2^0C) for 30 minutes in the presence of FCCP, DBMIB and methylviologen followed by far-red light excitation (730 nm) for 10 seconds - *state 1*.

Chlorophyll fluorescence analysis. The chlorophyll fluorescence was measured using a PAM-210 fluorometer according to Schreiber *et al.* (1986). The fluorescence parameters and quenching analysis was performed by applying the saturation pulse method. The quantum yield of the photochemical energy conversion was calculated according to the equation Yield = $\Delta F/F'_m$ and the ratio F_v/F_m (F_v/F_m = F_m-F_0/F_m) which gives information on the photochemical quantum yield of closed PS II reaction centers.

Results and discussion

During fluorescence measurement at room temperature on algae whole cells, the fluorescence emission is reversed proportionally with the photochemical yield of PS II and is proportional with the light capture antenna's size. It is possible to see the changes in the antenna's size if the PS II's photochemistry is inhibited using DCMU

(Finazzi *et al.*, 2001b). The 650 nm light excites mainly the PS II photosystem inducing a increased sensitivity of PS I, and the far-red light excites the PS I, inducing a increased sensitivity of PS II (Wollman, 2001).

FCCP (carbonyl cyanide p-trifluoromethoxy-phenylhydrazone) is a decoupling agent which causes the transition to *state 2* by decreasing the ATP and the membrane potential. Iodoacetamide inhibits the activity of Rubisco enzyme (Calvin cycle), and DCMU [3-(3,4-diclorofenil)-1,1-dimetilurea] inhibits the reduction of Q_B from PS II so that the plastoquinone is oxidated by light.

The minimal fluorescence (F_0) has decreased in *state 2* in the presence of preillumination with intense light associated to low temperature, more significantly in the anaerobiosis variants (V_4) (fig. 1). In *state 1*, favorable to the photochemical activity of PS I, in the presence of DCMU inhibitor which affects the linear electron transport and the methylviologen which is the artificial acceptor of electrons from PS I, the F_0 fluorescence has increased reaching the control value (V_5). This proves that in the presence of methylviologen, DCMU inhibitor does not produce negative effects over the electron transport chain. F_0 became almost equal to F_m. *State 2- state 1* transitions is stimulated by oxygen and electron acceptors of PS I such as methylviologen. The oxygen is an electron acceptor acting on the reducing side of PS I – the transfer of electrons to O_2 is done by the Mehler reaction which is involved s*tate 2- state 1* transitions. The increase of F_m in *state 1* transition shows an increase of LHC II antenna. Methylviologen is an acceptor for the electrons from PS I being reoxidated through O_2 and produces O_2^- which is used in the Mehler reactions. When the oxidation of Q_A does not take place, the elctrons are blocked and the PS II does not pump electrons in the electron transport chain as in *state 2*, and F_0 is equal to F_m. Methylviologen accelerates the electron transport towards O_2 (Forti and Caldiroli, 2005).

The maximal fluorescence (F_m) has decreased significantly both in *state 1* and *state 2*. Is notable the almost equal values of F_0 and F_m in the *state 1* of photosystems (V_5) (fig. 1). The decline in the F_m has lead to an decrease of the variable fluorescence (F_v). The results are contradictory. Thus, methylviologen is used as a base for the linear electron transport and produces the F_m diminish, and DBMIB in the presence of methylviologen contributes to the F_m recovery (Gilmore and Yamamoto, 1991). In the preilluminated cells the inhibiting effect of DBMIB over the electron transport is increasing. DBMIB inhibits the kinase activation in the presence of light because reacts with cytochrome b_6f and acts like a fluorescence quencher by binding to the Q_B place in PS II where DCMU also bonds. In *state 2* in dark, DBMIB does not inhibit the kinase activation – there is an increased level of LHC II phosphorylation, and when *state 2* has been reached under illumination, DBMIB inhibits the LHC II phosphorylation.

The results obtained regarding the evolution of maximal and variable fluorescence emphasizes the appearance of photoinhibition in the electron transport chain which is induced by low temperature in association with intense light. Photochemical activity carries on in „down regulation" conditions.

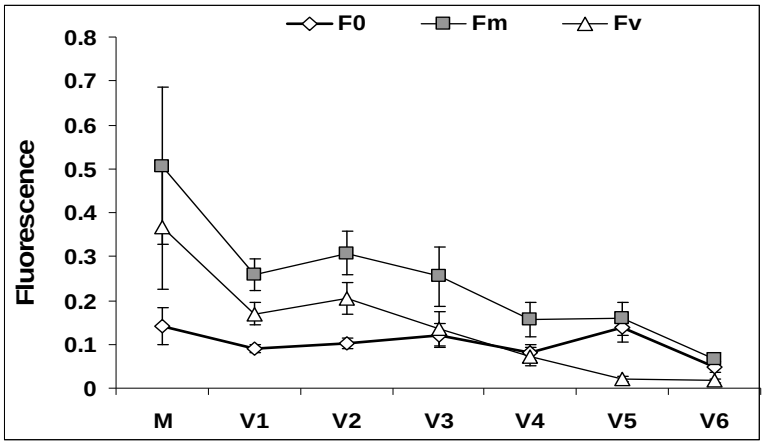

Fig. 1. Evolution of minimal, maximal and variable fluorescence in the conditions of photosystems' *state 1* and *2*. M= control; V_1-V_6 (see material and method)

The photochemical efficiency (F_v/F_m) as well as the quantum yield of the photosynthetic electrons transport chain have decreased significantly in both redox states of the photosystems, highlighting the photoinhibition of the closed reaction centers (fig. 2). In *state 1* in the presence of DBMIB inhibitor it was recorded a slight recovery of the photochemical activity, although DBMIB inhibits the linear electron flow (Joët *et al.*, 2002). This recovery is assigned to the cyclic electron current around PS I. The close numeric values for photochemical effieciency and quantum yield in all variants emphasized the lack of energized state in the thylakoidal membrane. In the state transitions, a decrease in the photochemical efficiency and quantum yield is due greatly to inhibitor effects of low temperature.

Low light exposure produces reversible decrease of photochemical efficiency because photoinhibition appears. The extent of the photoinhibition depends on the capacity of energy usage in photochemical reactions or in thermal dissipation, processes which are used for decreasing the excitation energy for the purpose of decreasing the photosystem's vulnerability to photoinhibition (Kornyeyev *et al.*, 2002). The lack of balance between synthesis and degradation of D_1 protein produces an inhibition of the PS IIs' electrons transport during photoinhibition (Briantais *et al.*, 1988).

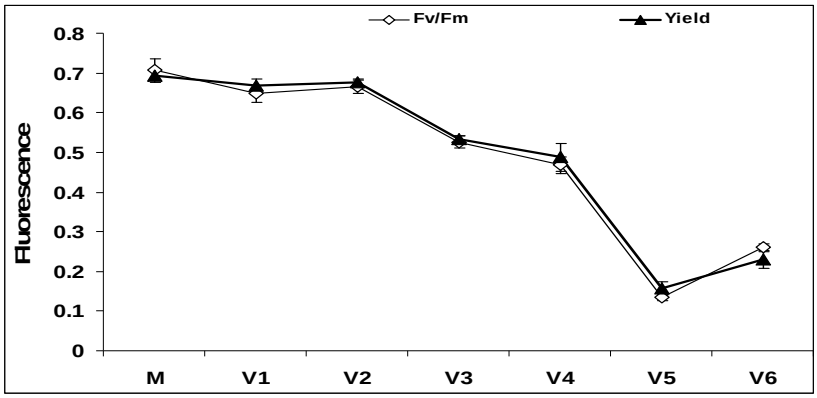

Fig. 2. Evolution of photochemical efficiency (F_v/F_m) and quantum yield in redox *states 1* and *2*.

The photochemical activity of photosystem II in *state 2* unreeled under a decreased excitation pressure reported to the control sample (fig. 3). In *state 1* in the presence of DBIMB the excitation pressure has increased significantly, stating an increase in the proportion of closed (reduced) Q_A (V_6). Functionally, a growth in the excitation pressure is translated in an increased proportion of primary acceptors Q_A in the reduced state, an increased concentration of zeaxanthin and a decreased antennary proteins LHC II. The state transitions are designated by the changes in the redox state of the plastoquinone pool, namely the reduced PQ leads to *state 2* as the core of oxidized PQ leads to *state 1*. The state transitions are accompanied by changes in the phosphorylation of LHC II which suggests that LHC II-kinase might be itself or be associated with a plastoquinol-binding protein. Two protein complexes display quinone/quinol-binding sites in the membrane-embedded photosynthetic electron transport chain: PS II and the cytochrome b_6f complex (Wollman, 2001). The *state 1* favourises the cyclic phosphorylation around PS I and cytochrome b_6f helping the ATP production, and the *state 2* favourises the lineary phosphorylation, producing NADPH for CO_2 fixation.

The state transitions are controlled by the need of ATP: the cells addapted to dark are in *state 2* when the ATP concentration is reduced, and the passing to *state 1* shows a restoration in the ATP content (Finazzi *et al.*, 2001b). The light dependent electron transport from water to monodehydroascorbate is coupled to ATP formation with a ratio $ATP/O_2 = 2$ (Forti and Elli, 1995). The cyclic electron transport around PS I prevents photoinhibition in stress conditions by maintaining a low pH in the thylacoid lumen which allows the dissipation of the excitation energy excess (Heber and Walker, 1992).

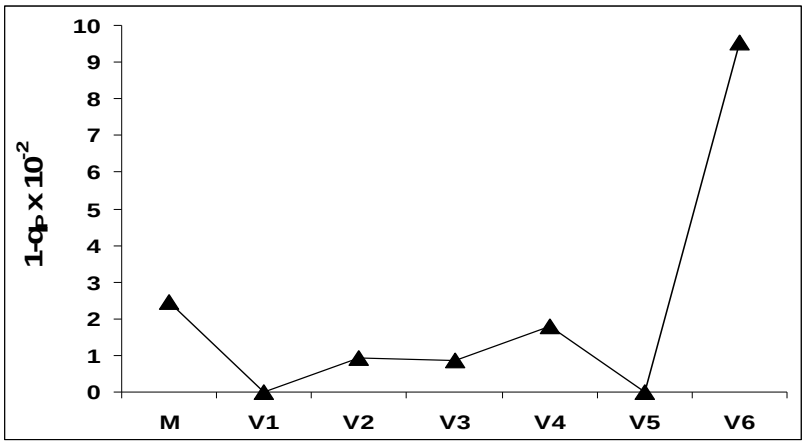

Fig. 3. Evolution of excitation pressure in photosystems' *state 1* and *2*.

In conditions which reduce the light energy consuption in photochemistry and thermic dissipation, the chlorophyll fluorescence increases, while an increase in the excitation energy usage leads to fluorescence quenching (Kornyeyev *et al.*, 2002). The non-radiative dissipation of excitation energy in the photosystems' antenna decreases F_0 and F_m proportionally, and dissipation from reaction centers reduces the F_m only (Gilmore and Yamamoto, 1991). The fluorescence quenching associated to photoinhibition is not correlated directly to degradation of PS II reaction centers (Briantais *et al.*, 1988).

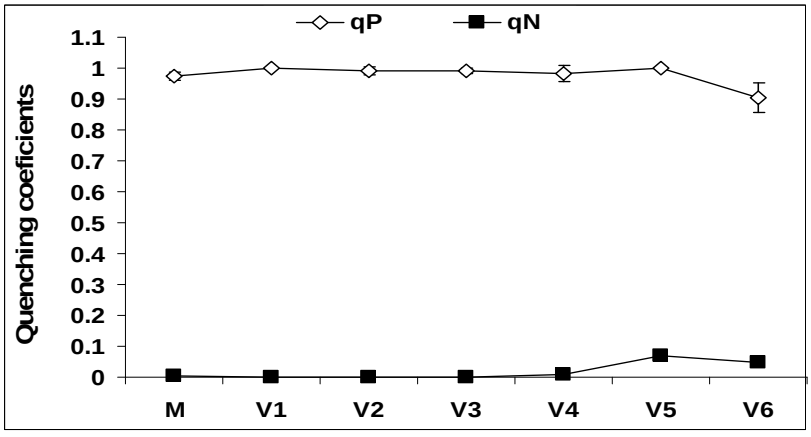

Fig. 4. Evolution of the photochemical (q_P) and non-photochemical (q_N) coefficients in photosystems' *state 1* and *2*.

The photochemical coefficient q_P has maintained at high values in *state 2*, overcoming the control value which states an increase in the proportion of open Q_A (fig. 4). Functionally, the excitation energy has been effectively converted to photochemistry and has been correlated to the quenching of chlorophyll fluorescence. In *state 1*, in the presence of DCMU inhibitor, q_P has reached its maximum value, leading to a reach of the maximum level of photochemical energy conversion. Along with methylviologen, DCMU does not inhibit the electron flow between the two photosystems. In the presence of DBMIB, the linear transport of photosynthetic electrons has been inhibited (V_6), leading to a decrease in the open Q_A proportion and to an increase in the non-photochemical dissipation of the excitation energy, respectively to an increase of the non-photochemical coefficient q_N which corelates to the excitation pressure (Fig. 4).

Conclusions

1. The inducement of chlorophyll fluorescence with quenching analysis on a short period of time in *state 1* and *2* on algae whole cells marks out the proportionality ratio with the light harvesting antenna's size. The minimal fluorescence has decreased in *state 2* in the presence of preillumination with intense light and in association with low temperature or in anaerobiosis conditions, while in *state 1* in the presence of DCMU and methylviologen F_0 has equaled the control values. In the presence of methylviologen, DCMU does not inhibit the electron transport chain, and F_0 has become almost equal to F_m. The maximal fluorescence has decreased in both *state 1* and *2*, which lead to a decrease of the variable fluorescence. The photochemical efficiency as wel as the quantum yield were reduced in both redox states, emphasizing the inhibition of the closed reaction centers.

2. The photochemical activity in *state 2* carried on under a low excitation pressure, and in *state 1* in the presence of DBIMB the excitation pressure increased which states a growth in the closed (reduced) Q_A proportion, respectively, the decrease of LHC II antenna proteins. *State 1* favourises cyclic phosporilation around PS I and cytochrome b_6f, helping the ATP production, and *state 2* favourises linear phosporilation, producing NADPH for CO_2 fixation. The photochemical coefficient values have increased in *state 2* which states an increase of the opened Q_A proportion. Functionally, the excitation energy was effectively converted to photochemistry and was correlated with a decrease in the chlorophyll fluorescence. In the presence of DBMIB, the linear transport of photosynthetic electrons was inhibited, leading to a decrease of the opened Q_A proportion and to an increase of the non-photochemical dissipation of the excitation energy, respectively to a growth of the non-photochemical coefficient which is correlated to the excitation energy.

3. The results obtained reveal the photoinhibition state at the level of the electron transport chain which is induced by low temperature in association with intense light. The photochemical activity unreeles in down regulation conditions. The

Mehler reaction and the cyclic electron current around PS I can contribute to the increase of ATP/NADPH ratio. Maintaining the electron flow in thylakoids in the presence of an enough quantity of $NADP^+$ as an electron acceptor is essential to the protection of chloroplasts against photooxidative stress, process in which participate the cyclic electron current and the water-water cycle around PS I.

REFERENCES

Allen, J.F. (1992). Protein phosphorylation in regulation of photosynthesis. *Biochim. Biophys. Acta*, **1098** (3), 275-335

Bonaventura, C., Myers, J. (1969). Fluorescence and oxygen evolution from *Chlorella pyrenoidosa*. *Biochim. Biophys. Acta*, **189** (3), 366-383.

Briantais, J.M., Cornic, G., Hodges, M. (1988). The modification of chlorophyll fluorescence of *Chlamydomonas reinhardtii* by photoinhibition and chloramphenicol addition suggests a form of photosystem II less susceptible to degradation. *FEBS Lett*., **236**, 1, 226-230

Canaani, O., Barber, J., Malkin, S. (1984). Evidence that phosphorylation and dephosphorylation regulate the distribution of excitation energy between the two photosystems of photosynthesis *in vivo*: Photoacoustic and fluorimetric study of an intact leaf. *Proc. Natl .Acad. Sci. USA*, **81** (6), 1614-1618.

Dragoş, N., Péterfi, L.Şt., Momeu, L., Popescu, C. (1997). An introduction to the algae and the culture collection of algae at the Institute of the Biological Research Cluj-Napoca. Cluj Univ. Press.

Finazzi, G., Rappaport, F., Furia, A., Fleischmann, M., Rochaix, J.D., Zito, F., Forti, G. (2002). Involvement of state transitions in the switch between linear and cyclic electron flow in *Chlamydomonas reinhardtii*. *EMBO Rep*., **3** (3), 280–285.

Finazzi, G., Barbagallo, R.P., Bergo, E., Barbato, R., Forti, G. (2001 a) Photoinhibition of *Chlamydomonas reinhardtii* in state 1 and state 2: damages to the photosynthetic apparatus under linear and cyclic electron flow. *J. Biol. Chem.,* **276** (25), 22251-22257.

Finazzi, G., Zito, F., Barbagallo, R.P., Wollman, F.A. (2001 b). Contrasted effects of inhibitors of cytochrome b_6f complex on state transitions in *Chlamydomonas reinhardtii*: the role of Q_o site occupancy in LHC II kinase activation. *J. Biol. Chem*., **276** (13), 9770-9774.

Forti, G., Caldiroli, G.(2005). State transitions in *Chlamydomonas reinhardtii*. The role of the Mehler reaction in state 2-to-state 1 transition. *Plant Physiol.,* **137** (2), 492-499.

Forti, G., Elli, G. (1995). The function of ascorbic acid in photosynthetic phosphorylation. *Plant Physiol.,***109** (4), 1207 - 1211.

Gilmore, A.M., Yamamoto, H.Y. (1991). Zeaxanthin formation and energy-dependent fluorescence quenching in pea chloroplasts under artificially mediated linear and cyclic electron transport. *Plant Physiol.,* **96** (2), 635-643.

Heber, U., Walker, D. (1992). Concerning a dual function of coupled cyclic electron transport in leaves. *Plant Physiol.*, **100** (4), 1621-1626.

Joët, T., Cournac, L., Peltier, G., Havaux, M. (2002). Cyclic electron flow around photosystem I in C_3 plants. In vivo control by the redox state of chloroplasts and involvement of the NADH-dehydrogenase complex. *Plant Physiol.*, **128** (2), 760-769.

Kornyeyev, D., Logan, B.A., Holaday, A.S. (2002). A chlorophyll fluorescence analysis of the allocation of radiant energy absorbed in photosystem 2 antennae of cotton leaves during exposure to chilling. *Photosynthetica*, **40** (1), 77-84.

Nilsson, A., Stys, D., Drakenberg, T., Spangfort, M.D., Forsén, S., Allen, J.F. (1997). Phosphorylation controls the three-dimensional structure of plant light harvesting complex II. *J. Biol. Chem.*, ***272***,(29), 18350-18357.

Schreiber, U., Schliwa, U., Bilger, W. (1986). Continuous recording of photo-chemical and non-photochemical chlorophyll fluorescence quenching with a new type of modulation fluorometer. *Photosynth. Res.*, **10** (1,2), 51-62.

Vallon, O., Bulte, L., Dainese, P., Olive, J., Bassi, R., Wollman, F.A. (1991). Lateral redistribution of cytochrome b6/f complexes along thylakoid membranes upon state transitions. *Proc. Natl. Acad. Sci. USA*, **88** (18), 8262-8266.

Vener, A.V., Kan, P.J.M., Rich, P.R., Ohad, I., Andersson, B., (1997). Plastoquinol at the quinol oxidation site of reduced cytochrome bf mediates signal transduction between light and protein phosphorylation: Thylakoid protein kinase deactivation by a single-turnoverflash. *Proc. Natl. Acad. Sci. USA*, **94** (4), 1585-1590.

Weis, E. (1985). Light- and temperature-induced changes in the distribution of excitation energy between photosystem I and photosystem II in spinach leaves. *Biochim. Biophys. Acta*, **807 (**2), 118-126.

Williams, W.P., Allen, J.F. (1987). State 1/state 2 changes in higher plants and algae. *Photosynth. Res.*, **13** (1), 19-45.

Wollman, F.A. (2001). State transitions reveal the dynamics and flexibility of the photosynthetic apparatus. *EMBO J.*, **20** (14), 3623-3630.

Zito, F., Finazzi, G., Delosme, R., Nitschke, W., Picot, D., Wollman, F.A. (1999). The Q_o site of cytochrome b_6f complexes controls the activation of the LHCII kinase. *EMBO J.*, **18** (11), 2961-2969.

STUDIA UNIVERSITATIS BABEŞ – BOLYAI, BIOLOGIA, LV, 1, 2010, p. 91-101

MODIFICATION OF THE BONE MINERAL DENSITY, T-SCORE AND Z-SCORE VALUES ACCORDING TO AGE AND ANATOMIC REGION IN OSTEOPOROSIS CASES

RODICA TÖRÖK-OANCE[1], VIRGILIU NICULESCU[2] and MARIOARA NICOLETA FILIMON[3]

SUMMARY. The bone resistance largely depends on the bone mineral density. Osteoporosis is a disease in which the bone resistance is affected, and establishing a diagnostic of certainty can be achieved by determining the bone mineral density. The present paper is based on the analysis of the results of the osteodensitometric investigation conducted on 361 patients who had been diagnosed with primary or secondary osteoporosis. The investigation took into account the hip bone and the vertebral column, and the following parameters have been analyzed: bone mineral content, bone mineral density, T-score and Z-score. We analyzed the evolution of the bone mineral density with increasing age, the existence of a connection between the bone mineral density determined at the vertebral column and at the hip, the connection between the T- and Z-score and age at the population we took into account, as well as the existence and the type of discordance in diagnosis for the two points of determination.

We found out that there is a decrease in the bone mineral density above the age of 40; concerning the T-score, there is an obvious decrease tendency with ageing, both at the vertebral column and at the hip, while in the case of the Z-score, the tendency is that of increasing with age. The most frequent discordance in diagnosis found in the population we analyzed is the minor one. The axial skeleton is preponderantly affected.

Keywords: age, bone mineral density, osteoporosis, T-score, Z-score

Introduction

The bone mineral density represents the decisive element of bone resistance, explaining for the most part its variability. The bone density expresses the bone quantity

[1] *West University of Timişoara, Faculty of Chemistry, Biology and Geography, Department of Biology, str. Pestalozzi, 16, Timisoara, Romania. E-mail: rodica.torok@cbg.uvt.ro*
[2] *University of Medicine and Pharmacy „Victor Babeş" Timişoara, Department of Anatomy;*
[3] *West University of Timişoara, Faculty of Chemistry, Biology and Geography, Department of Biology.*

per unit of surface (g/cm^2) or per volume unit (g/cm^3). The planimetric estimation of a bone mineral density is realized by using the dual energy X-ray absorptiometry.

The analysis of the bone mineral density is essential for the osteoporosis diagnostic of certainty. Osteoporosis is the most frequent bone disease (Werner and Vered, 2000) which affects millions of people around the world, and its prevalence is increasing as a result of population ageing. In 1994, the World Health Organization defined osteoporosis as a disease characterized by reduced bone mass and deterioration of the bone micro architecture, with a resulting increase in bone fragility and an increased risk of fracture.

Given the fact that the microarchitectural deterioration cannot be directly measured, the World Health Organization has recommended that the osteoporosis diagnosis should be done by measuring the bone mineral density with the help of the dual energy X-ray absorptiometry. The bone mineral density (BMD) values can be quantified in g/cm^2 or can be converted into T-score and Z-score, respectively. Thus, in what concerns the reduction in bone mass, the following diagnostic categories have been established: normal BMD, corresponding to a T-score with a standard deviation of -1 or greater, osteopenia, corresponding to a T-score with a standard deviation between -1 and -2.5, and osteoporosis, corresponding to a T-score with a standard deviation of -2.5 or below.

In the last fifteen years, a major progress has been made in understanding, preventing and treating osteoporosis. This progress is a result of the new technologies, which allowed for accurately measuring the bone mineral density and for introducing efficient treatments, which reduced the incidence of osteoporotic fractures.

Oftenly osteoporosis goes undiagnosed and untreated; the fact that, frequently, this disease does not manifest itself clinically until a bone fracture occurs contributes to this situation. The identification of those individuals with an increased risk and the carrying out of a prevention treatment are extremely important, because they can lead to a decrease in morbidity and mortality.

The purpose of this paper is to analyze the modification of the bone mineral density and of the T-score and Z-score according to age and region of BMD determination. The significance of this analysis resides in the fact that the appearance of this disease is directly connected with the decrease of the bone mineral density.

Materials and methods

The present paper is based on the analysis of the results of the osteodensitometric investigation conducted on 361 patients who had been diagnosed with primary or secondary osteoporosis (**Table 1**). The osteodensitometry was performed at the Timişoara Clinical Hospital no. 1, with the help of a Hologic QDR apparatus, Delphi W model. The investigation was performed at the hip bone and at the vertebral column, and the following parameters have been analyzed: bone mineral content, bone mineral density, T-score and Z-score.

Table 1.

Types of osteoporosis, age and sex distribution of osteoporosis in 361 patients.

Parameter		Number of patients		
		Male	**Female**	**Total**
Type of osteoporosis	Idiopathic juvenile osteoporosis	1	2	**3**
	Postmenopausal osteoporosis	0	246	**246**
	Senile osteoporosis	4	72	**76**
	Secondary osteoporosis	15	21	**36**
Age group	< 40	2	11	**13**
	40 - 44	1	12	**13**
	45 - 49	2	28	**30**
	50 - 54	0	67	**67**
	55 - 59	5	62	**67**
	60 - 64	2	35	**37**
	65 - 69	3	56	**59**
	70 - 74	2	41	**43**
	75 - 79	2	26	**28**
	≥ 80	0	4	**4**

The T-score is calculated on the basis of the difference between the patient's bone mineral density and the average bone mineral density of a healthy adult population (of the same sex and race), related to the standard deviation of that population. The Z-score is calculated on the basis of the difference between the patient's bone mineral density and the average bone mineral density of a population of the same age, related to the standard deviation of that population.

A patient's Z-score indicates the number of standard deviations which are below or above the mean value of the same age persons. A Z-score value of 0 means that the patient's bone mineral density coincides with the bone mineral density mean value for the respective age. A Z-score value of -1, for example, shows that the patient's bone mineral density is lower than the mean value for the respective age, being 1 standard deviation below the mean value.

The T-score indicates the number of standard deviations which are below the mean value of the bone mineral density of young adults (25-45 years old). A T-score value of 0 shows that the patient's bone mineral density corresponds to the mean value found in the case of young adults (Cummings *et al.*, 2002*)*.

The individual data have been introduced in research tables and quantified. For processing the data and for the graphs, we used Excel and GraphPad InStat 3.05 programs. In the statistical tests, we used the following interpretation of the p-

values (Marzillier, 1990): $p < 0.05$ = significant, $p < 0.01$ = highly significant, $p < 0.001$ = extremely significant and $p > 0.05$ = nonsignificant.

Results and discussion

Modification of bone mineral density with age and skeletal region

Since osteoporosis is directly connected with the decrease of bone mineral density, we analyzed the evolution of the bone mineral density with increasing age, at the patients who have been diagnosed with osteoporosis. We calculated the mean value of the bone mineral density for each age group. We observed (**Fig. 1.A**) that the bone mineral density decreases with age, both for the determinations performed at the vertebral column, and for those performed at the hip bone. We noticed a beginning of the decrease in the bone mineral density after the age of 40. Our results correspond to what has been observed in other studies, namely the fact that bone reduction starts after the age of 40 (Center and Eisman, 1997).

Although the reduction of the bone mineral density both at the vertebral column and at the hip bone is obvious, we observed that, between the age of 50 and 65, the decrease is more significant at the vertebral column, while after the age of 65 the decrease at the hip bone surpasses that at the vertebral column.

It is well known that in the first 5-10 years after the installation of menopause, the reduction of the spongy bone tissue is predominant (25-30%), as opposed to the compact bone tissue, which undergoes a reduction of 10-25% in this period (Pajouhi *et al.*, 2004). This reflects in the greater decrease of the bone mineral density at the vertebral column, because the spongy bone tissue is dominant here, with only a thin covering of compact bone. There are also studies (Arlot *et al.*, 1997) that show that, after the age of 75, a massive bone reduction takes place in most parts of the skeleton. We noticed the same thing in what concerns the vertebral column and the hip bone: a massive decrease occurs, in both these regions, after the age of 70.

We analyzed the connection between the mean value of the bone mineral density at the vertebral column and the mean age determined for each of the age groups in discussion. The calculated correlation quotient has a negative value ($R = -0.8193$, while $R^2 = 0.6713$), which demonstrates the fact that there is an inverted connection between these two parameters: an increase in the age leads to a decrease of the bone mineral density. Since the value of the correlation quotient is high, the connection is tight and very significant ($p=0.0038$) (**Fig. 1.B**).

We performed the same analysis for the mean value of the bone mineral density at the hip bone and the mean age for each age group. In this case, the correlation quotient is -0.853 ($R^2 = 0.7276$), the connection is inverted as well, even tighter than in the case of the vertebral column, and very significant, the p-value being smaller than in the previous case ($p=0.0017$) (**Fig. 1.C**).

Modification of T and Z- score values with age and skeletal region

We also analyzed, for all patients, the existence of a connection between the bone mineral density determined at the vertebral column and that determined at the

hip bone. Our results (**Fig. 2**) show there is a direct, but not very tight connection between the bone mineral density at the vertebral column and at the hip bone, the value of the R correlation quotient being 0.4521 (R^2 = 0.2044, p=0.6786).

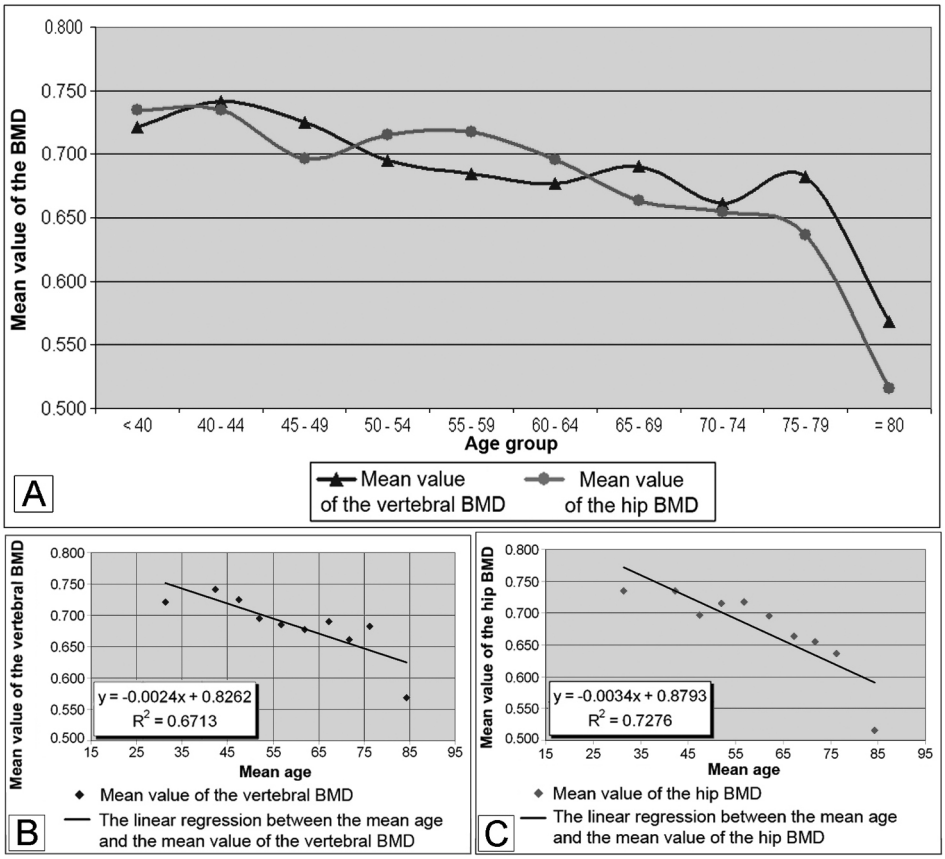

Fig. 1. A. Evolution of bone mineral density (BMD) with age; B. The regression between age and BMD mean values, as determined at the vertebral column; C. The regression between age and BMD mean values, as determined at the hip bone.

Since the T-score is calculated by taking into account the absolute value of the bone mineral density, the correlations between regions are similar, even if they are made in accordance with the bone mineral density (**Fig. 1**), or with the T-score.

By realizing the regressions between the patients' age and the T- and Z-scores at the vertebral column and hip bone, we can notice that the correlation quotient does not show a tight connection in none of these cases. Nevertheless, in the case of the regression between age and the T-score (**Fig. 3**) there is, for the T-

score values, an obvious decrease tendency with increasing age, both at the vertebral column and at the hip bone, which is consistent with the decrease in the bone mineral density that comes with age (**Fig. 1.A**).

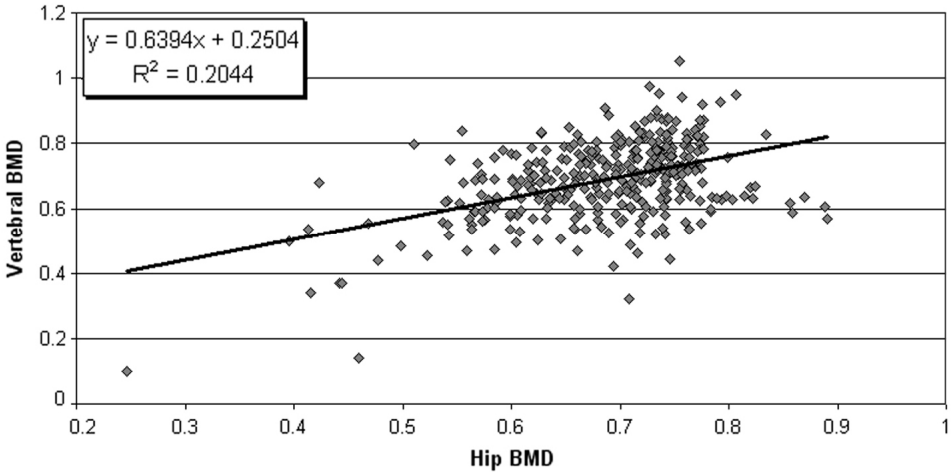

Fig. 2. The regression between the BMD determined at the hip bone and the BMD determined at the vertebral column in all cases. According to the values of the correlation quotient there is a not very tight connection between the bone mineral density determined at the hip and at the vertebral column.

On the other hand, the Z-score, which also takes into account the patient's age, has a tendency of increasing with age, both in the case of the vertebral column, and in that of the hip bone (**Fig. 4**). This also explains the correlation quotient's greater values, as compared with the previous situation. Thus, in what concerns the regression between the Z-score and age, we noticed that age explains 27.26% of the Z-score variability at the vertebral column (R^2= 0.2726, p<0.0001) and 7.01% of the Z-score variability at the hip bone (R^2=0.0701, p<0.0001). The situations in which the Z-score has very low values at some patients contribute to a decrease of the correlation quotient's value and is motivated by the fact that we have included, in our research, the secondary osteoporoses as well. Abrahamsen *et al.*, (1997) have found the same evolutions of the T- and Z-scores at the vertebral column and hip bone.

The literature (Maghraoui *et al.*, 2007) has shown the fact that, although there is a correlation between the bone mineral density as determined in different anatomic regions, a certain discordance in diagnosis between them can be found as well. Our results reflect the same thing: the fact that the connection between the bone mineral density as determined at the level of the two anatomic regions under

discussion is not very tight leads, in some cases, to different diagnostic categories for these regions.

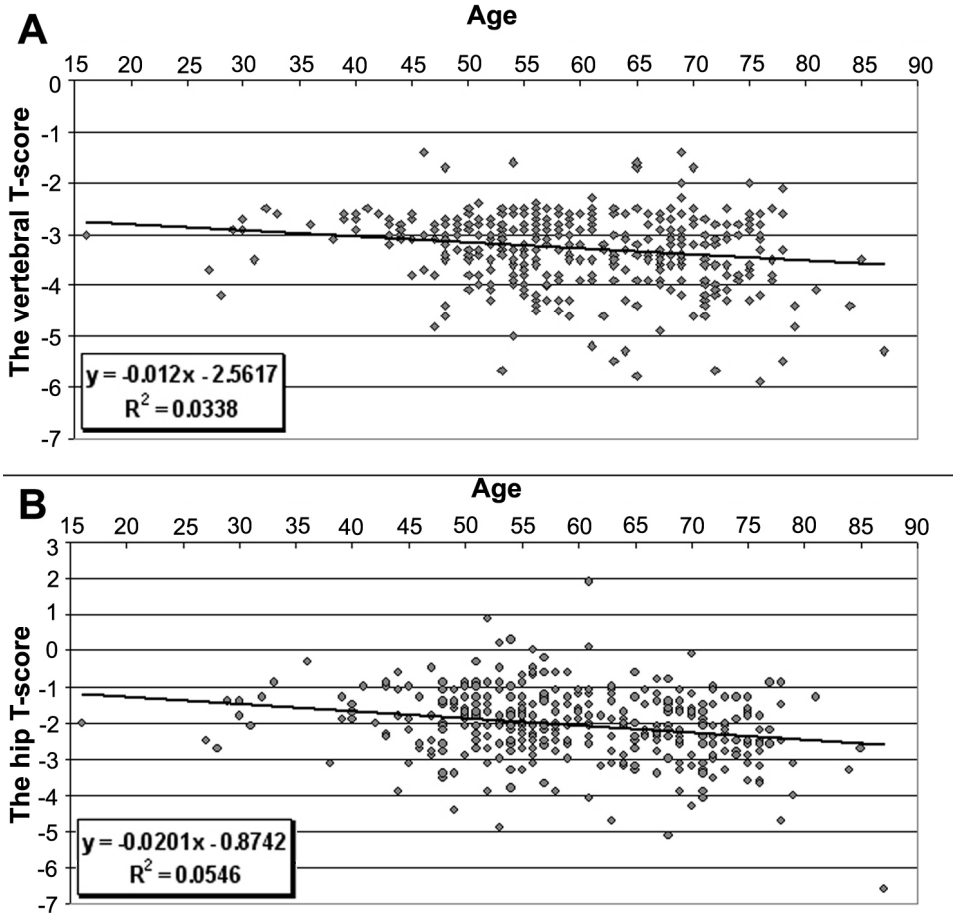

Fig. 3. The relation between the T-score and age: A, vertebral column; B, hip. In both cases, at the vertebral column and at the hip, there is a decrease tendency of the T-score with increasing age. This is related to the fact that the calculation of the T-score takes into account the bone mineral density of a healthy adult population.

Taking into account the T-score values at the level of the two determination regions, the vertebral column and the hip, the following situations can occur in the case of the patients who have been diagnosed with osteoporosis: vertebral osteoporosis – hip osteoporosis, vertebral osteoporosis – hip osteopenia, vertebral osteoporosis – normal

values at the hip, vertebral osteopenia – hip osteoporosis. Theoretically speaking, there is also the possibility of having normal values at the vertebral column and osteoporosis at the hip, but we haven't encountered this situation in the set we analyzed.

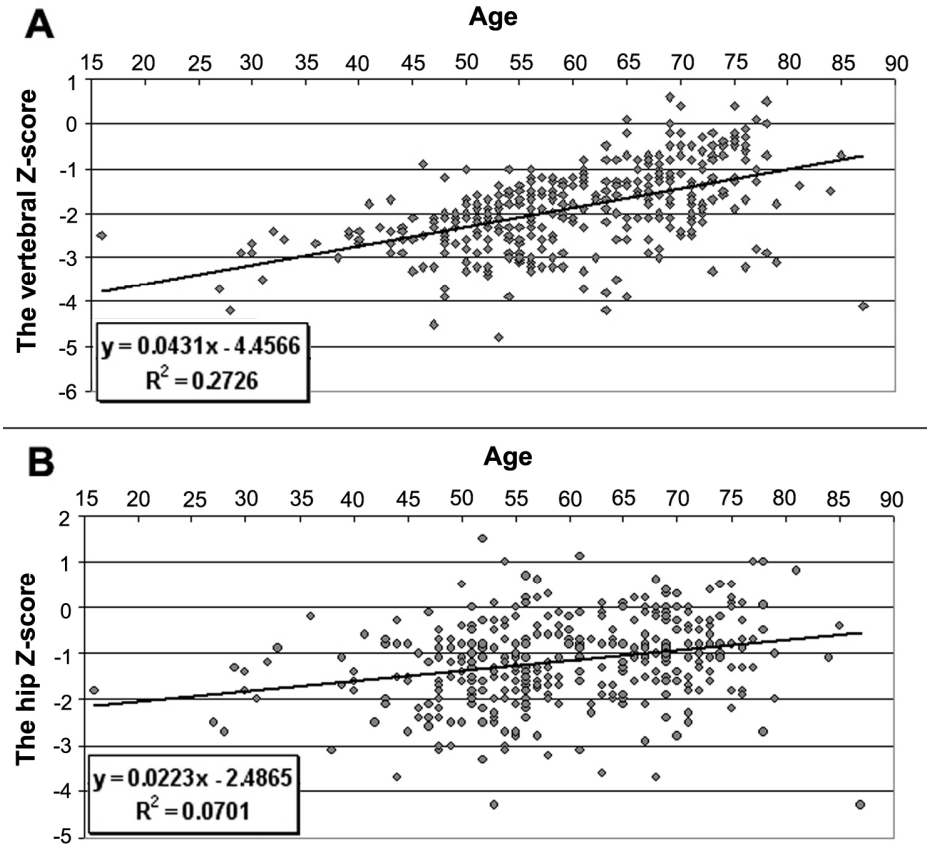

Fig. 4. The relation between the Z-score and age in the analyzed set:
A, vertebral column; B, hip.
The Z-score has an increase tendency with increasing age, both at the vertebral column and at the hip bone. This is related to the fact that the calculation of the Z-score takes into account the bone mineral density of a population of the same age.

We noticed that the most numerous cases are those of vertebral osteoporosis and hip osteopenia (56.94%). They are followed by the cases of both vertebral osteoporosis and hip osteoporosis (29.17%), and then by those with normal values at the hip and vertebral osteoporosis. The least numerous cases are those of hip osteoporosis and vertebral osteopenia (4.44%) and those of vertebral osteoporosis, with

normal values at the hip bone (9.72%). According to these values (**Fig. 5**) we noticed that the axial skeleton is preponderantly affected. The fact that we included, in our research, the secondary osteoporosis cases contributes to these results; the main part of these causes (the excess of glucocorticoid hormones, the hyperthyroidism, the malabsorption syndrome, the rheumatoid polyarthritis, certain medication) have as a result the initial damage at the vertebral column (Moayyeri *et al.*, 2005).

The existence of two different T-score categories for two anatomic regions of the same patient has been described in the literature as discordance in diagnosis. The discordance is minor if the diagnostic categories are adjacent (osteoporosis – osteopenia, osteopenia – normal values). When the diagnostic categories are osteoporosis – normal values, the discordance is major.

There are multiple causes for the discordance in diagnosis. They can be of a physiological nature, connected to the natural adaptive reaction of the skeleton to internal and external factors, of a physiopathological nature, as a consequence of an anatomical affection and connected to the presence and composition of the surrounding tissues, of technical nature, concerning the equipment used for determination or the faulty determination. Moayyeri *et al.*, (2005) have researched this discordance in diagnosis in osteoporosis. Most of the patients included in their research (58.3%) had the same T-score categories both at the vertebral column and at the hip bone, a minor discordance in diagnosis was encountered in 38.9% of the cases, while a major discordance was found in only 2.7% of the cases.

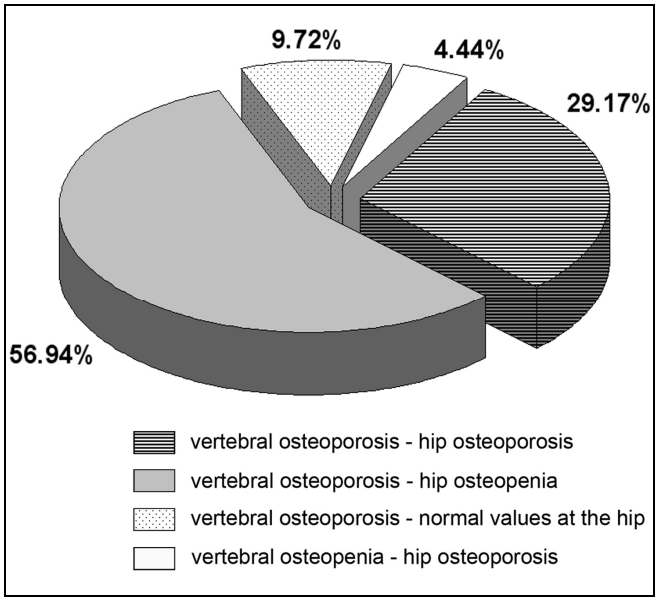

Fig. 5. Diagnostic categories at the vertebral column and at the hip. According to the T-score determined for each patient both at the vertebral column and at the hip bone we

noticed four different situations. The most frequent was the situation of vertebral osteoporosis associated with hip osteopenia. In all cases there was affected the vertebral column.

There are multiple causes for the discordance in diagnosis. They can be of a physiological nature, connected to the natural adaptive reaction of the skeleton to internal and external factors, of a physiopathological nature, as a consequence of an anatomical affection and connected to the presence and composition of the surrounding tissues, of technical nature, concerning the equipment used for determination or the faulty determination. Moayyeri *et al.*, (2005) have researched this discordance in diagnosis in osteoporosis. Most of the patients included in their research (58.3%) had the same T-score categories both at the vertebral column and at the hip bone, a minor discordance in diagnosis was encountered in 38.9% of the cases, while a major discordance was found in only 2.7% of the cases.

Our results are slightly different. The cases with a major discordance in diagnosis are the rarest situation as well (9.72%). This is followed by the situation in which osteoporosis is diagnosed for both regions, the most frequent being the minor discordance in diagnosis (61.38%). According to Masud and Francis (2000), the discordance is more frequent in the first years of postmenopause than in women over 60 years old.

Conclusions

In the set of patients we analyzed, the decrease of the bone mineral density starts after the age of 40, both at the vertebral column, and at the hip bone. This decrease of the bone mineral density becomes more significant after the age of 70, in both determination regions.

There is an inverted connection, tight and very significant ($p=0.0038$), between the bone mineral density determined at the vertebral column and age. Likewise, there is an inverted connection, tight and very significant, between the bone mineral density determined at the hip bone and age ($p=0.0017$), the connection being even tighter than in the previous case ($p=0.0017$).

We also noticed the existence of a direct and not very tight connection between the bone mineral density determined at the vertebral column and, respectively, at the hip bone; the R correlation quotient's value is 0.4539 ($R^2 = 0.2044$, $p=0.6786$).

There is also an obvious decrease tendency, with increasing age, of the T-score values, both at the vertebral column, and at the hip bone. On the other hand, the Z-score, which also takes into account the patient's age, shows an increase tendency both at the vertebral column, and at the hip bone.

In the set of patients we analyzed, we noticed, according to the T-score, that the axial skeleton is preponderantly affected. The most frequent situations are those of minor discordance of diagnosis between the two regions under investigation, followed by the cases of the unitary diagnosis. The least frequent was the major discordance of

diagnosis. Also, there were no cases of T-score normal values for the vertebral column related to T-score values that could indicate osteoporosis at the hip.

REFERENCES

Abrahamsen, B., Hansen, T., Jensen, B., Herman, A., Eiken, P. (1997). Site of osteodensitometry in perimenopausal women: correlation and limits of agreement between anatomic regions, *J. Bone Miner. Res.*, **12** (9)**,** 1471-1479

Arlot, M., Sornay-Rendu, E., Garnero, P., Vey-Marty, B., Delmas, P. (1997). Apparent pre- and postmenopausal bone loss evaluated by DXA at different skeletal sites in women: the Ofely Cohort, *J. Bone Miner. Res.*, **12** (4)**,** 683-690

Center, J., Eisman, J. (1997). The epidemiology and pathogenesis of osteoporosis, *Bailliere's Clinical Endocrinology and Metabolism*, **11**, (1), 23-62

Cummings, S., Bates, D., Black, D. (2002). Clinical Use of Bone Densitometry, *JAMA*, **288** (15), 1889-1897

Maghraoui, A., Abayi, D., Ghazlani, I., Mounach, A., Nouijai, A., Ghazi, M., Achemlal, L., Bezza, A. (2007). Prevalence and risk factors of discordance in diagnosis of osteoporosis using spine and hip bone densitometry, *Ann. Rheum. Dis.*, **66**, 271-272

Masud, T., Francis, R. (2000) The increasing use of periferal bone densitometry, *BMJ*, **321**, 396-398

Marzillier, L. (1990). *Elementary statistics*, William C. Brown Publishers, U.S.A., pp.500

Moayerri, A., Soltani, A., Tabari, N., Sadatsafavi, M., Hossein-neghad, A., Larijani, B. (2005). Discordance in diagnosis of osteoporosis using spine and hip bone densitometry, *BMC Endocr. Disord.*, **5** (3), doi:10.1186/1472-6823-5-3

Pajouhi, M., Maghbooli, Z., Hejri, S., Keshtkar, A., Saberi, M., Larijani, B. (2004). Bone mineral density in 10 to 75 year-old Iranian healthy women: population base study, *Iranian J Publ Health, a supplementary issue on Osteoporosis*, 57-63

Werner, P., Vered, I., (2000). Management of osteoporosis: a survey of Israeli physicians knowledge and attitudes, *Isr. Med. Assoc. J.*, **2**, 361-364.

STUDIA UNIVERSITATIS BABEŞ – BOLYAI, BIOLOGIA, LV, 1, 2010, p. 103-110

THE ELECTRICAL RESISTANCE OF ACUPUNCTURE SOURCE POINTS AS A RELEVANT FACTOR FOR INNER ORGAN STATUS

ŞTEFAN-CLAUDIU MIRESCU[1, 2], LIDIA CIOBANU[2, 3], VASILE ANDREICA[2, 3] and CORINA-LUMINIŢA ROŞIORU[1]

SUMMARY. The galvanic skin response (GSR), is the skin's resistance to electrical current. Responsible for the variation of the GSR are the sweat glands, which react to nearly all stimuli. The variation of the GSR has been used for decades in biofeedback research, polygraph tests and even religion. The purpose of the study is to review the behavior of the skin's electrical resistance. The GSR was measured using a Wheatstone bridge, of our own manufacturing. The study was conducted on patients with internal diseases. The initial resistance was recorded, then the GSR was recorded for one minute. The subjects were asked a number of questions and data were computer recorded. On the first minute of measurement, the GSR followed a linear pattern. The measurements revealed a decrease of the electrical resistance during the dialogue, especially when the subject was asked questions with emotional content. There is a correlation between the GSR and the relaxed state of the subject. The GSR is a prompt and efficient tool for evaluating the subjects' state of mind. Further research will be conducted to indicate other uses of this measurement.

Keywords: galvanic skin response, acupuncture source points, electrodermal response.

Introduction

Galvanic skin response (GSR), also known as electrodermal response, psychogalvanic reflex, or opposite of the skin conductance, is a measure of the electrical resistance of the skin. Most of the researches at the moment investigate the spontaneous fluctuations of the GSR according to the emotional state of the subject (Jaggar and Robbins, 2001). These studies suggested GSR as a reference method for polygraph tests, biofeedback therapy or sleep apnea investigation. GSR has also proven to be a valid method for neurological studies (Fitzgerald and Folan-Curran, 2002). The purpose of the study is to test the relevance of the GSR measurements in specific acupuncture points, called source (Chinese - Yuan) points, for describing inner organ health status.

[1] *Faculty of Biology and Geology, Chair of Experimental Biology "Babeş-Bolyai" University, Cluj-Napoca*
[2] *Faculty of Medicine, University of Medicine and Pharmacy "Iuliu Haţieganu", Cluj-Napoca*
[3] *"Octavian Fodor" Third Medical Clinic, Cluj-Napoca*

Materials and methods

Source points localization. According to the Chinese traditional medicine, there are 12 meridians along the body, each corresponding to an organ or system (Dumitrescu and Constantin, 1977). Each meridian has its source (or Yuan) point (Popa, 2000). All these points are located equally on the hands and on the feet.

Many early researches tried to find out the morphological and functional substrate of acupuncture meridians and points, especially the source points (Jaggar and Robinson, 2001). Histological sections and imagistic methods did not prove to be useful in identifying meridians. Electrical studies were performed and revealed that there were points on the body in which the electrical resistance was clearly modified compared to the electrical resistances of the nearby skin. These points resembled the meridians from the Chinese traditional meridians. The electrical resistance was found to be tenfold lower than in other extra-meridian points. Electrical potential measurements were also performed and demonstrated that the voltage was slightly increased in these points. A low electrical resistance, corroborated with higher electrical potential in these points led the researchers to the conclusion that these points are the *energetic batteries* of the human body (Van der Valk and Groen, 1952). Further researches were based on these conclusions (Zimlichman *et al.*, 2005; Lurie *et al.*, 2007).

The instrumentation. A four arms Wheatstone bridge of our own manufacturing was used for measurements (Fig. 1.). The reference electrode was taped on the back of the left hand and the 12 measurement electrodes were taped to the corresponding source points (six on the hand and six on the foot). For commuting between the points, a 12 positions rotary switch was used. The bridge was connected to a 6 V power source and the output was connected to a precision voltmeter. By adjusting the voltmeter to zero using the potentiometer included in the circuit, the electrical resistance between the electrodes was displayed. This cycle was repeated 12 times for each patient.

The patients. The study was performed on 17 patients with gastroenterological and rheumatismal disorders. The measurements were taken at approximately the same hour of the day, because some studies suggest that the acupunctural response is time dependant (Şteflea, 1986). Consent was obtained from each patient and from hospital's director.

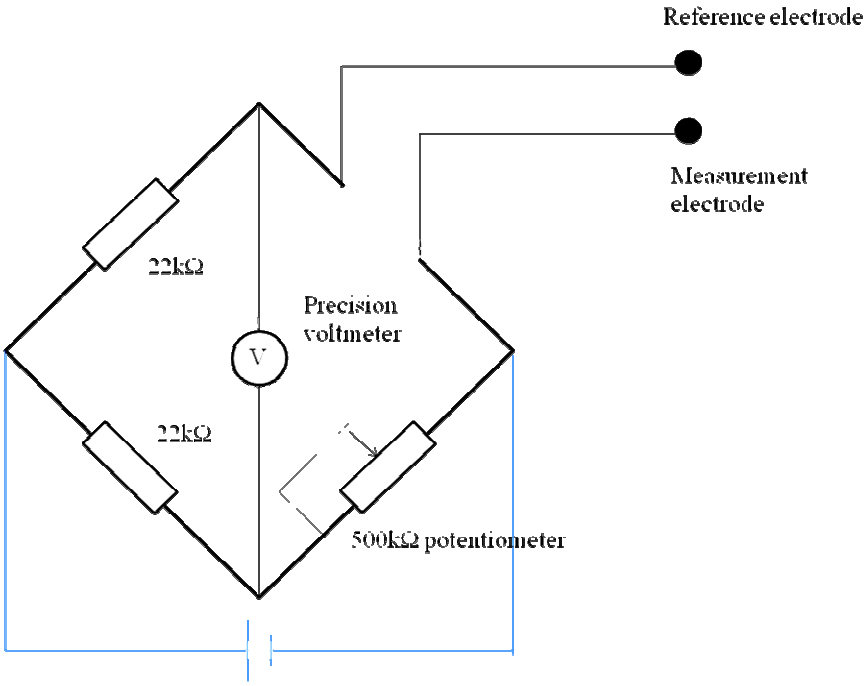

Fig. 1. The Wheatstone bridge used in the measurements (Osiac *et al.*, 2000)

Results

Because of the low number of participants included in the study, a statistical analysis could not be performed. The results are based on individual cases, eliminating the redundancy of presenting one pathological entity twice or more.

Testing the bridge. After the initial implement of the device, the bridge was tested to verify its precision. It is a well-known fact that the electrical resistance of the skin is modified by the subject's physical and mental state. With two electrodes connected to the finger 2 and 4 of the left hand, the subject was asked to perform some simple motor acts with the right hand, like making the fist. Then, the subject was asked to cough and to keep his eyes closed for 10 seconds, followed by the opening of the eyes.

At the beginning of the measurement, the electrical resistance was increasing slightly, as the patient entered a relaxed state of mind. At the beginning of the motor acts, the electrical resistance registered an abrupt decrease, for a few seconds. Likewise, when the subject opened his eyes, after a few seconds of closure, the electrical resistance slightly dropped (Fig. 2.).

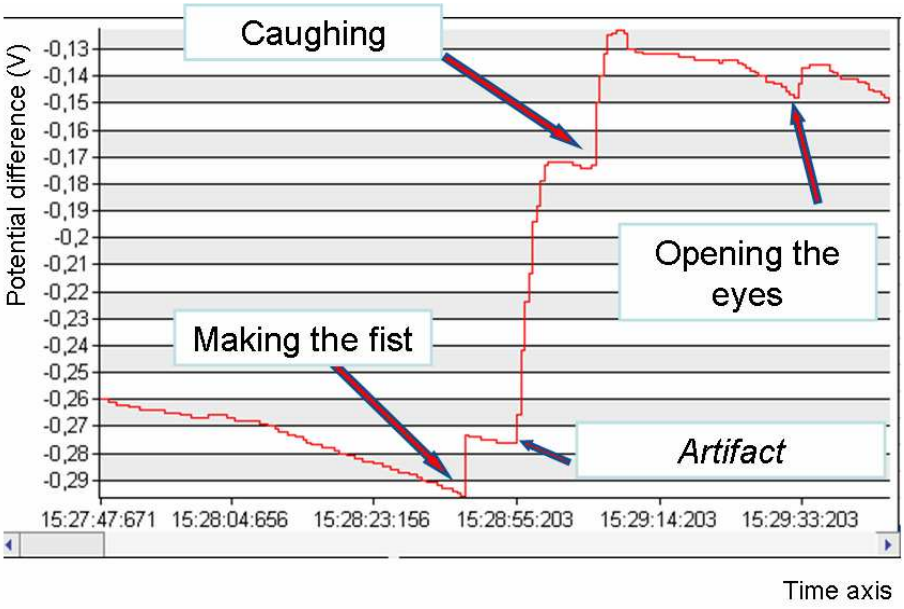

Fig. 2. The variation of the electrical resistance during some simple motor acts. The Y axis represents the voltage, which varies inversely with resistance

With the same electrodes connected, the subjects were tested for the psycho galvanic reflex. They were asked a number of neutral questions (e.g. *Do you live in Cluj-Napoca at the moment?* or *Do you have a cat at home?*) and a number of emotional content questions (e.g. *Have you ever witness a tragic auto accident?* or *Do you get along well with your spouse?*). On asking the emotional content questions, the decrease in electrical resistance was significantly greater than when asking the neutral questions (Fig. 3.).

Precisely revealing the psycho galvanic reflex, the bridge proved its accuracy in measuring the electrical resistance of the skin.

Pathological measurements. The main criterion for the patients to be included in the study was to exhibit at most two internal pathologies. Patients with more than two distinct pathologies could influence the accuracy of the determination. The investigated pathologies included: liver steatosis, surgical organ ablation, biliary diskinesia, rheumatismal disease, hepatitis C and heart failure.

The data obtained from the measurements were compared to the medical documents, which were considered gold standard for diagnosis.

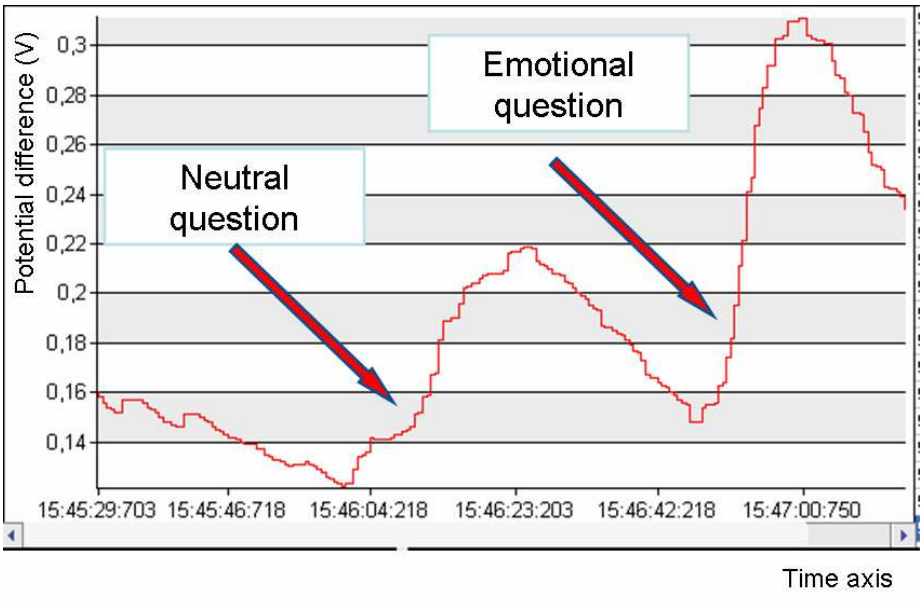

Fig. 3. The variation of the electrical resistance during answering neutral and emotional questions answering. The Y axis represents the voltage, which varies inversely with resistance.

The following are examples of measurements, corresponding to the pathologies above mentioned:

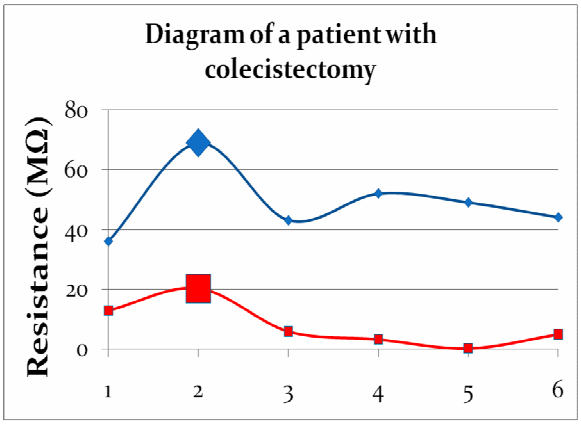

Fig. 4. Diagram of a patient with colecistectomy; legend of the points: 1=bladder; 2=gall bladder; 3=liver; 4=kidney; 5=spleen; 6=stomach

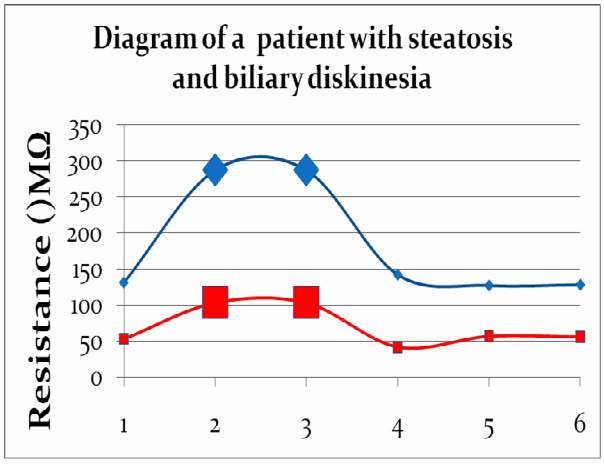

Fig. 5. Diagram of a patient with steatosis and biliary diskinesia; legend of the points: 1=bladder;2=gall bladder; 3=liver; 4=kidney; 5=spleen; 6=stomach

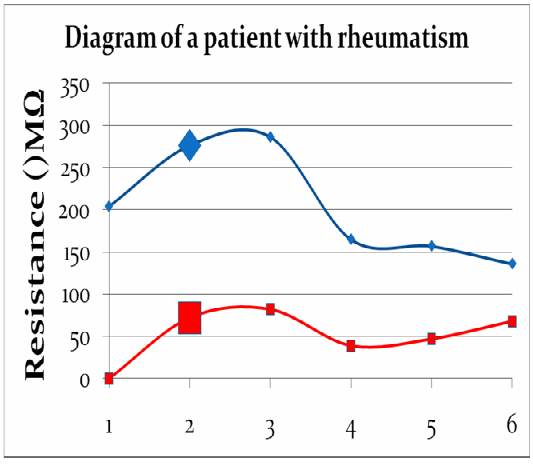

Fig. 6. Diagram of a patient with rheumatismal disease of the hand; legend of the points: 1=small intestine; 2=rheumatismal point; 3=large intestine; 4=lung; 5=pericardium; 6=heart

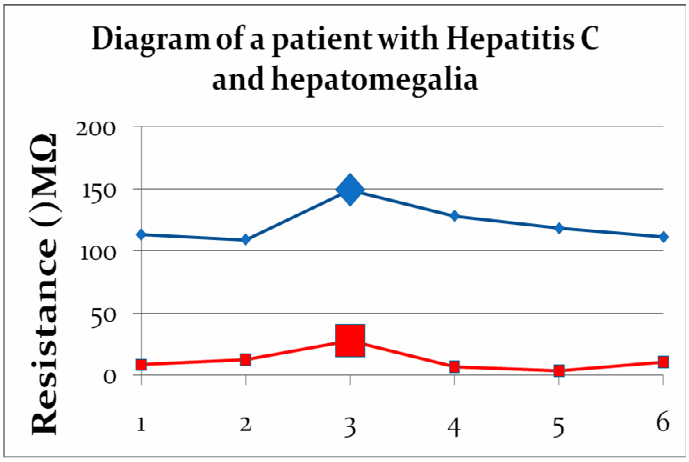

Fig. 7. Diagram of a patient with hepatitis C and hepatomegalia; legend of the points: 1=bladder; 2=gall bladder; 3=liver; 4=kidney; 5=spleen; 6=stomach.

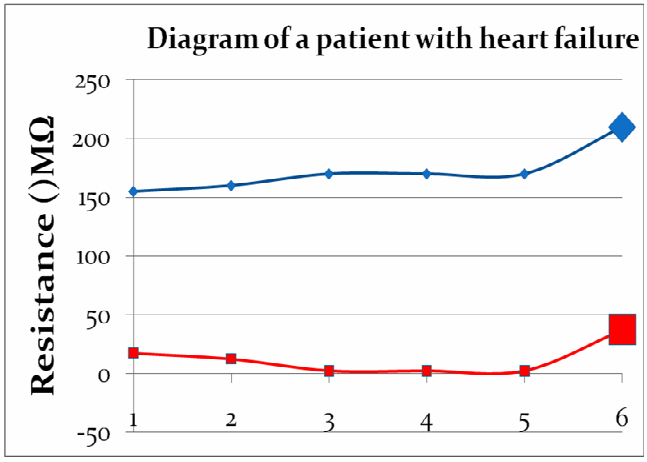

Fig. 8. Diagram of a patient with heart failure; legend of the points: 1=small intestine; 2=rheumatismal point; 3=large intestine; 4=lung; 5=pericardium; 6=heart

Discussions

As concluded from the testing of the device, the electrical resistance is a very sensitive and precise measure of changes in the body. Somatic movement and also emotional status are expressed in electrical resistance terms.

In pathological terms, patients with inner organ diseases presented a modified electrical resistance in the corresponding source points. At some instance, a patient who had undergone laparoscopic surgery for colecistectomy, said that she electrocutes herself when touching any metal object. At measurement, this patient expressed a very low electrical resistance.

Further studies will be made to test different currents' performances in providing clearer data and a more accurate diagnosis.

REFERENCES

Dumitrescu, I.F., Constantin, D. (1977) *Acupunctură ştiinţifică modernă*, Ed. Junimea, Iaşi, pp. 382

Fitzgerald, M.J.T., Folan-Curran, J. (2002) *Clinical neuroanatomy*, Saunders, Londra, pp. 323

Jaggar, D.H., Robinson, N.G. (2001) *History of veterinary acupuncture, 2nd Edition*, Mosby, St. Louis

Lurie, Y., Landau, D.A., Kanevsky, A., Pel, S., Zelber-Sagie, S., Oren, R. (2007) Medex Test, a novel modality for liver disease diagnosis, *J Clin Gastroenterol*, **41**, 700-705

Osiac, A., Petrescu, Z., Roşu, V., Vîlceanu, S. (2000) *Fizică*, Ed. Corint, Bucureşti, pp 176

Popa, A. I. (2000) *Electropunctură*, Ed. Fundaţia Mirabilis, Bucureşti, pp. 165

Şteflea, D. (1986) *Cronobiologia şi medicina*, Editura Medicală, Bucureşti, pp. 384

Van der Valk, J.M., Groen, J. (1952) Electrical resistance of the skin during induced emotional stress. A study of normal individuals and of patients with internal disease, *World Federation for Mental Health International Congress*

Zimlichman, E., Lahad, A., Aron-Maor, A., Kanevsky, A., Shoenfeld, Y. (2005) Measurement of electrical skin impedance of dermal-visceral zones as a diagnostic tool for inner organ pathologies: a blinded preliminary evaluation of a new technique, *IMAJ*, **7**, 631-634

STUDIA UNIVERSITATIS BABEŞ – BOLYAI, BIOLOGIA, LV, 1, 2010, p. 111-118

=== REVIEW ===

OXIDATIVE STRESS AND INFLAMMATION – KEY PLAYERS IN TUMOR ANGIOGENESIS

MARIUS COSTEL ALUPEI[1]*, RAMONA MARIA MAXIM[1]* and MANUELA BANCIU[1]

SUMMARY. Tumor angiogenesis has a crucial role in tumor development and the metastasis. Initiation and angiogenesis development is a result of the interaction of two tumor-associated processes: inflammation and oxidative stress. Therefore, a better understanding of molecular mechanisms that play a key role in tumor angiogenesis-associated inflammation and oxidative stress can offer promising strategies for future anticancer therapies.

Keywords: cancer, angiogenesis, oxidative stress, inflammation

Introduction in tumor angiogenesis

Angiogenesis-formation of new blood vessels from pre-existing vasculature or progenitors of endothelial cells, has a crucial role in physiological events, like embryogenesis and wound healing, as well as, in tumor growth and metastasis (Hall and Ran, 2010). This process is regulated by the balance between proangiogenic and antiangiogenic factors (Rosen, 2002, Sato,2003). The presence of excessive angiogenesis is usually associated with pathology such as cancer (Crowther et al. 2001). Since 1971, Judah Folkman has shown that the growth of the tumor beyond a size of 2 mm^3 depends on the development of its own vasculature. The newly-formed blood vessels ensure maintenance of tumor cellular viability via favoring the efficient metabolic exchange of oxygen, nutrients, and waste products in tumor tissue.

Tumor angiogenesis is two stage-process in tumor development. In the first stage called "**angiogenic switch**", tumor cells express an proangiogenic phenotype via the activation of various oncogenes and/or mutation of tumor supressor genes in tumor cells (Banciu, 2008; Crowther *et al*., 2001; Gupta and Qin, 2003; Sato, 2003). Several studies have been shown that hypoxia is a potent cause for the switch of the balance between proangiogenic and antiangiogenic factors favoring the release of pro-angiogenic factors by tumor cells (Crowther *et al*., 2001). A major role in hypoxia response involves activation of hypoxia inducible factor-1 (HIF)-1 (Sato,2003).

[1] *Faculty of Biology and Geology, Babes-Bolyai University, 400006, Cluj-Napoca Romania.*
**Both authors have equal contribution to this review*

HIF-1 is a transcription factor that induces further activation of various oncogenes and/or mutation of tumor suppressor genes in tumor cells, which collectively activate the proangiogenic/proinflammatory genes (encoding for **v**ascular **e**ndothelial **g**rowth **f**actor (VEGF), **b**asic **f**ibroblast **g**rowth **f**actor (bFGF) **c**yclo**ox**ygenase (COX)-2) (Crowther *et al*., 2001; Sato, 2003). Moreover, in tumor cells, hypoxia induces production of excessive reactive oxygen species (ROS), which in turn modulates HIF-1 and proangiogenic protein synthesis.

The second angiogenic stage is called "**inflammatory angiogenesis"** due to the involvement of infiltrated inflammatory cells overstimulated by microenvironmental stress factors secreted by tumor cells (Crowther *et al*., 2001; Gupta *et al*., 1984; Albini *et al*., 2005). In tumors, inflammatory cells such as macrophages, T cells, neutrophils, eosinophils, monocytes, mast cells fully participate in the angiogenesis steps by production of the majority of pro-angiogenic/pro-inflammatory factors that stimulate recruitment, proliferation, migration and activation of the endothelial cells and finally tumor blood vessel formation (Albini *et al.* 2005, Banciu, 2008; Naldini and Carraro, 2005).

Consequently, oxidative stress and inflammation seems to be central forces in tumor angiogenesis. Therefore, this review will briefly summarize the current findings related to the involvement of oxidative stress and inflammation in tumor angiogenesis.

Oxidative stress in tumor development

The oxidative stress is a state of the cell characterized by excessive production of reactive oxygen species (ROS) (Dayem *et al*., 2010). In cellular metabolism there is equilibrium between production of ROS and the antioxidant mechanisms. Disturbance in the balance between oxidant and antioxidant mechanisms in the favor of the generation of ROS will lead to the major damaging effects on the important cellular components- proteins, nucleic acids and lipids (Wienberg *et al*., 2010). In healthy cells, the physiological levels of ROS are maintained by non-enzymatic and enzymatic antioxidant agents like glutathione, thioredoxin, superoxide dismutase , catalase and peroxidases (Wang and Yi, 2008).

ROS have a major contribution in initiation, promotion and progression of tumor cell phenotypes. ROS-mediated DNA damage is known to play an important role in initiation of carcinogenesis due to their interaction with pyrimidines, purines and chromatin proteins. As a result, tumor cells develop an increased rate in DNA base modifications, genomic instability and modifications in gene expression (Fruehauf and Meyskens, 2007). Oxidative stress induced by ROS is one of the most important regulatory mechanisms involved in carcinogenesis through induction of nuclear or mitochondrial DNA mutations, and oxidation of intracellular proteins and lipids structures (Tandon *et al*., 2005)**.**

In tumor cells, ROS can be generated from a variety of sources, including mitochondrial electron transport system, activities of xanthine oxidase, the cyotochrome p450 and NADPH oxidase (Ushio-Fukai and Nakamura, 2008). Nevertheless, in tumors, ROS generation is a consequence of the common characteristics of tumor tissues such as ischemia, excessive glycolysis, inadequate neovascularization and infiltration of inflammatory cells (Benz and Yau, 2008)**.** These features enable production of excessive levels of ROS, superoxide anions (O_2^-) and hydrogen peroxide (H_2O_2) (Lopez-Lazaro, 2010).

Key players in oxidative stress

For many years, oxidative stress has been shown to have negative influence on cells, these studies being focused on the suppression of ROS. Cells have developed antioxidant mechanisms, comprising of enzymatic and low molecular weight compounds, in order to counteract oxidative stress and to detoxify the free oxygen radicals. With great importance for these processes are the enzymes, *superoxide dismutase* (SOD), which catalyses the dismutation of superoxide radicals to hydrogen peroxide, and both *catalase* (CAT) and *glutathione peroxidase* (GPX) which convert hydrogen peroxide to water (Gonzales *et al*., 1984). The balance between ROS and the antioxidant enzymatic activity is very important for cellular homeostasis. Low levels of ROS are involved in cellular signalling and have an crucial role in normal cell proliferation. In tumor cells, there is a negative correlation between tumor suppressor protein p53 and SOD activity. In tumor cells p53 is present in low amounts and SOD activity is increased with the production of high levels of H_2O_2 that favor cell proliferation and a very high rate of mutagenesis (Chung-man Ho *et al*., 2001). Moreover, several studies suggested that elevated H_2O_2 levels promote the activation of the hypoxia inducible factor (HIF) pathway. HIF is a family of transcription factors that act as cellular oxygen sensors, initiating an activation of the cellular response (Guzy and Schumacker, 2006).

One of the most important causes responsible for ROS generation is hypoxia (Lopez-Lazaro, 2007). Hypoxia is also able to activate a signalling cascade that leads to induction or repression of the transcription of a multitude of genes implicated in angiogenesis, glucose metabolism and cell survival/death (Brahimi-Horn and Pouyssegur, 2007). The most important mediator in response to low oxygen availability is HIF-1. HIF-1 is a heterodimer composed of HIF-1α, a subunit tightly regulated by tissue oxygen levels and HIF-1β which is constitutively expressed (Rapisarda *et al.*, 2009). Several studies have shown a high level of HIF-1 expression in tumors, together with other transcription factors involved in modulation of oxidative stress induced by increased hypoxia. Although a high amount of ROS are generated in tumors, HIF-1 expression is maintained at a relatively constant concentration (Guzy and Schumacker, 2006). This fact is explained by various intracellular regulatory mechanisms that involve activation of oncogenes which are important for initiation of Ras-Raf-ERK/(mitogen-activated protein kinase) MAPK

pathway involved for tumor cell proliferation (Denko, 2008). Although the secondary effects of oncogenes are not fully understood, oncogenes have a major contribution for the increased accumulation of HIF-1α (Brahimi-Horn and Pouyssegur, 2007). Mitochondrial ROS ensure HIF-1α stabilization by blocking the activity of prolyl hydroxylase involved in mechanisms of recognition HIF-1α for proteasomal degradation (Denko, 2008).

Besides this positive effect exerted by ROS on HIF-1, several studies have been shown that ROS can decrease HIF-1α levels by signaling an increase in prolyl hydroxylase activity (Denko, 2008, Qutub and Popel, 2008).

Involvement of oxidative stress in tumor angiogenesis

Tumor angiogenesis – is a key process in tumor progression (Miller *et al*., 2009). Angiogenic mechanisms are activated by various cellular stress factors, such as hypoxia, low pH, nutrient deprivation and ROS (Eichhorn *et al*., 2007). Endothelial cells are responsible for high ROS generation, such as O_2^- and H_2O_2, involved in different pathophysiological responses. The primary source of ROS in endothelial cells is the activity of NADPH oxidase. In low concentrations ROS can act as signalling molecules that mediate endothelial cell proliferation and migration, facilitating angiogenesis (Ushio-Fukai, 2006).

In tumor cells, oxidative stress increases the production of angiogenic factors. The hypoxic states present during tumor development generate a high amount of ROS (Sihvo *et al*., 2003). Hypoxia also activates HIF-1 expression, the main regulator of vascular endothelial growth factor (VEGF) and of other pro-angiogenic proteins. ROS is also responsible for activation of NF-kB, a transcription factor capable to upregulate HIF-1 (Xia *et al*., 2007). Moreover, ROS, in particularly H_2O_2, have been demonstrated to directly stimulate angiogenesis in tumor cells and endothelial cells by enhancing the production of VEGF (Miller *et al*., 2009). Even more important, it is widely known that H_2O_2 is increased in cancer cells due to the lack of catalase activity (Chung-man Ho *et al*., 2001).

Inflammation – role in tumor angiogenesis

Since 1863, Virchow has shown the relation between inflammation and cancer, suggesting that tumors tended to occur at sites of chronic inflammation. Moreover, epidemiologic studies presented that chronic inflammatory diseases are frequently associated with increased risk of cancers (Balkwill and Mantovani, 2001). Chronic inflammation is involved in all stages of carcinogenesis. Recent findings have proven that the tumor development from inflammation might be a process driven by inflammatory cells as well as a variety of mediators, including cytokines, chemokines, and enzymes, which altogether could create an inflammatory microenvironment (Coussens and Werb, 2004). After „angiogenic switch" in tumor cells, the inflammatory cells infiltrating the tumor fully participate in the angiogenic process by recruitment,

proliferation, migration and activation of the endothelial cells as well as by production of the majority of proangiogenic factors: vascular endothelial growth factor (VEGF), hepatocyte growth factor (HGF), matrix metalloproteinase-2 (MMP2) and interleukin-8 (IL-8) (Albini *et al.*,2005; Banciu, 2008; Balkwill *et al*., 2005; Naldini and Carraro, 2005; Zou, 2005). For that reason this step of angiogenesis is also called tumor **inflammatory angiogenesis** (Albini *et al*., 2005; Banciu, 2008; Naldini and Carraro, 2005). Consequently, inflammation-dependent angiogenesis seems to be a central force in tumor growth and expansion, a concept supported by the observation that the use of anti-inflammatory drugs leads to angiogenesis inhibition (Albini *et al*., 2005; Banciu, 2008).

Key cell players in tumor inflammation

The inflammatory microenvironment of neoplastic tissues include neutrophils, T cells, neutrophils, eosinophils, monocytes that expressed Tie-2 receptors, dendritic cells, macrophages, and mast cells. All these cell types possess the capacity to produce cytokines, cytotoxic mediators like ROS, serine and cysteine proteases, metalloproteinases (MMPs) and membrane perforating agents (Balkwill and Mantovani, 2001; Coussens and Werb, 2002; Nakayama *et al*., 2004).

The innate immune cells contribute to cancer development through direct and indirect mechanisms. The direct mechanisms are: DNA damage induced by generation of ROS and regulation of intracellular pathways via activaition of transcription factors such as NF-κB and HIF-1. The indirect mechanisms include promotion of angiogenesis and tissue remodeling by the production of growth factors, cytokines, chemokines and matrix metalloproteinases; COX-2 upregulation; suppression of antitumour adaptative immune responses. The adaptive immune cells also contribute to modulation of cancer by direct and indirect mechanisms. The direct mechanisms comprise: inhibition of tumor growth by antitumor cytotoxic-T-cell activity and inhibition of tumor growth by cytokine-mediated lysis of tumour cells (de Visser *et al*., 2006).

Among the immune cell populations present in tumor tissue, tumor-associated macrophages (TAM) seem most important in promoting and coordinating tumor growth (Banciu *et al*., 2008). TAM are a major component of tumor leukocyte infiltrate, being recruited by chemokines *i.e.* monocyte chemotactic protein (MCP). Chronic inflammation induced by TAM represents a source of **r**eactive **o**xygen **s**pecies (ROS) which, depending of their level, could modulate the immune system, and affect cell proliferation, stimulating angiogenesis by activation of oxidative stress enzymes responsible for stabilization of HIF-1α (Fruehauf and Meyskens, 2007). ROS generated in TAM but also in neutrophils via a plasma membrane bound nicotinamide adenine dinucleotide phosphate, reduced form (NADPH)-oxidase deliver a sublethal oxidative stress to tumor cells. Tumor cells exposed to sublethal oxidative stress will have a higher capacity of metastasis due to the reduction of tumour cell adhesion to basement membrane components (Brown and Bicknell, 2001). TAM are an important source of pro-inflammatory cytokines and chemokines (TNF α (**t**umor **n**ecrosis **f**actor α),

inter**l**eukins IL-1, 6, 8, IL12p40, MCP-1, 3, 4 (**m**onocyte **c**hemoattractant **p**roteins 1, 3, 4) and pro-angiogenic factors (VEGF, bFGF, IGF (**i**nsulin-like **g**rowth **f**actor), cellular adhesion molecules, metalloproteinases etc) involved in all steps in tumor angiogenesis. TAM also secrete anti-apoptotic proteins for tumor cell protection (FasL - Fas ligand) (Allavena *et al*., 2008; Banciu *et al*., 2006; Banciu *et al*., 2008, Schoppmann *et al*., 2002). Besides protumoral functions of TAM described above, tumor macrophages have antitumoral functions such as: direct cytotoxic effects on tumor cells by inducing phagocytosis of debris and presenting tumor antigens to T cells; indirect antitumoral effects by production of anti-inflammatory (IL-2, interferons and IL-12) and anti-angiogenic proteins (TIMP-1 and 2 (**t**issue **i**nhibitor of **m**etallo**p**roteinases 1, 2)) (Naldini *et al*., 2005; Banciu *et al*., 2008; van der Bij *et al*., 2005). Furthermore macrophages were reported to exert great protective capacity against metastases outgrowth in melanoma-bearing rats with tumor-infiltrating macrophages than in the same experimental models with depleted TAM (van der Bij *et al*., 2005).

Conclusions and perspectives

This review deals with tumor angiogenesis-associated processes: inflammation and oxidative stress. The two processes have both pro- and antitumor actions in tumor development. A proper understanding of both functions offers promise for identification of therapeutic targets for antiangiogenic therapy of cancer.

REFERENCES

Albini A., Tosetti F., Benelli R., Noonan D.M., (2005) Tumor inflammatory angiogenesis and its chemoprevention. *Cancer Res.*, **65** (23), 10637-10641.

Allavena P, Sica A, Garlanda C, Mantovani A., (2008) The Yin-Yang of tumor-associated macrophages in neoplastic progression and immune surveillance. *Immunol Rev*., **222**, 155-161.

Balkwill F, Mantovani A. (2001). Inflammation and cancer: back to Virchow? *Lancet*, **357**, 539 – 545.

Brown N.S., Bicknell R., (2001) Hypoxia and oxidative stress in breast cancer Oxidative stress: its effects on the growth, metastatic potential and response to therapy of breast cancer, *Breast Cancer Res.*, **3**, 323–327.

Banciu, M., Glucocorticoids - a Potential Anti-Angiogenic Cancer Therapy, (2008) *Studia Univ. Babes-Bolyai, Biologia*, **53** (2), 101-114.

Banciu, M., Metselaar, J.M., Schiffelers, R.M., Storm, G. (2008) Antitumor activity of liposomal prednisolone phosphate depends on the presence of functional tumor-associated macrophages in tumor tissue. *Neoplasia*, **10** (2), 108-117.

Banciu, M., Schiffelers, R.M., Fens, M. H. A. M., Metselaar, J.M., Storm, G. (2006) Anti-angiogenic effects of liposomal prednisolone phosphate on B16 melanoma in mice, *J. Control. Release*, **113** (1), 1-8.

Benz, C.C., and Yau, C. (2008). Ageing, oxidative stress and cancer: paradigms in parallax. *Nat. Rev. Cancer*, **8** (11), 875-879.

Brahimi-Horn, M.C., Pouyssegur, J. (2007). Harnessing the hypoxia-inducible factor in cancer and ischemic disease. *Biochem. Pharmacol.*, **73** (3), 450-457.

Chung-man Ho, J., Zheng, S., Comhair, S.A.A., Farver, C., Erzurum, S.C. (2001). Differential Expression of Manganese Superoxide Dismutase and Catalase in Lung Cancer. *Cancer Res.*, **61**, 8578-8585.

Coussens, L.M., Werb, Z., (2002) Inflammation and cancer. *Nature* **420**, 860 – 867.

Crowther, M., Brown, N.J., Bishop, E.T., Lewis, C. E. (2001). Microenvironmental influence on macrophage regulation of angiogenesis in wounds and malignant tumors. *J. Leukoc. Biol.*, **70**, 478-490.

Dayem, A.A., Choi, H.-Y., Kim, J.-H. and Cho, S.-G. (2010) Role of Oxidative Stress in Stem, Cancer, and Cancer Stem Cells, *Cancers* **2:** 859-884.

Denko, N.C. (2008). Hypoxia, HIF1 and glucose metabolism in the solid tumour. *Nat. Rev.*, **8 (**9**)**, 705-713.

De Visser, K.E., (2006) Paradoxical roles of the immune system during cancer development, *Nat. Cancer Rev.*, **6** (1), 24-37.

Eichhorn, M.E., Kleespies, A., Angele, M.K., Jauch, K.W., Bruns, C.J., (2007). Angiogenesis in cancer: molecular mechanisms, clinical impact. *Langenbecks Arch, Surg*,, **392**, 371-379.

Fruehauf, P.J., Meyskens, F.L. (2007). Reactive Oxygen Species: A Breath of Life or Death?. *Clin. Cancer Res.*, **13** (3), 789-794.

Gonzales, G. Auclair, C, Voisin, E., Gautero H., Dhermy, D., Boivin, P (1984). Superoxide Dismutase, Catatase, and Glutathione Peroxidase in Red Blood Cells from Patients with Malignant Diseases. *Cancer Res.*, **44**, 4137-4139.

Gupta, C., Katsumata, M., Goldman, A.S., Herold, R., Piddington, R. (1984). Glucocorticoid-induced phospholipase A2-inhibitory proteins mediate glucocorticoid teratogenicity in vitro. *Proc Natl Acad Sci U S A*, **81**, 1140-1143.

Gupta, M. K., Qin, R. Y. (2003). Mechanism and its regulation of tumor-induced angiogenesis. *World J. Gastroenterol.*, **9**:, 1144-1155.

Guzy, R.D., Schumacker, P.T. (2006). Oxygen sensing by mitochondria at complexIII: the paradox of increased reactive oxygen species during hypoxia. *Exp. Physiol.*, **91** (5), 807-819.

Hall K, Ran S., (2010). Regulation of tumor angiogenesis by the local environment. *Front Biosci.*, **15**, 195-212.

Lopez-Lazaro, M. (2007). Excessive superoxide anion generation plays a key role in carcinogenesis. *Int. J. Cancer*, **120**, 1378-1380.

Lopez-Lazaro, M. (2010). A New View of Carcinogenesis and an Alternative Approach to Cancer Therapy. *Mol. Med.*, **16**, 144-153.

Miller, T.W., Isenberg, J.S., Roberts, D.D. (2009). Molecular Regulation of Tumor Angiogenesis and Perfusion via Redox Signaling. *Chem. Rev.*, **109 (7)**, 3099-3124.

Nakayama, T., Yao, L., Tosato, G. (2004). Mast cell-derived angiopoietin-1 plays a critical role in the growth of plasma cell tumors. *J. Clin. Invest.* **114**, 1317–1325.

Naldini, A., Carraro, F. (2005). Role of inflammatory mediators in angiogenesis. *Curr. Drug Targets Inflamm. Allergy*, **4**, 3-8.

Qutub A.A, Popel A.S., (2008) Reactive Oxygen Species Regulate Hypoxia-Inducible Factor 1α Differentially in Cancer and Ischemia. *Mol. Cell. Biol.* **28** (16), 5106–5119.

Rapisarda, A., Shoemaker, S.H., Melillo, G. (2009). Antiangiogenic agents and HIF-1 inhibitors meet at the crossroads. *Cell Cycle*, **8** (24), 4040-4043.

Rosen, L.S. (2002). Clinical experience with angiogenesis signaling inhibitors: focus on vascular endothelial growth factor (VEGF) blockers. *Cancer Control*, **9**:, 36-44.

Sato, T.N., (2003), Emerging concept in angiogenesis: specification of arterial and venous endothelial cells, *Br. J. Pharmacol.*, **140**, 611-613.

Sihvo, E.I.T., Ruohtula, T., Auvinen, M.I., Koivistoinen, A., Harjula, A.L., Salo, J.A. (2003). Simultaneous progression of oxidative stress and angiogenesis in malignant transformation of Barrett esophagus. *J Thorac Cardiovasc. Surg.*, **126** (6), 1952-1957.

Tandon, V.R., Sharma, S., Mahajan, A., Bardi, G.H. (2005). Oxidative Stress: A Novel Strategy in Cancer Treatment. *JK SCIENCE*, **7** (1), 1-5.

Ushio-Fukai, M. (2006). Redox signaling in angiogenesis: Role of NADPH oxidase. *Cardiovasc. Res.*, **71**, 226 - 235.

Ushio-Fukai, M. and Nakamura, Y. (2008), Reactive Oxygen Species and Angiogenesis: NADPH Oxidase as Target for Cancer Therapy. *Cancer Lett.*, **266**, 37-52.

van der Bij G.J., Oosterling S.J., Meijer S., Beelen R.H., van Egmond M., (2005) The role of macrophages in tumor development. *Cell Oncol.*, **27** (4), 203-213.

Wang, J., Yi, J. (2008). Cancer cell killing via ROS. *Cancer Biol. Ther.*, **7** (12), 1875-1884.

Wienberg, F., Hamanak, R., Wheaton, W.W., Weinberg, S., Josep, J., Lopez, L., Kalyanaraman, B., Mutlu, G.M., Budinger, G.R.S., Chandel, N.S. (2010). Mitochondrial metabolism and ROS generation are essential for Kras-mediated tumorigenicity. *Proc. Natl. Acad. Sci. USA.*, **107** (19), 8788-8793.

Xia, C., Meng, Q., Liu, L-Z., Rojanasakul, Y., Wang, X-R., and Jiang, B-H. (2007). Reactive Oxygen Species Regulate Angiogenesis and Tumor Growth through Vascular Endothelial Growth Factor. *Cancer Res.*, **67** (22), 10823-10830.

Zou, W. (2005). Immunosuppressive networks in the tumour environment and their therapeutic relevance. *Nature Rev. Cancer*, **5**, 263–274.

STUDIA UNIVERSITATIS BABEŞ – BOLYAI, BIOLOGIA, LV, 1, 2010, p. 119-130

OBTAINING AND CHARACTERIZATION OF AN α-AMYLASE BY A STRAIN OF *BACILLUS SUBTILIS*

MIHAIL DRĂGAN-BULARDA[1], RAHELA CARPA[1], MIHAELA MIŞCA[1]and VICENȚIU CĂLEAN[1]

SUMMARY. This paper presents the results of obtaining a *Bacillus subtilis* strain, by UV irradiation, a strain that should produce alpha-amylase. We had in view the increase of biomass on a mineral medium with yeast extract, to which soluble starch 2% was added, and we used therefore, an installation with fermentation pot. The production of alpha-amylase was monitored, determining the maximum specific increase rate, respectively the relation between the increase of the cell mass and the enzyme production. We had also in view to obtain a raw enzymatic preparation and a partial purified one, for which K_m and V_{max} of reaction were determined. The enzyme production proved to be closely correlated with the quantity of biomass. The bacteria culture reached constant production efficiency after the lag phase. The raw enzymatic preparation presented a slightly higher alpha-amylase activity than the partial purified one, probably because of the starch traces present in the raw enzymatic extract.

Keywords: α-amylase, *Bacillus subtilis*, characterization, enzyme kinetics, fermentation, purification

Introduction

Amylases are among the most important starch-converting enzymes, and they can be derived from several sources. However, bacterial and fungal amylases have dominated applications in the industrial sector (breweries, alcohol production, bakeries, juice production from various fruits) (Vasilescu, 1963; Pandely, 2003; Drăgan-Bularda and Samuel, 2008). Also, the amylolytic enzymes find a wide spectrum of applications in food industry for production of glucose syrups, high fructose corn syrups, maltose syrups, reduction of viscosity of sugar syrups, reduction of haze formation in juices, and find a wide range of application in baking, paper, textile and detergent industry (Sivaramakrishnan et al., 2006). The alpha-amylase hydrolyses the α-1.4 bonds within the amylose and amylopectin chains (dextrinogenous amylases), resulting many maltodextrins, some maltose and

[1] *Babeş-Bolyai University / 1 Kogălniceanu St., 400084 Cluj-Napoca, Romania*
e-mail: mihai.dragan@ubbcluj.ro
e-mail: k_hella@yahoo.com
e-mail: vicentiu_84@yahoo.com

glucose from amylose, respectively, many maltodextrins and limit dextrin (with ramifications through α-1.6 bonds), some maltose and glucose from amylopectin (Baig *et al*., 1984; Banu *et al*., 1987; Dan, 2000; Jurcoane, 2000; Malhontra *et al*., 2000; Iorga and Câmpeanu, 2004; Drăgan-Bularda and Samuel, 2008).

The α-amylase produced by bacteria is a metalloenzyme with high molecular mass of about 50,000 Da, characterized by the presence in its structure of some inorganic ions, related to the polypeptide chains (Zarnea *et al*.,1988). These are Ca^{2+} (1-3) ions for stabilizing the structure and 1-2 Zn^{2+} ions that determine the dimer formation of the enzyme (*www.resb.org*). Due to the fact that it is a protein, the biosynthesis of the alpha-amylase takes place at ribosome level and is secreted by the bacteria in the culture medium (Drăgan-Bularda and Samuel, 2008).

In the last decades, more and more microorganisms were used as potential sources for various biotechnologies (Zarnea and Dumitru, 1994). Bacterial α-amylase, which are usually produced by bacteria belonging to *Bacillus* genus (Nigam and Singh, 1995) are widely used in the starch-processing industry for the hydrolysis of starch (Lonsane and Ramesh, 1990). There were tested conditions for optimizing the biosynthesis of some enzymatic complexes (protease-amylase complex) by using *Bacillus subtilis* strains (Bahrim and Dan, 1994; Dan *et al*., 1994), respectively, there was studied the influence of the input of aminoacids on the biosynthesis of some enzymes, among these also the alpha-amylase on *Bacillus subtilis* strains, or the effect of some water-soluble vitamins on the biosynthesis in case of fermentation with *Bacillus subtilis* strains. In most cases the enzymatic process is inhibited by high substrate and product concentration and also instability of the enzyme repetitive or prolonged use. Immobilization is an important technique for continuous and repeated use of enzymes in industrial application and also rapid separation of the enzyme from the reaction medium. The general methods employed for immobilization are entrapment, microencapsulation, copolymerization, cross-linking, physical adsorption, chemical attachment and covalent binding (Gangadharan *et al*., 2009).

Tests were conducted for immobilizing some microbial hydrolases with protease and amylase activity on collagen support (Tcacenco *et al*., 1994). α-amylase produced by *Bacillus amyloliquefaciens* ATCC 23842 was immobilized in calcium alginates. Also, alginate beads have been successfully used for entrapment of α-amylase of *Bacillus subtilis* and effectively used for starch hydrolysis (Rajagopalan and Krishnan, 2008). Immobilization is a very effective alternative in overcoming problem of instability and repetitive use of enzymes. Entrapment method of immobilization is advantageous over other methods that do not involve chemical modification of the enzyme (Gangadharan *et al*., 2009).

It should be emphasized that the application of α-amylase in different industrial processes demands specific characteristics including thermostability, particular pH activity profiles, pH stability and Ca-independency, consequently, demand for novel amylases is increasing worldwide, as the variety of enzyme applications is increasing in various industrial sectors (Pandely *et al*., 2000). Industrially

important enzymes have traditionally been produced by submerged fermentation, but in recent years slide-state fermentation processes have been increasingly used for the production of these enzymes. In fact, solide-state fermentation has gained renewed interest from researches for the production of these enzymes in view of its economic and engineering advantages (Pandely, 1992). Inexpensive agriculture and agro-industrial residues are generally considered the best substrates for solid-state fermentation and for enzyme production in the systems (Pandely, 2003).

Our research aims at obtaining a valuable strain of *Bacillus subtilis* for producing alpha-amylase, using the UV-irradiation technique. We have also tested an enzymatic preparation of alpha-amylase under laboratory conditions, followed by partial purification and enzyme kinetics studies of alpha-amylase.

Materials and methods

Microbiological analyses. The *Bacillus subtilis* strain with amylolytic capacity was obtained by using a culture medium made of nutritive agar to which soluble starch was added to 0.5 %. There were used for inoculation several sources of microorganisms (fertile soils, therapeutic mud, aquatic sediments, compost). There were selected 5 bacterial strains with an intense amylolytic activity (that hydrolysed all the starch from the solution). There were obtained pure cultures and the specific affiliation as *Bacillus subtilis* strains was determined by microscopic, physiological and biochemical tests. The isolated strains were exposed to UV radiation (250 nm), and then the amylolytic activity was tested again, both from qualitative and quantitative point of view (by the Somogy-Nelson method) (Drăgan-Bularda, 2000).

Fermentation studies. There was used for fermentation a bubbling vessel of 500 ml capacity. After the thermal sterilization, the vessel opening was sealed with a rubber plug, provided with a sampling tube, so as to keep the aseptic condition of the vessel. The vessel was placed in a water-bath with adjustable temperature and connected to an adjustable-flow air-pump. In order to prevent the contamination of the culture medium, the air supply was provided with a filtering system with pores of 5, 2 and 1 μm. The discharged air was bubbled into a disinfecting solution before its exhausting, in order to ensure aseptic conditions and to prevent the release of culture microorganisms in the atmosphere.

Preparation of the culture medium. It had the following composition (Atlas, 2004): soluble starch 2%, yeast extract 0.3 %, $(NH_4)_2SO_4$ 0.3%, K_2HPO_4 0.1 %, $MgSO_4$. 7 H_2O 0.02%, NaCl 0.1 %, $CaCl_2$. 2 H_2O 0.008%. The medium was sterilised at 110^0C, for 30 minutes.

Preparation of inoculum. The *Bacillus subtilis* strain, growth on a solid medium with starch was inoculated on a liquid nutritive medium with starch. The incubation was made at 28^0C, for 24 hours. Then, there were introduced 15 ml of culture from the liquid medium into 100 ml of nutritive medium. This mixture was kept for 4 hours at 28^0C. Further on, it is added to the fermentation vessel, that contains 385 ml nutritive medium. The inoculum was mixed with the medium in

the bubbling vessel. The water-bath was adjusted at 30^0C and the inlet air-flow was set at 1.5 L air/L medium/minute. The fermentation process took 14 hours.

Analyses performed. *Measuring the increase of biomass.* It took place at the beginning of the fermentation and then every 30 minutes. The increase of the cell mass was determined by measuring the absorbance at 600 nm.

Monitoring the α-amylase production. Every 30 minutes, a small quantity of *culture medium* (4 ml) was taken under aseptical conditions. This sample was centrifugated for 5 minutes at 8000 rpm in order to separate the bacterial cells and the supernatant was used for enzymatic tests. The quantity of dry cell mass was determined (after drying in the drying chamber at 105^0C, for 48 hours). The Metais and Bieth method (Popa, 1990) was used for determining the α-amylase activity. The principle of this method consists in using a starch solution that will be treated with an enzymatic solution. The substrate remained unhydrolised was dosed spectrophotometrically at 565 nm, after the reaction with iodine. There was used a reaction mixture of enzymatic solution + enzymatic substrate (starch solution 0.4% as buffer Na_2HPO_4 0.2 M – citric acid 0.1 M, pH7). The incubation took place at several temperatures (20-70^0C), for 5 minutes. The enzymatic reaction was stopped with 5 ml of 6% acetic acid solution. Iodine solution N/1500 was added, and the resulting violet complexe passed trough a colorimetric analyse at 565 nm, towards distilled water. In order to determine the initial starch concentration in the reaction medium, the enzymatic reaction was stopped at zero time. The amylase activity is indicated in U/ml/min and is calculated as follows:

Enzymatic activity = $OD_{control} - OD_{sample}$ *x 1.2 x 5 x 1/5 per* $OD_{control}$ (where OD is optical density; 1.2 – quantity of starch, expressed in mg, added to the reaction).

The above relation was multiplied by 5 in order to determine the enzymatic units in 1 ml of protein preparation, respectively by 1/5 in order to determine the activity during 1 minute.

Obtaining the raw extract. After 14 hours, the content was centrifugated for 15 minutes at 800 rpm. The supernatant was collected and filtered, getting the raw extract (in total 220 ml).

Obtaining the partial purified preparation. To the raw extract there was added cold acetone up to 80% (V/V) saturation. We worked on ice bath. The suspension was centrifuged for 30 minutes at 800 rpm. The supernatant was removed. The precipitation was redisolved in buffer phosphate 0.1 mol/L.

Calculation of K_m *and* V_{max}. In order to determine the reaction rate, there were used 5 starch solutions of known concentrations. To each of these, there was added 1 ml of enzymatic preparation. After homogenisation, there was taken 1 ml of mixture, to which 0.2 ml iodine solution N/100 was added and the adsorbance at 565 nm was measured. The rest of the sample was indroduced in a water bath at 30^0C. After 1 minute there were added 0.4 ml iodine solution N/100 and the adsorbance at 565 nm was measured. For calculating the starch concentration in the sample, there was used a standard curve with 6 concentrations of starch (0.333 – 2 mg/ml). The reaction rate was calculated as follows: $V= (C_{inițial}-C_{final})/60$.

Results and discussion

1. *The maximum specific increase rate*

The maximum specific increase rate of the *Bacillus subtilis* strain used, was determined by the relation $dx/dt=\mu x$

where x = quantity of biomass

t = time of growth

μ = specific increase rate

By separating the variables and integration we obtain:

$Ln \cdot x_0/x = \mu(t-t_0)$

Thus, by the graphic presentation of the values for $Ln \cdot x_0/x$ depending on the time we obtained a line, with the slope indicating the specific increase rate. The dependence between the optical density at 600 nm and the quantity of biomass in the sample is considered to be a linear one. Knowing the quantity of biomass (0.15 mg) corresponding to an absorbance of 1.42, the absorbance of the samples at 600 nm was correlated with the quantity of biomass, using the data in Table 1.

Table 1.

Data used for calculating the maximum specific increase rate

Time (h)	Absorbance at 600 nm	Dry cell mass (mg)	$Ln \cdot x_0/x$
2	0.227	0.023979	0.024527
2.5	0.365	0.038556	0.499474
3	0.581	0.061373	0.964328
3.5	0.61	0.064437	1.013036
4	0.835	0.088204	1.327009
4.5	0.79	0.083451	1.27161
5	1.235	0.130458	1.718403
5.5	1.452	0.15338	1.880274
6	1.58	0.166901	1.964757
6.5	1.828	0.193099	2.110555
7	1.95	0.205986	2.175162

Based on the data in Table 1 we drawn the graphic in figure 1. We calculated this way the slope of the line, which is actually the maximum increase rate (μ_{max}). For the *Bacillus subtilis* strain, this value was of $\mu_{max}=0.504\ h^{-1}$, which is considered to be a normal value for a cell culture.

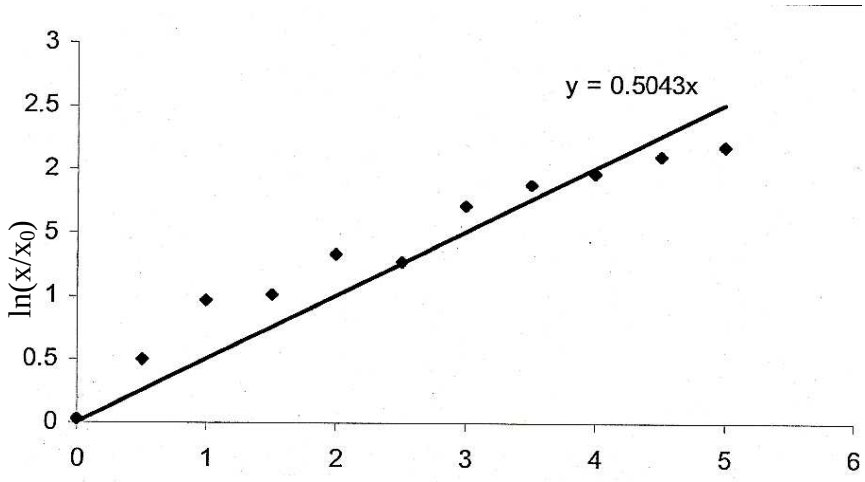

Fig. 1. Calculation of the maximum increase rate

2. The relation between the increase of the cell mass and the enzyme production

The Table 2 shows the data from measuring the optical density (absorbance) of the culture at 600 nm.

The data in Table 2 were used for determining the relation between biomass and the enzymatic activity of the medium (see Fig. 2). One can observe analysing the graphic, a correlation between the accumulation of cell mass and the intensification of the enzymatic activity of the culture medium. This dependence indicates that the alpha-amylase is a prime metabolite with constitutive synthesis. In such cases, the relation between the enzyme production (P) and the biomass (x) is described as follows:

$1/dx \cdot dP/dt = dP/dx \cdot 1/x \cdot dx/dt$,

where

$1/dx \cdot dP/dt = q_p$ is the specific rate for biomass product forming and

$dP/dx = Y_{p/x}$ is the efficiency coefficient,

while $1/x \cdot dx/dt = \mu$ is the specific increase rate of biomass.

Making the substitution in the first relation, it resulted that $q_p = Y_{p/x}$, which represents μ.

Table 2.

Data obtained during the fermentation, based on which, the enzymatic activity and the dry cell mass were calculated

Time (h)	Adsorbance at 600 nm	Dry cell mass (mg)	Enzyme production		
			Control Absorbance at 565nm	Absorbance of sample at 565nm	Activity (U/ml/min)
0	0.221	0.0233	0.725	0.715	0.0165
0.5	0.21	0.0222	0.735	0.729	0.0095
1	0.252	0.0266	0.714	0.707	0.0123
1.5	0.183	0.0193	0.718	0.651	0.112
2	0.227	0.024	0.702	0.682	0.0342
2.5	0.365	0.0386	0.712	0.703	0.0151
3	0.581	0.0614	0.72	0.703	0.0285
3.5	0.61	0.0644	0.702	0.664	0.0642
4	0.835	0.0882	0.699	0.510	0.324
4.5	0.79	0.0835	0.71	0.482	0.385
5	1.235	0.1305	0.715	0.380	0.563
5.5	1.452	0.1534	0.72	0.327	0.655
6	1.58	0.1669	0.716	0.346	0.62
6.5	1.828	0.1931	0.695	0.185	0.88
7	1.95	0.206	0.708	0.159	0.93
7.5	2.275	0.2403	0.721	0.252	0.78
8	2.105	0.2224	0.7	0.099	1.03
8.5	2.422	0.2558	0.698	0.047	1.12
9	2.125	0.2245	0.71	0.030	1.15
9.5	2.355	0.2488	0.695	0.046	1.12
10	2.42	0.2556	0.7	0.058	1.1
10.5	2.252	0.2379	0.703	0.158	0.93
11	2.158	0.228	0.695	0.145	0.95
11.5	1.852	0.1956	0.698	0.128	0.98
12	1.905	0.2012	0.71	0.089	1.05
12.5	1.937	0.2046	0.685	0.143	0.95
13	1.45	0.1532	0.698	0.134	0.97
13.5	1.35	0.1426	0.685	0.211	0.83
14	1.42	0.15	0.693	0.144	0.95

The specific product forming rate and the efficiency coefficient can be calculated and these offer information on the efficiency of the fermentation process. Thus, at the end of the fermentation, based on the obtained data, it resulted that:

$q_p = 1/0.15 \cdot (0.95\text{-}0.0165) / 14 \cdot 60$, so q_p=7.4 U enzyme/g biomass/min

The efficiency coefficient was calculated using the same data, and we obtained

$Y_{p/x} = (0.95\text{-}0.0165) / (0.15\text{-}0.233)$, so Yp/x=7370 U enzyme/g biomass.

These data indicate that the enzyme production is in this case, a poor one. The Fig. 2 presents the enzyme production related to the biomass, and the relation proved to be a constant one, after the *lag* phase. This result indicates also that the enzyme production is constitutive.

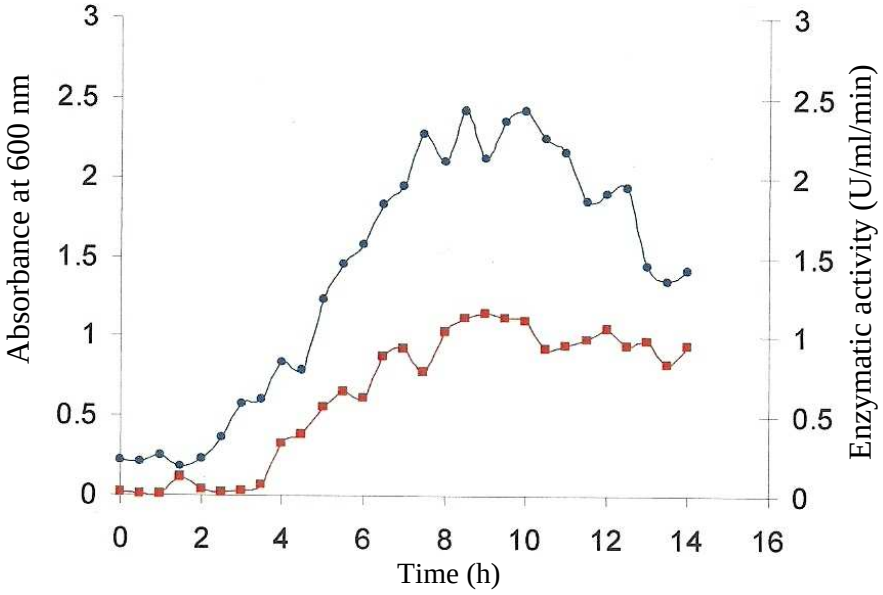

Fig. 2. Relation between the increase of biomass (circles) and the enzymatic activity (squares) of the *Bacillus* strain.

Using the values obtained for q_p and $Y_{p/x}$ we calculated the value of the biomass increase rate, and it resulted that $\mu = 7.4/7370\ 60$, so $\mu = 0.0602\ h^{-1}$. This increase rate is a relatively poor one, probably because of the low oxygen supply, which proved to be a limitative factor.

3. Obtaining the raw and the purified enzymatic preparation

The data we obtained in this respect are shown in Table 3, respectively in Fig. 3.

It was observed that the activity of alpha-amylase oscillated depending on the temperature at which the enzymatic activity took place, with a maximum value at 40^0C, and a decrease of the values after this temperature, probably because of the inactivation or thermal distortion of the alpha –amylase. We also observed that the raw extract had a higher enzymatic activity than the purified preparation (see Fig.3).

Table 3.

Enzymatic activity of the raw enzymatic preparation and of the purified enzyme preparation

Temperature (^{O}C)	Raw extract			Purified preparation		
	OD Control	OD Sample	Activity	OD Control	OD Sample	Activity
20	0.56	0.215	0.7392857	0.385	0.178	0.645195
30	0.565	0.16	0.860177	0.379	0.16	0.693404
40	0.558	0.11	0.9634409	0.382	0.132	0.78534
50	0.56	0.122	0.9385714	0.372	0.138	0.754839
60	0.58	0.132	0.9268966	0.378	0.156	0.704762

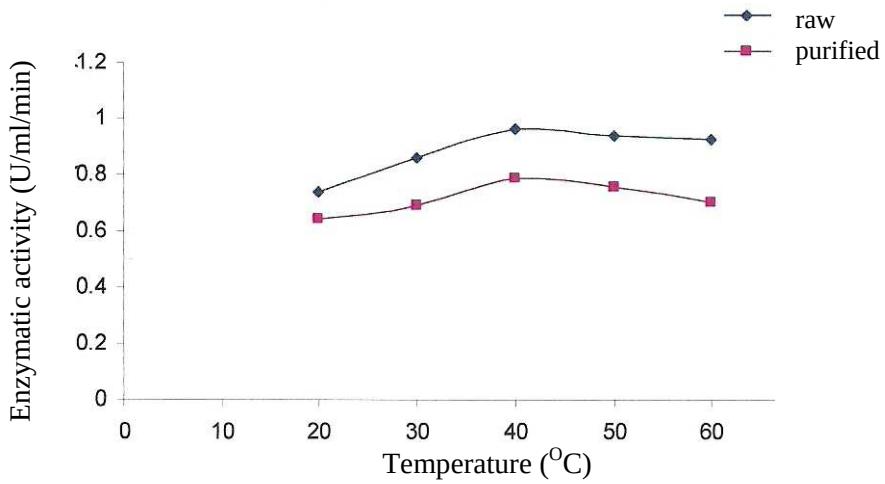

Fig. 3. Evolution of the alpha-amylase activity.

This phenomenon can be explained by an incomplete precipitation of the alpha-amylase in the raw extract and on the other hand by the presence of starch rests in the raw extract, which influenced the experiment. Analysing the figure, we observe also that the enzymatic activity of the of the raw extract seems to remain approximatively at the same value, between 40 and 60^{0}C.

4. Determining the enzymatic kinetics

There was determined the Michaelis-Menten constant and V_{max} of reaction. The data used for calculating K_m and V_{max} are indicated in Table 4.

Table 4.

Calculating K_m and V_{max} in the case of *Bac.subtilis* alpha-amylase

No.	[S] (mg/ ml)	L/[S] (ml/ mg)	Adsorbance		Concentration		V (mg/s)	L/V (s/mg)
			Initial	Final	Initial	Final		
1	0.2	5	0.023	0.021	0.214	0.188	0.000433	2307.692
2	0.4	2.5	0.044	0.039	0.398	0.356	0.0007	1428.571
3	0.6	1.66	0.066	0.058	0.599	0.522	0.001283	779.2208
4	0.8	1.25	0.089	0.082	0.802	0.738	0.001067	937.5
5	1	1	0.106	0.092	0.955	0.832	0.00205	487.8049

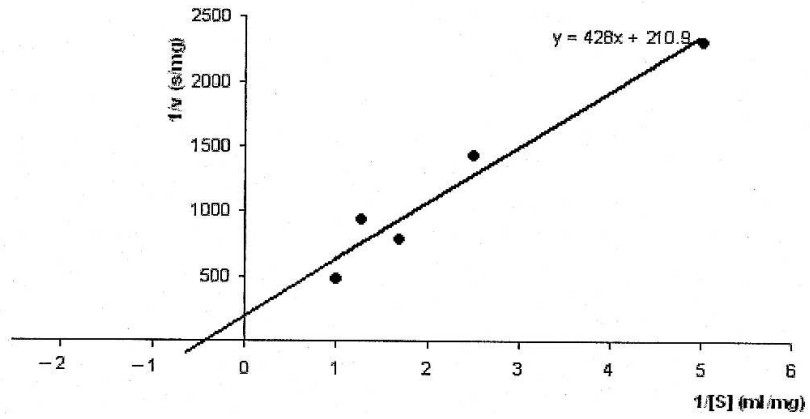

Fig. 5. The calculation of K_m and V_{max} by Lineweaver-Burk method.

The Fig.5 shows the calculation of K_m and V_{max} by the Lineweaver-Burk method. Thus, $1/V_{max}$ = 210.9, so thati V_{max}=0.0047 mg/s, respectively 0.284 mg/min, while

K_m/V_{max} = 428
K_m=428 x V_{max}, so that K_m = 2.011 mg/ml

The values obtained for V_{max} suggest that the preparation of alpha-amylase hydrolised the starch with a lower speed, probably because of an excessive dilution during the resuspension in buffer solution, and because of an inactivation arosen during handling and storage, on the other hand. In the mean time, the value for K_m indicates a lower affinity of the enzyme for the substrate, which can be explained by the variations as shape and structure of the alpha-amylase substrate.

Conclusions

1. The amylolytic activity of a *Bacillus subtilis* strain was tested, and it proved to have a quite important amylolytic capacity. The enzyme production takes place constitutively, parallel to the biomass increase. The bacteria culture reached a constant production efficiency after the *lag* phase, confirming that the enzyme production is not correlated with the culture age.
2. The enzyme production proved to be closely related with the cell mass quantity. The biomass quantity was relatively lower, probably because of a poor aeration, as the oxygen dissolved in the medium has a limitative influence.
3. The enzymatic preparation obtained after partial purification showed a slightly lower enzymatic activity than the raw extract, partly because of the starch rests in the raw extract, due to its low solubility.
4. The kinetic analyse indicated a relatively high value of the Michaelis-Menten constant, this fact shoving a lower affinity of the enzyme for the substrate, probably because of the wide dimension range of the substrate. The maximum rate was relatively low, possibly because of the purification method, whose efficiency was not good enough.

REFERENCES

Atlas, R.M. (2004). *Handbook of Microbiological Media, 3rd edition,* CRC Press, New York.

Bahrim, G., Dan, V.(1994). The optimization of biosynthesis conditions for protease-amylase complex bysp.MIVG 6.61, *Proc.8th Nat .Symp. Ind. Microbiol. Biotehnol. (Bucharest),* pp. 237-240.

Baig, M.A., Pazlarova, J., Votruba, J. (1984). Kinetics of α-amylase production in a batch and fed-batch culture of *Bacillus subtilis*, *Folia Microbiol.*, **29**, 359-364.

Banu, C., Vasu, S., Stoicescu, A. (1987). *Biotehnologii în industria alimentară,* Ed. Tehnică, Bucureşti.

Dan, V.(2000). *Microbiologia produselor alimentare,vol.2,*Ed. S.C. Alma, Galaţi.

Dan, V., Bahrim, G., Nicolau,A.(1998). Condiţii de obţinere a complexului amilazo-proteazic prin cultivarea tulpinii *Bacillus subtilis MIUG 9.61* pe medii semisolide. *Lucr. IX Symp. Microbiol. Biotehnol. (Iaşi),* pp. 37-44.

Drăgan-Bularda, M.(2000). *Microbiologie generală – lucrări practice*, Ed. III. Univ.Babeş-Bolyai, Cluj-Napoca.

Drăgan-Bularda, M., Samuel, A.D. (2008). *Biotehnologii microbiene*, Ed. Univ. Oradea.

Gangadharan, D., Nampoothri, K.M., Sivaramakrishnan, S., Pandey, A. (2009). Immobilized bacterial α-amylase for effective hydrolysis of raw and soluble starch, *Food Res. Internat.*,**42**, 436-442.

Hefco, G., Olteanu, Z., Tănase, A., Rugină, V. (1998). Influența unor vitamine hidrosolubile asupra biosintezei α-amilazei şi catalazei în fermentația cu *Bacillus subtilis, Lucr. IX Symp. Microbiol. Biotehnol. (Iaşi)*, pp. 671-675.

Iorga, E., Câmpeanu, G. (2004). *Utilizarea enzimelor în panificație*, Ed. Univ. Șt. Agron. Med. Vet., Bucureşti.

Jurcoane, Ş. (2000). *Biotehnologii*, Ed. Tehnică, Bucureşti.

Lonsane, B.K., Ramesh, M.V. (1990). Production of bacterial thermostable α-amylase by solid-state fermentation: a potential tool for achieving economy in enzyme productioin and starch hydrolysis, *Adv. Appl. Microbiol.*, **35**, 1-56.

Malhontra, R., Noorwez, S.M., Satyanarayana, B. (2000). Production and partial characterisation of thermostable and calcium-independent α-amylase of an extreme thermophyle *B.thermoleovorans NP54, Let. Appl. Microbiol.*, **31**, 378-384.

Nelson, A. (1944). A photometric adaptation of the Somogyi method for the determination of glucose, *J. Biol. Chem.*, **153**, 375-380.

Nicolau, A. (1998). Utilizarea culturilor mixte de fungi selecționați pentru producerea de amilaze, *Lucr. IX. Symp. Microbiol. Biotehnol. (Iaşi)*, 105-113.

Nigam, P., Singh,D. (1995). Enzyme and microbial systems involved in starch processing, *Enzyme Microb. Technol.*, **17**, 770-778.

Pandely, A. (2003). Solid state fermentation, *Biochem. Eng. J.*, **13**: 81-84.

Rajagopalan, G., Krishnan, C. (2008). Immobilization of malto-oligosaccharide forming α-amylase from *Bacillus subtilis* KCC103: Properties and application in starch hydrolysis, *J. Chem. Technol. Biotechnol.*, doi:10.1002/jctb.1922.

Rugină, V., Hefco, G., Olteanu, Z., Tănase, A., Ciornei, A., Dănălache, B. (1998). Influența adaosului de aminoacizi în biosinteza enzimelor α-amilază, amiloglucozidază, catalază, în fermentația speciei *Bacillus subtilis, Lucr. IX Symp. Microbiol. Biotehnol.(Iaşi)*, pp.657-665.

Sivaramakrishnan, S., Gargadharan, D., Nampoothiri, K.M.,Pandey, A. (2006). α-amylase from microbial sources – An overview on recent developments, *Food Technol. Biotechnol.*, **44** (2), 173-184.

Somogyi, M. (1952). Notes on sugar determination, *J. Biol. Chem.*, **195**, 19-23.

Tcacenco, L., Ioniță, A., Teodor, E., Rugină, A. (1998). Imobilizarea unor hidrolaze microbiene cu activitate proteazică şi amilazică pe suport colagenic, *Lucr. IX Symp. Microbiol. Biotehnol. (Iaşi)*, pp.863-867.

Vasilescu, I.(1963). *Tehnoloigia şi aplicațiile industriale ale enzimelor*, Ed. Tehnică, Bucureşti.

Zarnea, G., Dumitru, L. (1994). Biodiversitatea microorganismelor, sursa potențială de progres în biotehnologie, *Proc. 8th Nat. Symp. Ind. Microbiol. Biotehnol. (Bucharest)*, pp.15-45.

STUDIA UNIVERSITATIS BABEŞ – BOLYAI, BIOLOGIA, LV, 1, 2010, p. 131-138

MICROBIOLOGICAL AND ENZYMOLOGICAL STUDY ON SEDIMENTS AND WATER OF THE RIVER SOMEŞUL MIC UPSTREAM THE GILĂU (CLUJ COUNTY) TREATMENT PLANT

VASILE MUNTEAN[1], COSMINA-GABRIELA MAIER[1], RAHELA CARPA[1], CORINA MUREŞAN[2] and ANCUȚA CRISTINA FARKAS[2]

SUMMARY. Seasonal analyses were carried out on the waters from 5 sampling sites situated on the Someşul Mic river, upstream the water treatment plant in Gilău. The total coliform germs and the faecal coliforms were analysed. The presence in water of the two bacterial groups was detected in each sampling site, in each season, with higher values in autumn, and lower in winter. A positive correlation with good statistical significance ($p<0.01$) was registered between the two groups of coliforms. In order to differentiate the genera of coliforms, 7 biochemical tests have been carried out on the water sampled in autumn at the P2 site, where the highest number of coliforms had been registered: indole production, methyl red test, Voges-Proskauer test, citrate utilization, malonate utilization, urea hydrolysis and H_2S production on the TSI medium. On the base of the results obtained from the 7 biochemical tests, four bacterial genera have been identified: *Escherichia, Klebsiella*, *Enterobacter* and *Citrobacter*. The three enzymatic activities studied in sediments (phosphatase, catalase and potential dehydrogenase) gave values of enzymatic indicators of sediment quality slightly lower than those registered by other researchers five years earlier.

Keywords: Someş river, coliform germs, faecal coliforms, enzymatic activity

Introduction

The water quality is always an actual and serious problem of mankind. The microbiological pollution of water is even a more pressing matter when it affects rivers used as sources of drinking water for large populations. In order to avoid contamination of people with pathogenic microorganisms, many studies aim at identification in natural waters of so called **indicator organisms**. According to Bitton (2005), the main criteria for an ideal indicator organism would be the following:

[1] *Babeş-Bolyai University, Faculty of Biology and Geology, Department of Experimental Biology, Kogălniceanu street, No.1, 400084 Cluj-Napoca, Romania*
[2] *Water Company Someş SA, 22 Decembrie 1989 street, No.79, 400604 Cluj-Napoca, Water Treatment Plant Gilău, Romania*

- it should be a member of the intestinal microbiota of warm-blooded animals;
- it should be present when pathogens are present, and absent in uncontaminated samples;
- it should be present in greater numbers than the pathogen;
- it should be at least equally resistant as the pathogen to environmental factors and to disinfection in water and wastewater treatment plants;
- it should not multiply in the environment;
- it should be detectable by means of easy, rapid, and inexpensive methods;
- the indicator organism should be non pathogenic.

The group of coliform bacteria fulfils these criteria and was adopted as an indicator of faecal contamination of drinking water as early as the beginning of last century. These indicators are useful for determining the quality of potable water, shellfish harvesting waters, and recreational waters. In water treatment plants, total coliforms are one of the best indicators of treatment efficiency of the plant.

The **total coliforms** belong to the family Enterobacteriaceae, order Enterobacteriales, class Gammaproteobacteria, phylum BXII – Proteobacteria (Garrity, 2005). The total coliforms include the aerobic and facultative anaerobic, non-spore-forming, Gram-negative, rod-shaped bacteria that ferment lactose with gas production within 48 hours at 35°C. The group includes four bacterial genera: *Escherichia, Klebsiella, Enterobacter and Citrobacter*.

Faecal coliforms are thermotolerant bacteria that include all coliforms that can ferment lactose at 44.5°C. The presence of faecal coliforms indicates the presence of faecal material from warm-blooded animals. Faecal coliforms display a survival pattern similar to that of bacterial pathogens, but they are not reliable with regard to contamination of aquatic environments with viruses and protozoans.

Grimes *et al.* (1984) study the microbiological effects caused by the dump of used water in the coastline waters of Puerto Rico, resulting in the increase in number of faecal indicator bacteria and in water pollution with pathogen microorganisms. Gerba and Speed (1997) show the effects of pollution indicator bacteria living in a small tropical river and their impact on the quality of water used for leisure activities. A surface water with faecal pollution is recorded by Venter *et al*. (1997) in South Africa.

Noble *et al.* (2003a) compare the bacterial indicators (total coliforms, faecal and enterococci) of water quality for ocean water used in leisure activities. Same year, Noble *et al*. (2003b) make another comparison of measurement methods for bacterial indicators of water quality in oceanic water from seashore zone.

Many studies were also carried out in our country, pursuing the same task, especially on the water of the Mureş river (Millea *et al.,* 1993; Papp and Fodorpataki, 2002; Muntean *et al.*, 2008). The present study aimed to detect the presence in the Someşul Mic river water of microorganisms used as faecal pollution indicators. We

also aimed to appreciate the level of the enzymatic activity in sediments of the same river, at the same 5 sampling sites situated upstream the Gilău treatment plant.

Materials and methods

The microbiological analyses pursued the presence of coliform germs in water of the Someş river before it reached the treatment plant in Gilău. The analyses were carried out seasonally, in 2007, on water sampled from five sites, as follows:

P1 – Someşul Cald, 300 m upstream the filtration station Gilău;

P2 – Someşul Rece, 500 m upstream the filtration station Gilău;

P3 – the confluence of the rivers Someşul Cald and Someşul Rece;

P4 – left side of the Gilau dam reservoir;

P5 – right side of the Gilau dam reservoir.

We determined the total and faecal (thermotolerants) coliform bacteria, according to the STAS 3001-91. In order to differentiate the genera of coliforms, seven biochemical tests have been carried out on the water sampled in autumn, at the P2 site, where the highest number of coliforms had been registered: indole production, methyl red test, Voges-Proskauer test, citrate utilization (the four IMViC tests), malate utilization, urea hydrolysis on Christensen medium and H_2S production on TSI medium (Drăgan-Bularda, 2000, Atlas, 2004, Garrity, 2005).

We also analysed the enzymatic potential of sediments at the same five sampling sites in autumn. The following three enzymatic activities were studied: phosphatase (Krámer and Erdei, 1959), catalase (Kappen, 1913) and potential dehydrogenase (Casida *et al.*, 1964).

Results and Discussion

Fig. 1 presents the seasonal variation of the number of total coliform germs in the 5 sampling sites. High values of the number of total coliform germs (calculated by McCrady matrix) have been noticed in most of the cases. The number of total coliform germs was lower in winter and sometimes in spring, and higher in summer and autumn. The highest value (35000 germs/l) was registered in P2, in autumn, and the lowest one (54 germs/l) in P1, in winter.

A similar situation can be noticed in the case of the faecal coliforms (fig. 2). The number of faecal coliforms was lower, generally by an order of magnitude as compared to the total coliforms. The higest value (6400 germs/l) was also registered in autumn in P2. A positive correlation ($r = +0,983$) with a good statistical significance ($p<0.01$) was established between the number of total coliforms and faecal coliforms.

The results of the seven biochemical tests carried out in order to differentiate the genera of the coliforms present in the water sampled in the autumn of 2007, at the P2 site, where the highest number of coliforms had been registered are presented in tab. 1.

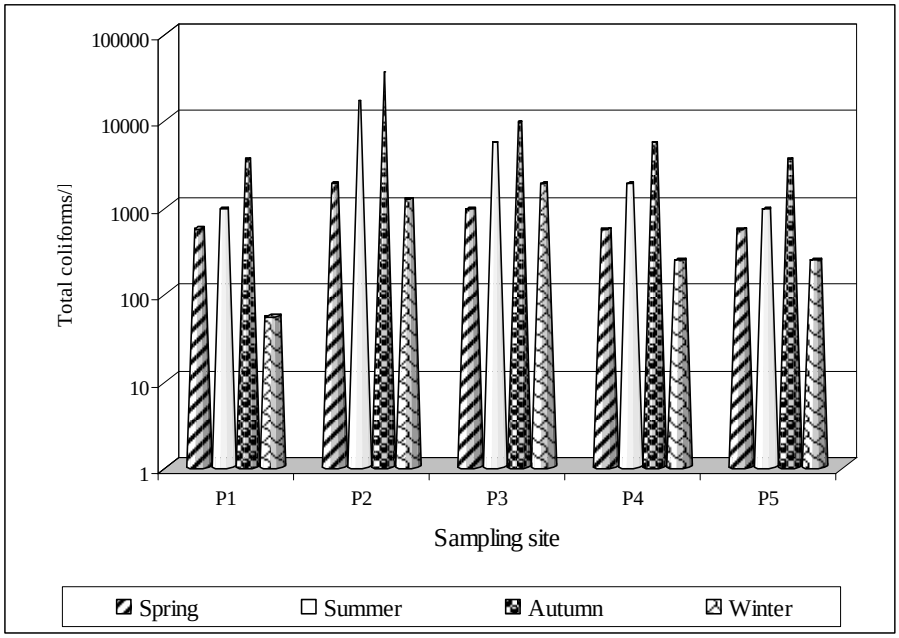

Fig. 1. The number of total coliforms (logarithmic expression).

One can notice that: strain 1 (S1) gave positive results only for indole production and methyl red test; strain 2 (S2) was positive for methyl red test, citrate utilization and urea hydrolysis; strain 3 (S3) was positive for Voges-Proskauer test, citrate and malonate utilization, and for urea hydrolysis; strain 4 (S4) was positive for six tests and negative only for the Voges-Proskauer test. According to these results, we assume that the four analysed strains belong to the following bacterial genera: *Escherichia* (S1), *Klebsiella* (S2), *Enterobacter* (S3) and *Citrobacter* (S4).

We notice the efficiency of the water treatment plant in Gilău. The applied treatment methods assure the complete elimination of coliforms in water, as the regular analyses at the treatment plant demonstrate. But we also notice the high negative potential of the permanently increasing number of habitations built along the river upstream the water treatment plant. The attention must be watchful and permanent, taking into account that the coliforms are discharged daily in numbers of billions by each human or animal being, in their faeces. And what is more important, the presence of coliforms indicates the possible presence in water of the pathogenic enteric bacteria.

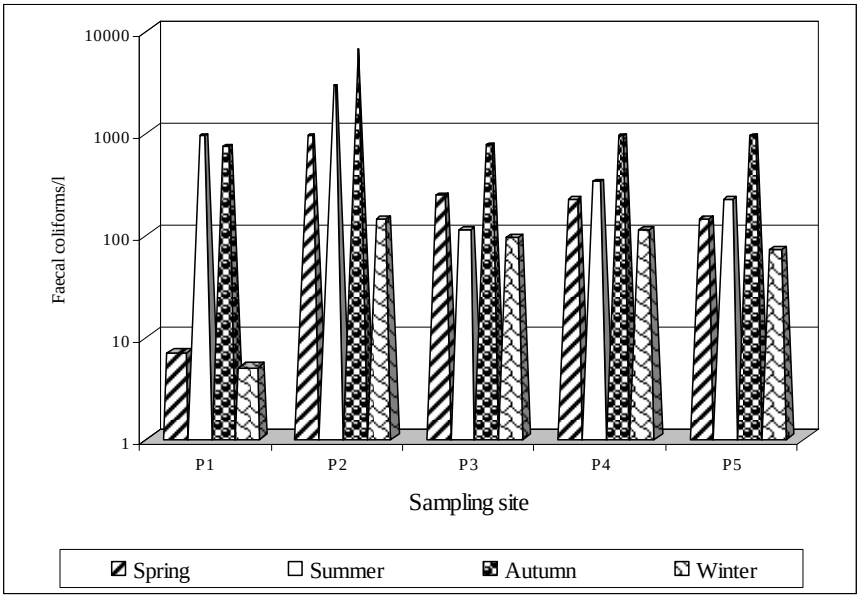

Fig. 2. The number of faecal coliforms (logarithmic expression).

Table 1.

Results of the biochemical tests for differentiation of the coliform species.

Test	Bacterial strain tested			
	S1	S2	S3	S4
Indole production	+	-	-	+
Methyl red test	+	+	-	+
Voges-Proskauer test	-	-	+	-
Citrate utilization	-	+	+	+
Malonate utilization	-	-	+	+
Urea hydrolysis	-	+	+	+
H_2S production on TSI medium	-	-	-	+
Genus to whom belong the strains	*Escherichia*	*Klebsiella*	*Enterobacter*	*Citrobacter*

The three enzymatic activities studied in autumn have been detected in all the sediments analysed. On the base of the absolute values of each enzymatic activity, the enzymatic indicator of sediment quality (EISQ) was calculated, according with Muntean *et al.* (1996). The values of the EISQ follow an increasing curve along the five sampling sites: the lowest value (EISQ = 0.159) in P1 and the highest value (EISQ = 0.286) in P5 (fig. 2). We mention that the minimal theoretical value of the EISQ is 0, and the maximal one is 1.

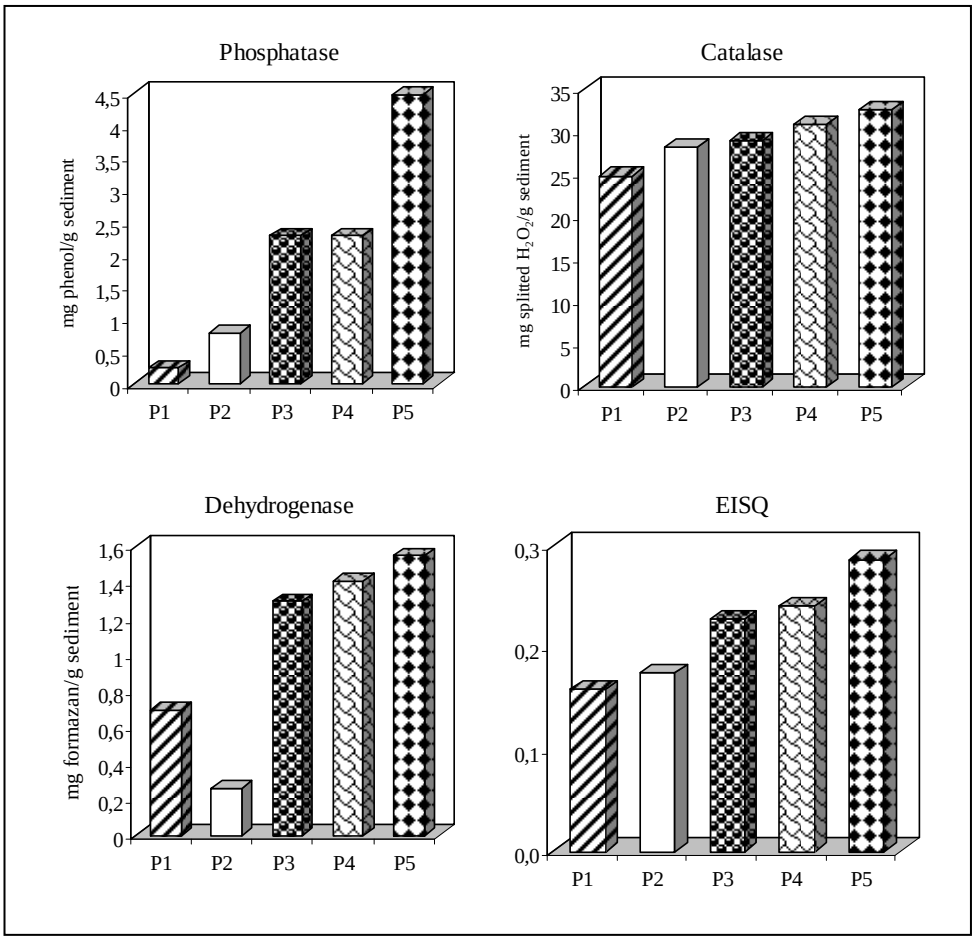

Fig. 3. Enzymatic activity in sediments. EISQ = enzymatic indicator of sediment quality.

The highest individual values have been registered as follow:

- phosphatase activity (4.5 mg phenol/g dry matter sediment) in P5;
- catalase activity (28.98 splitted H_2O_2/g dry matter sediment) in P3;
- potential dehydrogenase activity (1.408 mg formazan/g dry matter sediment) in P4.

The values of the phosphatase activity are significantly lower than those registered in the same dam sediments by Curticăpean and Drăgan-Bularda (2007). The catalase and the potential dehydrogenase activites proved to be higher than those obtained by the same authors. The EISQs calculated by the cited authors are higher than ours, because of the very high level of the phosphatase activity.

Positive correlations were calculated between the three enzymatic activities, but only the correlation between the phosphatase activity and the catalase activity ($r = +0.917$) has statistical significance ($p<0.05$). Slightly negative correlations without any statistical significance were established between the enzymatic activities and the total and faecal coliforms.

Conclusions

The presence of the total and faecal coliforms was registered in each season in the water samples in all the five sampling sites. Their number was lower in winter and sometimes in spring, and higher in summer and especially in autumn. The number of total coliforms was generally higher by an order of magnitude as compared to the faecal coliforms. Positive correlation with good statistical significance was noticed between the two bacterial groups.

Based on the results of the 7 biochemical tests (indole production, methyl red test, Voges-Proskauer test, citrate utilization, malonate utilization, urea hydrolysis on the Christensen medium and H_2S production on the TSI medium) four bacterial genera have been identified in the water sampled in autumn: *Escherichia, Klebsiella, Enterobacter* and *Citrobacter*.

The three enzymatic activities studied (phosphatase, catalase and potential dehydrogenase) were present in all the analysed sediments. The enzymatic indicators of sediment quality have all values under 0.3, lower than those registered by other researchers five years earlier.

REFERENCES

Atlas, R.M. (2004). *Handbook of Microbiological Media*, 3rd edition, CRC Press, New York.

Bitton, G. (2005). *Wastewater Microbiology*, 3rd edition, Wiley-Liss, Hoboken, New Jersey.

Casida, L.E.Jr., Klein, D.A., Santoro, T. (1964). Soil dehydrogenase activity, *Soil Sci.*, **98**, 371-376.

Curticăpean, M.-C., Drăgan-Bularda, M. (2007). The enzymatic activity from the sediment of the Gilau dam reservoir – Cluj county, *J. Biochem. Biophys. Methods*, **69**: 261-272.

Drăgan-Bularda, M. 220. *Microbioogie generală. Lucrări practice*, Universitatea Babeş-Bolyai, Cluj-Napoca.

Garrity, G.M. (ed. in chief), Brenner, D.J., Krieg, N.R., Staley, J.T. (ed. vol. 2) (2005). *Bergey's Manual of Systematic Bacteriology*, 2nd edition, vol. 2 – *The Proteobacteria*, Springer, New York.

Gerba, C.P., Speed, D.J. **(**1997). Source of fecal indicators bacteria in a brackish, tropical stream and their impact on recreational water quality, *Water Sci. Technol.*, **35** (11-12): 179-186.

Grimes, D.J., Singleton, F.L., Stemmler, J., Palmer, L., Brayton, P., Colwell, R.R. (1984). Microbiological effects of wastewater effluent discharged into coastal waters of Puerto Rico, *Water Res.*, **18**: 613-619.

Kappen, H. (1913). Die katalytische Kraft des Ackerbodens, *Fühlings Landw. Ztg*., **62**, 377-392.

Krámer, M., Erdei, G. (1959). Primenenie metoda opredeleniya aktivnosti fosfatazy v agrokhimicheskikh issledovaniyakh. *Pochvovedenie*, 9, 99-102.

Millea, L.C., Drăgan-Bularda, M., Lengyel, J., Muntean, V. (1993). Studiul bacteriologic al unor probe de ape din oraşul Aiud, *Stud. Univ. Babeş-Bolyai, Biol.*, **38** (1-2): 111-117.

Muntean, V., Crişan, R., Paşca, D., Kiss, S., Drăgan-Bularda, M. (1996). Enzymological classification of salt lakes in Romania, *Int. J. Salt Lake Res.*, **5** (1): 35-44.

Muntean, V., Carpa, R., Pojar, L.C., Grozav, M.A. (2008). Research concerning the faecal pollution of the Mureş River in the Ocna Mureş zone, *Stud. Cercet. Biol.*, **13**: 15-22.

Noble, R.T., Moore, D.F., Leecaster, M.K., McGee, C.D., Welsberg, S.B. (2003a). Comparison of total coliform, fecal coliform, and enterococcus bacterial indicator response for ocean recreational water quality testing, *Water Res.*, **37**: 1637–1643.

Noble, R.T., Weisberg, S.B., Leecaster, M.K., McGee, C.D., Ritter, K. Walker, K.O., Vainik, P. (2003b). Comparison of beach bacterial water quality indicator measurement methods, *Environ. Monit. Assess.*, **81**: 301–312.

Papp, J., Fodorpataki, L. (2002). Evaluation of the organic pollution of the Mureş river on the study of the indicator microflora, *Contrib. Bot.*, **37**: 231-237.

Venter, S.N., Steynberg, M.C., Wet, C.M.E., Hohls, D., Plessis, G., Kfir, R.. (1997). A Situational analysis of the microbial water quality in a peri-urban catchement in South Africa, *Water Sci. Technol.*, **35**(11-12): 119-124.

STAS 3001-91. *Apa – analiză bacteriologică*.